JPRS-UPM-90-003
30 JULY 1990

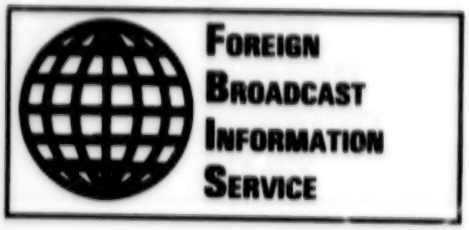

JPRS Report

Science & Technology

USSR: Physics & Mathematics

Science & Technology
USSR: Physics & Mathematics

JPRS-UPM-90-003 30 JULY 1990

CONTENTS

Lasers

Magnetohydrodynamics

Nuclear Physics

Optics, Spectroscopy

Plasma Physics

Superconductivity

Numerical Analysis, Algorithms

UDC 533.6

Experimental Determination of Parameters of Flow Behind Spherical Shock Waves

907L0057A Moscow VESTNIK MOSKOVSKOGO UNIVERSITETA, SERIYA 3: FIZIKA, ASTRONOMIYA in Russian Vol 30 No 6, Nov-Dec 89 pp 44-47

[Article by A. M. Galkin, D. A. Mazalov, N. N. Sysoyev, and F. V. Shugayev, Chair of Molecular Physics and Physical Measurements]

[Abstract] Essential characteristics of flow behind spherical shock waves were measured, shock waves having been generated by explosion on the surface of a barrier upon incidence of a laser beam. Graphite as well as steel and copper barriers with plane and spherical surfaces were placed inside a hermetic air chamber. Explosion was initiated by normally incident radiation pulses of 20 ns duration from a ruby laser (694.3 nm wavelength), their energy E being varied over the 0.01-1 J range and the power density q on the barrier surface correspondingly varying over the 10^8-10^{11} W/cm^2 range. The diameter of the focal spot was also varied, over the 100-500 μ range. In the the experiment the initial gas pressure was varied over the 0.1-1 atm range, the chamber with optical windows was placed in one arm of a Mach-Zehnder interferometer, and a monopulse laser provided brightening light pulses of 20 ns duration. The air density behind the front of a shock wave was calculated from pertinent data with the aid of the inverse Abel integral. The flow characteristics of concern are the length of time within which the flow pattern remains consistent with the theory of "point" charge explosion, the dependence of this time parameter on the power density q of incident radiation, and its dependence as well as that of the gas density on the distance from the laser spot. For the purpose of a general dimensionless analysis, that time and that distance as well as gas density and pressure P have been normalized to their quiescent values. The analysis of interferograms and processed numerical data, also of data on the flow pattern behind cylindrical shock waves, indicates that the gasdynamic processes occurring under conditions of this experiment are adequately described by the theory of "point" charge explosion when back-pressure is also taken into account. While 90% of the high incident laser energy sustains an absorption wave inside the laser beam channel and 5-10% of it initiates a cylindrical shock wave outside that channel, the theory of "point" charge explosion remains valid for a dimensionless time not longer than $0.05(E/2P_0)^{1/3}c_0^{-1}$. Here c_0 denotes the speed of sound in quiescent gas. With a different energy balance, at lower power density of incident radiation, it remains valid for a dimensionless time not shorter than $0.07(E/2P_0)^{1/3}c_0^{-1}$. Figures 5; references 7.

Mechanisms of Excitation of Atoms Ahead of Shock Wavefront During Optical Breakdown of Mixture of Inert Gases

907L0054A Leningrad PISMA V ZHURNAL TEKHNICHESKOY FIZIKI in Russian Vol 15 No 21, 12 Nov 89 pp 12-17

[Article by V.V. Apollonov, S.I. Derzhavin, D.A. Norayev, and A.A. Sirotkin, Institute of General Physics, USSR Academy of Sciences, Moscow]

[Abstract] An experiment with a mixture of inert gases was made, for a study of the mechanisms by which their atoms, upon absorption of radiation from a CO_2-laser, become excited ahead of the shock wavefront during optical breakdown of such a mixture. The mixture of xenon and helium in a Xe:He = 1:1000 ratio was pumped by a 50 W CO_2 - laser in pulses of 50 J energy, the pressure of the mixture being varied from 1 atm down and the duration of laser pulses being varied from 150 ns to 5 μs. The radiation was focused by a cylindrical lens onto a 0.8 mm wide and 6-9 mm strip so that optical breakdown of the gas mixture in the target cell occurred under radiation intensities covering the 10^7-10^8 W/cm^2 The electron concentration was measured by with a double-exposure holographic interferometer with a ruby laser as light source and the concentration of excited atoms was determined on the basis of absorption resonance. The interferograms revealed a cylindrical plasma expansion geometry and a nearly cylindrical shock wave propagation, with stronger refraction of the laser radiation at the caustic surface in the plasma, in the shock wave, and ahead of the shock wavefront upon normal incidence and upon incidence at a 45° angle. The minimum recorded electron concentration was 3.5 x 10^{15} cm^{-3}, much higher than 10^{15} cm^{-3} and thus hardly attributable to photoionization by ultraviolet radiation emitted by the optical-breakdown plasma alone. Absorption of CO_2-laser radiation by preionized gas plays probably a role here, optical breakdown in this experiment having occurred not with attendant avalanche ionization but with ionization ahead of the shock wavefront at a rate comparable with and thus compensating the loss of electrons due to diffusion, adhesion, elastic and inelastic collisions, and recombination. No absorption of radiation ahead of the shock wavefront was recorded in pure helium, the Penning effect being responsible for this. The recorded space-time distribution of excited Xe and He atoms indicates that their concentrations depend on the laser pulse duration, their concentrations increasing during short pulses and then quickly relaxing after such pulses. This too does not correspond to the dynamics of ultraviolet radiation emission by the optical-breakdown plasma. The authors thank S.I. Yakovlenko for his stimulating comments. Figures 2; references 7.

UDC 536.36-541.12

Parameters of Air Shock Waves Generated During Transition From Combustion to Detonation

907L0028A Novosibirsk FIZIKA GORENIYA I VZRYVA in Russian Vol 25 No 5, Sep-Oct 89 18 Jan 88 pp 111-115

[Article by S.A. Gubin and V.A. Shargatov, Moscow]

[Abstract] A spherical cloud of a stoichiometric acetylene + oxygen reactant mixture is considered floating in

air, the pressures of both being initially equal. Combustion of the mixture starts at the center and spreads in the form of a spherical deflagration wave until it transforms into a spherical detonation wave, whereupon the latter propagates farther until it reaches the reactant-air boundary and an air shock wave is consequently generated outside the cloud. Assuming that chemical equilibrium prevails everywhere within the reactant cloud at any time and not being concerned with the cause of transition from combustion to detonation, also assuming that both detonation wave and shock wave have infinitesimally thick fronts, the parameters of both waves have been calculated numerically by the method of finite differences on a grid constructed according to a "cross" scheme. Calculations were made for three modes of combustion propagation: 1) with detonation occurring at the center of the reactant cloud; 2) at a constant velocity of 400 m/s until detonation occurs when the radius of the flame becomes 0.82 times the initial cloud radius; 3) at a constant velocity of 200 m/s until detonation occurs when the radius of the flame becomes 1.08 times the initial cloud radius. An analysis of the results indicates among others that the air shock wave may be much stronger when detonation occurs farther from the center. Figures 4; references 5.

UDC 539.4

Strength of Aluminum, Copper, and Steel Behind Front of Shock Wave

907L0028B Novosibirsk FIZIKA GORENIYA I VZRYVA in Russian Vol 25 No 5, Sep-Oct 89 pp 126-132

[Article by Yu.V. Batkov, V.L. Glushak, and S.A. Novikov, Moscow]

[Abstract] An experiment was performed for the purpose of determining the rheological behavior and also the shear strength of copper, AD1 commercial aluminum, AMg6 aluminum alloy, and St3 plain carbon steel in shock waves by measuring the principal normal stresses σ_x,σ_y in two orthogonal planes. These stresses were measured and recorded with Π-form gages made of 3-12 Ni-Mn manganin wire 0.05 mm in diameter or 0.2 mm wide and 0.02 mm thick ribbon with thin polymer or mica insulation. The stresses were measured through all three elastic, elastoplastic, and flow ranges. A generalized analysis of the readings in terms of spherical pressure and deviatoric stress components reveals how the dynamic yield point Y_d, the Poisson ratio, and the shear modulus of these materials, both elastic and volume velocities of sound in them, and also the degree of nonhydrostatic stress distribution characterized by the ratio $2Y_d/3$ divides gs_x depend on the principal stress σ_x. Figures 7; tables 2; references 21.

UDC 621.7.044.2

Shock-Wave Compaction of Mechanically Activated Fe-Nd-B Powder

907L0028C Novosibirsk FIZIKA GORENIYA I VZRYVA in Russian Vol 25 No 5, Sep-Oct 89 pp 148-150

[Article by V.F. Nesterenko, Ye.G. Avvakumov, S.A. Pershin, Z.A. Kormilitsyna, A.N. Lazaridi, and M.Yu. Yazvitskiy, Novosibirsk]

[Abstract] The feasibility of compacting a mechanically activated stoichiometric Fe_2B + Fe + Nd powder mixture into bulk specimens of the $Fe_{14}Nd_2B$ alloy by means of shock waves was studied experimentally by the metallographic method supplemented with calorimetric measurements and x-ray structural examination. The powder mixture was mechanically activated in an AGO-2 planetary grinder with steel drums containing steel balls. It was then compacted into 125 mm long bars 3 x 25 mm^2 in cross-section. They were chemically homogeneous with grains of 1-3 μm and 10 μm size fractions, their density and microhardness being 7.46 g/cm^3 and 280-320 HV respectively. Pressing was followed by isochronous annealing, first at low temperatures (500-600-650°C) for 10 min at each and then at high temperatures (750-800-950°C) for 60 min at each. Subsequent magnetic measurements revealed an only small increase of the coercive force to 80 Oe, owing to oxidation of the particles, and no change in the shape of the hysteresis loop The material was found to be crystalline without a peak on the crystallization curve. Relaxation processes in it evidently begin at temperatures lower than 665°C, at which they begin in amorphous-crystalline tape produced by quenching, and the compacted is correspondingly also less stable than the quenched one. Figures 4; references 8.

The Effect of Ultrasonic Treatments on the Electrical and Photoelectrical Properties of CdS_xSe_{1-x} Semiconductor Solid Solutions S_xSe_{1-x} Semiconductor Solid Solutions

907L0015A UKRAINSKIY FIZICHESKIY ZHURNAL in Russian Vol 34 No 10, Oct 89 pp 1553-1556

[Article by G. Garyagdyev, I. Ya. Gorodetskiy, B. R. Dzhumaev, N. Ye. Korsunskaya, K. Nurmukhammedov]

[Abstract] This study investigates the effect of ultrasonic treatments on the photoelectric and electric properties of CdS_xSe_{1-x} solid solutions undoped high-resistance (dark resistivity of 10^7 to 10^9) single-crystal CdS_xSe_{1-x} specimens 4 to 8 mm in length cleaved along the c axis were analyzed. Ultrasound was generated from the natural piezoelectric effect by applying an electrical RF field along the c axis to the specimen by means of indium contacts. The ultrasonic frequency corresponded to the longitudinal resonance for this specimen. The study analyzes the electrical (conductivity) and photoelectrical (spectral and temperature dependences of the photocurrent, the lux-ampere characteristics and the temperature-stimulated conductivity) properties of initial specimens and those exposed to ultrasonic treatments. Ultrasonic treatment was found to have different effects on the spectral relations, as in certain specimens it served to increase the photocurrent while in others it resulted in a decrease. Measurements of the lux-ampere characteristics revealed that at low illumination levels these curves were linear and went to saturation at high levels. The study of temperature-stimulated conductivity revealed that the change in photocurrent is accompanied by a

corresponding change in the concentration of small adhesion centers for the electrons which generally have a donor character.

Effect of Sound on the Superconducting State of Lead Films

18620164a Leningrad PISMA V ZHURNAL TEKHNICHESKOY FIZIKI in Russian Vol 14 No 24, Dec 88 pp 2249-2253

[Article by K. V. Dyakonov, Yu. V. Ilisavskiy, E. Z. Yakhkind]

[Abstract] This study reports a new approach to investigating the effect of sound on the superconducting state in lead films. Surface acoustical waves (SAW) were used to influence the superconducting state of thin lead films; due to the localization of acoustic energy in the thin surface layer this made it possible to achieve substantial acoustic intensities (10^4 W per cm^2). Two interdigital converters separated by 26 mm were used to excite and detect the SAW in YZ-cut $LiNbO_3$ SAW pulses 1.5 mcs in duration were excited at an 87 MHz resonant frequency with a repetition rate of 50 Hz. The lead film resistivities were measured by the standard four-probe technique by passing pulsed current through the film. This study drafts R(T) relations for the case of both the presence and absence of surface acoustical waves. The R(T) relations show three characteristic film resistivity ranges. Each of these ranges corresponds to a specific type of sound action on the film. In the first region the change in resistivity is due to the thermal action of the surface acoustical waves. The second and third regions can be attributed to the development of film inhomogeneities and cannot be explained within the framework of thermal action. These experiments and calculations revealed that the primary behavioral characteristics of a thin lead film in the vicinity of the superconducting transition under the influence of powerful surface acoustical waves can be attributed to the effect of mechanical stresses generated by surface waves in the film.

Semiconductor—Metal Transition in Selenium Melt Under High Pressure

907L0018A Moscow PISMA V ZHURNAL EKSPERIMENTALNOY I TEORETICHESKOY FIZIKI Vol 50 No 9, 10 Nov 89 pp 392-395

[Article by V.V. Brazhkin, R.N. Voloshin, and S.V. Popova, Institute of High-Pressure Physics, USSR Academy of Sciences]

[Abstract] Transition of molten selenium from semiconductor to metal under high pressure was studied in an experiment, the melting point for hexagonal-phase crystalline selenium having been raised by raising the pressure in a toroidal chamber which had been calibrated at room temperature against transitions of Ce, Bi, Sn. A specimen of crystalline Se, compacted into a 2-3 mm high cylinder, was heated electrically and cooled over the 300-1700-300 K temperature range at rates of 0.1-100 K/s, for electrical resistance measurement through graphite contact tabs. Heating was done with a graphite or Mo element, temperature and pressure were measured accurately within plus/minus 10 K and plus/minus 0.3 Ga respectively, pressure jumps during heating were monitored with a Pt/(Pt + 10% Rh) thermocouple having a large positive pressure coefficient of thermo-e.m.f. relative to a Chromel-Alumel thermocouple having a small negative pressure coefficient of thermo-e.m.f. On the basis of anomalies recorded during both temperature-pressure and differential thermal analyses has been constructed the (P,T) constitution diagram for selenium, with a triple point at P_T= 3.1-4.1 GPa and T_T= 880-920 K. The melting curve peaks mildly to a maximum point within 975-995 K at a pressure of 8-9 GPa. The melt is metallic with an electrical conductivity of 3-5 $kS.cm^{-1}$ under pressures above 3.1-4.1 GPa, the electrical conductivity having jumped by several orders of magnitude during melting. Transition from liquid semiconductor to liquid metal is manifested by a steep jump of electrical conductivity over an about 50 K narrow temperature range, the jump being smaller under lower pressure and under pressures below 1.2 GPa degenerating intc a smooth increase by 1-2 orders of magnitude over an about 200 K wide temperature range. The authors thank L.N. Dzhavadov and N.D. Nikolayev for assisting in temperature-pressure analys in the performance of temperature-pressure analysis and R.G. Arkhipov for discussing the results. Figures 2; references 8.

Picosecond Superluminescence in GaAs Upon Interband Absorption of Strong Short Light Pulses

907L0040C Moscow PISMA V ZHURNAL EKSPERIMENTALNOY I TEORETICHESKOY FIZIKI in Russian Vol 50 No 11, 10 Dec 89 pp 462-465

[Article by Yu.D. Kalafati and V.A. Kokin, Institute of Radio Engineering and Electronics, USSR Academy of Sciences]

[Abstract] The possibility that, upon interband absorption of strong short light pulses, recombination superluminescence in GaAs can develop and then self-quench within picoseconds is demonstrated theoretically by considering relaxation of excess carriers upon their collisions with one another and with optical phonons. These relaxation processes are shown to significantly influence the evolution of an electron-hole plasma in the semiconductor during incidence of a strong excitation pulse. Analysis of this phenomenon is based on the equations of energy balance and numerical particle balance in the plasma and on the parabolic model of band structure. The results of calculations according to this theory indicate that the superluminescence pulse can be shorter than the excitation pulse, owing to its self-quenching attributable to heating of the plasma. Both intensity and duration of the superluminescence pulse, also both temperature and concentration of the plasma in the state of optical saturation, will depend on the diameter of the light spot focused on the semiconductor. The authors thank I.L. Bronev, S.Yc. Kumekov, and V.I. Perel for stimulating and helpful discussions. Figures 2; references 7.

UDC 537.32:546

New CeM_2(M=Fe,Co)X_8(X=Al,Ga) Kondo Lattices

907L0020C Leningrad FIZIKA TVERDOGO TELA in Russian Vol 31 No 10, Oct 89 pp 297-299

[Article by M.D. Koterlin, B.S. Morokhivskiy, R.V. Lapunova, and O.M. Sichevich, Lvov State University imeni I. Franko, Lvov]

[Abstract] An experimental study of CeM_2(M=Fe,Co)X_8 (X=Al,Ga) compounds and their solid solutions was made involving the density of states and the fine structure near the Fermi level in these new materials of the rhombic crystal class with the Pbam space group Measure-ments of their electrical resistivity, thermo-e.m.f., and magnetic susceptibility were made over a temperature range from below 77 K to 400 K. They revealed that the magnetic component of electrical resistivity equal to the difference $\rho(CeM_2X_8 - \rho(LaM_2 X_8)$ has maxima at approximately 40 K for $CeCo_2Al_8$, 120 K for $CeFe_2Ga_8$, and 150 K for $CeFe_2Al_8$, but remains almost constant at a high metallic residual level of 0.240 mohm.cm for $CeCo_2Ga_8$. While the Seebeck coefficient was found to be a negative one monotonically becoming more so with rising temperature for $CeCo_2Ga_8$, to cross over from negative to positive at about 50 K and to remain so after peaking to a maximum at about 120K for $CeFe_2Ga_8$, to be a positive one peaking at about 40 K for $CeCo_2Al_8$ and at about 150 K for $CeFe_2Al_8$ and then dropping into the negative range at respectively higher temperatures. The temperature of maximum Seebeck coefficient for solid solutions such as $CeCo_2Al_{8-x}Si_x$, $CeCo_{2-x}Fe_xAl_8$, $CeFe_{2-x}Co_xAl_8$ was found to be quite sensitive to change of x and to thus depend on the composition. Magnetic susceptibility measurements revealed a deviation of only

$CeFe_2Al_8$ from the usual trivalent state of Ce. The results indicate a magnetic state of Ce in $CeCo_2Ga_{8.2}Al_8$, an intermediate valence of Ce in $CeFe_2Al_8$, and a critical state of Ce within the range of transition from intermediate valence to Kondo lattice in $CeFe_2 Ga_8$ with pronounced coherent effects in the temperature dependence of the Seebeck coefficient. Figures 3; references 5.

UDC 05.3:07

Melting and Crystallizing Dynamics of Thin Amorphous-by-Implanation Si Layers During Action of Nanosecond Laser Pulses

907L0021A Leningrad PISMA V ZHURNAL TEKHNICHESKOY FIZIKI in Russian Vol 15 No 17, 12 Sep 89 pp 13-17

[Article by S.Yu. Karpov, Yu.V. Kovalchuk, V.Ye. Myachin, Yu.V. Pogorelskiy, M.Yu. Sipova, I.A. Sokolov, and M.I. Etinberg, Institute of Engineering Physics imeni A.F. Ioffe, USSR Academy of Sciences, Leningrad]

[Abstract] An experimental study of thin amorphous Si layers was made concerning the dynamics of their melting and crystallizing during pulsed laser action, implantation 60 keV Sb^+ ions in doses of 1.6×10^{15} cm^{-2} having amorphized an approximately 50 nm thick surface layer of chemically polished crystalline Si(111) plates without melting the material underneath. Such layers were treated with a radiation beam in pulses of 20 ns duration at half-amplitude level from a Q-switched YAG:Nd^{3+} laser operating at the 530 nm wavelength in the principal TEM_{00p} mode. Their surface layer was in the process probed by a beam of 630 nm light and a beam of 1150 nm radiation from a He-Ne laser, both beams having a diameter 15 times smaller than that of the heating laser beam and both incident at a 24.5° angle. The reflection coefficient for 630 nm probing light was measured over a repetition period of a heating pulse various levels of heating energy density, the reflection coefficient for 1150 nm probing radiation then found to vary analogously with a maximum within that period. Measurements revealed also that increasing the energy density had caused the maximum reflection coefficient at the surface of an amorphous layer to increase and the reflection coefficient at the surface of the crystallized semiconductor to decrease. The results indicate that the mass of molten silicon and the duration of liquid-phase existence both change jumplike within the 0.16-0.18 J/cm^2 range of laser action, but the mass of crystallized silicon remains the same. Figures 2; references 8.

UDC 532.783:548.14

Defects in Liquid Crystals: Linear and Point Singularities in Nematics

907L0023B Moscow IZVESTIYA AKADEMII NAUK SSSR: SERIYA FIZICHESKAYA in Russian Vol 53 No 10, Oct 89 pp 1880-1903

[Article by M.V. Kurik and O.D. Lavrentovich, Institute of Physics, UkSSR Academy of Sciences]

[Abstract] Characteristics and behavior of defects in liquid crystals are analyzed theoretically, nematic crystals having been researched most extensively and not only nonpolar uniaxial ones but also the much rarer nonpolar biaxial ones as well as the hypothetical polar phase of uniaxial ones being considered. A review of ordering in nematic crystals, these crystals consisting of molecules or micelles with ellipsoidal symmetry, is followed by a review of the defect topology in them. The evolution of linear defects is described in accordance with the Volterra model of a splitting circular cylinder and eventual relaxation into an equilibrium state with either disclinations or dislocations. The evolution of point defects is described in accordance with the more elucidating hedgehog model, taking into account the theoretically predicted but not yet experimentally confirmed Volovik-Mineyev effect. The physical characteristics of disclinations are analyzed according to the simpler Franck theory rather than the more general Landau-de Gennes theory. On this basis are covered the director distribution and the energy of elastic distortions, elastic interaction and dissipative interaction dynamics with an experimentally verifiable form of the interaction potential, the effect of anisotropy of elasticity constants on the stability of planar and steric disclinations, flexoelectric effects and specifically flexopolarization, the form of disclinations and the constitution of nuclei. The physical characteristics of point defects and specifically hedgehog defects covered here include their director distribution and elasticity, interaction and dissipative dynamics. Flexopolarization is evaluated for a radial hedgehog inside a spherical liquid drop and on the surface of a flat liquid drop, also for defects of any kind on the poles of a bipolar spherical liquid drop The constitution of nuclei is also considered in the case of point defects and of special interest are high-strength point defects, the measure of their strength being the number of complete turns through a 360° angle during one passage around a closed path on the crystal surface. The relation between these characteristics of linear as well as point defects and nonuniformity of the order-parameter distribution has been established theoretically with some experimental support. Figures 11; references 49.

UDC 539.2:538.915

Experimental and Theoretical Study of Optical Properties of MgO

18620223A Tomsk IZVESTIYA VYSSHIKH UCHEBNYKH ZAVEDENIY: FIZIKA in Russian Vol 32 No 5, May 89 pp 117-120

[Article by Ye.V. Stepanova, V.S. Stepanyuk, V.N. Kolobanov, S.V. Vlasov, O.V. Farberovich, V.V. Mikhaylin, and A.A. Katsnelson, Moscow State University imeni M.V. Lomonosov]

[Abstract] An experimental and theoretical study of MgO was undertaken for the purpose of reconciling the inconsistent available data on its optical properties. The

experiment was performed with an MgO single crystal grown at the Institute of Physics, ESSR Academy of Sciences. It was placed, for measurement of its reflection spectrum, in the synchrotron channel of the electron accelerator at the Institute of Physics, USSR Academy of Sciences, operating in the quasi-storage mode with a plateau of 0.4 s duration, with 570 MeV constant-energy electrons, and with a 6 s repetition period of acceleration cycles. Measurements were made using a normal-incidence monochromator without entrance slit in a Wadsworth mount with a horizontal dispersion plane for the 40-240 nm range of the spectrum, a diffraction grating with 1200 lines/mm, and a MgF_2 filter eliminating higher orders in the longwave part of the spectrum. For calculation of the optical constants, the reflection spectrum was supplemented with data on the refractive index in the low-energy range and the E^{-4}-approximation was used in the high-energy range. The frequency-dependent imaginary part of the refractive index was calculated according to the Kramers-Kronig relation. The electronic band structure was calculated by the self-consistent linear method of attached plane waves, in the local approximation of exchange-correlation effects according to the theory of the electron concentration functional. The values obtained for total and partial charges on Mg and O atoms indicate an ionic-covalent chemical bond in the MgO compound, this compound being a dielectric with a straight band structure. All its four bands are filled with electrons, the lowest one with s-electrons of oxygen and the three above with 2p-electrons of oxygen, both the bottom of the conduction band formed by 3s-states of magnesium and the top of the valence band being located at the common Gamma point. Theoretical calculations based on the local approximation for the exchange-correlation potential underestimated the width of the forbidden band, yielding only 5.22 eV as compared with 7.8 eV on the basis of experimental data. Figures 2; tables 2; references 16: 7 Russian, 9 Western (1 in Russian translation).

Theory of Two-Phonon Resonance of Photoexcited Electrons by Acoustical Phonons in a Quantizing Magnetic Field

18620181A Leningrad FIZIKA TVERDOGO TELA in Russian Vol 31 No 2, Feb 89 pp 7-11

[Article by M. D. Blokh and L. I. Magarill]

[Abstract] This study examines oscillations in the transverse electric conductivity of photoexcited electrons associated with the emission of two acoustic phonons at low lattice temperatures. The resonant behavior of the current is analyzed accounting for electron gas heating due to both the light and the electrical field. The analysis considers a nondegenerate semiconductor with an isotropic square law of electron dispersion. The theoretical analysis suggests that when the electrical and magnetic fields are parallel light will have no dynamic effect on the resonant portion of the current in the case of two-phonon resonance and, moreover, the cyclotron-two-phonon resonance effect is absent. The light begins to have an effect when the fields are perpendicular, which is manifested as the polarization dependence of these phenomena of photoexcited electrons. The dynamic effect of light on magnetic-two-resonance is also found to reduce the probability of electron-two-phonon interaction. The study emphasizes that these conclusions are valid for the case where light has no effect on the free electron concentration, which is a valid assumption at low crystal temperatures.

Application of Microsecond Laser Radiation to Deposition of Diamond-Like Carbon Films

18620164B Leningrad PISMA V ZHURNAL TEKHNICHESKOY FIZIKI in Russian Vol 14 No 24, Dec 88, pp 2257-2259

[Article by Yu. A. Bykovskiy, V. p Kozlenkov, I. N. Nikolaev, Ye. V. Charyshkin]

[Abstract] This study examines the application of microsecond laser radiation to the deposition of carbon films. A continuously pumped, periodically Q-switched YAG laser with a pulse duration 0.2 mcs was employed. At this laser pulse duration rapid vaporization of the carbon target was achieved near the vapor ionization threshold, making it possible to avoid the production of high-energy particles. The laser radiation surface flux density was 3×10^7 W per cm^2. Electron microscope analysis revealed that the deposited films had an amorphous homogeneous structure without any crystalline inclusions of greater than 10 angstroms in size. At room temperature the resistivity of samples .05 mcm in thickness was 1×10^9 ohms per cm. The authors also compared the properties of the aluminum-like films obtained using this technique to the properties of films deposited by ion beams. The laser films had a lower resistivity value, yet had a broader bandgap, transmission factor and composition homogeneity.

UDC 532.132

Critical Parameters of Superfluid Flow Through Narrow Channels

907L0091A Kharkov FIZIKA NIZKIKH TEMPERATUR in Russian Vol 15 No 11, Nov 89 pp 1123-1127

[Article by L.V. Kiknadze and Yu.G. Mamaladze, Institute of Physics, GSSR Academy of Sciences, Tbilisi]

[Abstract] The minimum width of a channel through which liquid helium can still flow in the superfluid state is determined in accordance with the Ginzburg-Pityakovskiy phenomenological Ψ theory, taking into consideration two different meanings of critical velocity as well as the shape of a channel. Analysis of this problem is based on the dimensionless second-order fifth-degree partial differential equation $d^2f/dx^2 + f(1-M)f^3-Mf^5 = v^2f$, f denoting the modulus of the wave function. It is applied to a cylindrical channel with circular cross-section with boundary conditions of $f = 0$ at its axis and periphery. This equation is solved by the "valid in-the-mean" method, with addition of the $(\pi/d)^2)f$ term to both sides (dnormalized diameter of channel). The solution yields not only the minimum diameter but also both critical diameter and velocity corresponding to transition from thermodynamically unstable to thermodynamically stable flow according to Ginzburg-Sobyanin and according to Kiknadze-Mamaladze. The equation has been solved numerically for several values of parameter M (9/7, 2, 3, 4.5, 7, 17) characterizing the relative weight of nonlinear f-terms in that fifth-degree equation. Tables 1; references 21.

UDC 538.945

Coulomb Mechanism of High-Temperature Superconductivity in Conducting Systems of Low Dimensionality

907L0091B Kharkov FIZIKA NIZKIKH TEMPERATUR in Russian Vol 15 No 11, Nov 89 pp 1204-1206

[Article by Yu.p Monarkha, Institute of Low-Temperature Engineering Physics, UkSSR Academy of Sciences, Kharkov]

[Abstract] A one-dimensional conducting system with a Fermi energy much lower than the electron-electron interaction energy in a plane perpendicular to the conduction channel but of the same order of magnitude as or higher than the mean Coulomb energy is considered, a new liquid state of a "quantum electronic chain" being predicted where the coherence length is much larger than the mean distance between electrons. The prediction is based on the model of infinitesimally weak attraction across an infinitely large radius and thus reduced to the Bardeen-Cooper-Schrieffer theory, except that pairing of electrons in this configuration occurs over the entire range of k rather than only within a narrow range near k_F. Inasmuch as two electron cannot interchange places when the interaction energy is so high, their noncoherent motion brings about a local departure from electroneutrality and a pure Coulomb attraction. The energy gap then corresponds to the energy an electron must receive in order to be able to move independently of its nearest neighbors in the chain. References 1.

UDC 538.945

Alternating-Current Josephson Effect in $Tl_2Ca_2Ba_2cu_3O_{10+x}$ Ceramic

907L0091C Kharkov FIZIKA NIZKIKH TEMPERATUR in Russian Vol 15 No 11, Nov 89 pp 1213-1215

[Article by B.A. Aminov, A.I. Akimov, N.B. Brandt, Nguen Min Thu, M.V. Sudakova, Yu.A. Pirogov, and Ya.G. Ponomarev, Moscow State University imeni M.V. Lomonosov]

[Abstract] An experimental study of $Tl_2Ca_2Ba_2Cu_3O_{10+x}$ ceramic was made concerning the effect of an external microwave field on the current-voltage characteristics of Josephson microbreak junctions in this high-temperature superconductor material with a critical transition temperature of 106-108 K. Square bars 3 mm long and 0.8 mm thick were glued with epoxy cement to a glass-fiber plate, with a set of 0.1 mm thick copper-foil current and potential electrodes soldered to each end. After polymerization of the epoxy cement, each bar was ground down to 0.1 mm thickness and a 0.1-0.2 mm wide slot was cut with leather cloth across the center leaving 0.1-0.2 mm wide bridge. The plate was mounted on a brass spring so deflection of the latter by a micrometer screw caused the plate to bend. After a microcrack had been produced in each bridge by bending of the plate, the current-voltage characteristics of Josephson junctions across them was measured at temperatures covering the 4.2-104 K range, first without and then in a microwave field at 52-75 GHz frequencies. In the latter case there appeared a series of Shapiro on the I-V curves and in some also subharmonic steps, the latter indicating departure from a sinusoidal phase-current characteristic. The height of all steps was found to decrease with rising temperature, the height of subharmonic steps faster than that of Shapiro steps. The charge of superconducting electrons, based on the width of Shapiro steps, was found to be (1.95-2.05)e. The effective bridge diamater, determining the weak link across the microcrack and determined from the dependence of the critical supercurrent on the magnetic field in the plane of the microcrack, was found to be 10-20 μm and thus comparable with the size of superconducting grains. The critical supercurrent I_c was found to decrease with rising temperature according to the (3/2)-power law from maximum at 4.2 K to zero at the critical superconducting transition temperature, the product I_cR_N (R_N denoting normal-state resistance) spreading over the 1-10 mV range. The authors thank K.K. Likharev for extremely helpful discussions. Figures 3; references 6.

Supercooling of Superfluid He-4 During Crystallization

18620239A Moscow PISMA V ZHURNAL EKSPERIMENTALNOY I TEORETICHESKOY FIZIKI in Russian Vol 50 No 2, 25 Jul 89 pp 87-89

[Article by V. L. Tsymbalenko, Institute of Atomic Energy imeni I. V. Kurchatov]

[Abstract] The theoretically predicted appearance of a tunneling supercritical seed during crystallization of helium at temperatures close to absolute zero has been confirmed in an experiment with liquid helium at temperatures up to 1.75 K. Metastable liquid He-4 was produced by monotonic cooling of a helium container made of stainless steel inside a vacuum jacket with a He-3 bath, a resistance thermometer mounted on a copper bar across the container measuring the temperature accurately within 0.005 K and deflection of one of the 0.55 mm thick container walls indicating the pressure inside accurately within 2 multiplied 10^{-4} atm. The experiment and the data processing were aided by an IBM PC and a CAMAC crate. With the temperature of the He-3 bath set at approximately 0.020 K below the He-4 crystallization point, the container was heated to approximately 0.020 K above that point. With the heater then turned off, the container was subsequently cooled at a rate of 0.0001-0.001 K/s till a crystal seed, after reaching its critical dimension, began to grow rapidly with an accompanying pressure fall in the container. This cycle was repeated several times. Based on an analysis of the data relating the magnitude of a pressure fall to the difference between chemical potentials of liquid helium at different temperatures with correction for the heat of crystallization and relating the number of pressure falls per unit time at a given temperature to the probability of a seed reaching the critical dimension, the rate of seed growth decreases with decreasing temperature. Evidently, therefore, a critical seed of He-4 crystal is formed within the 1.75-1.25 K temperature range by the classical mechanism of thermal activation. The author thanks S. N. Burmistrov, L. B. Lubovskiy, Yu. M. Kagan, and L. A. Maksimov for helpful discussions, Ye. p Krasnoperov, and N. A. Chernoplekov for support and interest. Figures 3; references 7: 6 Russian, 1 Western.

UDC 621.373.826.038.823

Emisssion of High-Intensity 222 nm Radiation by Ne(He)-Kr-HCl Gas Mixture Upon Pumping by Self-Sustained Discharge

907L0073B Moscow KVANTOVAYA ELEKTRONIKA in Russian Vol 16 No 12, Dec 89 pp 2409-2412

[Article by A.N. Panchenko, V.F. Tarasenko, and Ye.V. Bukatyy, Institute of High-Current Electronics, Siberian Department, USSR Academy of Sciences, Tomsk]

[Abstract] An experimental study of two KrCl-lasers with pumping by self-sustained transverse discharge and ultraviolet preionization was made, for a determination of their emission power and efficiency at the 222 nm wavelength on the pump power and the preionization intensity as well as on the length of the active-medium cell. The active medium in both lasers was a Kr-HCl mixture with Ne or He as buffer gas. In the 60 cm long LIDA-KT laser the interelectrode gap was 3.6 cm wide and the discharge column was 1.5 cm wide. In the 20 cm long LIDAN laser the interelectrode gap was 1.6 wide and the discharge column was 0.4 cm wide. The pumping power was varied by varying the excitation voltage and, in the LIDAN laser, also by varying both storing and peaking capacitances. The cavity of each laser was formed by plane highreflectance mirror with aluminum coating and a plane-parallel quartz plate. Preionization in the LIDAN laser by bulk discharge was aided by brightening discharges across 20 spark gaps. The emission pulse energy was measured with an IMO-2N calorimeter and the pulse shape was monitored through an FEK-22 SPU photodiode on the screen of a 6LOR-04 oscillograph. An approximately 0.5% maximum efficiency of the LIDA-KT laser was attained with neon as buffer gas and the discharge voltage lowered to the minimum necessary for operation of the spark dischargers, the pump power then being about 1.5 MW/cm^2 and the V_0/Nd ratio (V_0breakdown voltage for the active space, d-width of interelectrode gap, N-particle concentration in active mixture) being approximately 10^{-16} V.cm^2. With helium instead of neon the emission energy was two orders of magnitude lower, even though the pump power was the same. An analysis of chemical an d physical processes in these lasers indicates that ion-ion recombination is the main channel for formation of KrCl* molecules. Figures 3; references 12.

UDC 621.373.826.038.825.4

Charge-Carrier Concentration Autowaves in $PbS_{1-x}Se_x$ Injection Lasers

907L0073C Moscow KVANTOVAYA ELEKTRONIKA in Russian Vol 16 No 12, Dec 89 pp 2426-2432

[Article by M.S. Murashov and A.p Shotov, Institute of Physics imeni pN. Lebedev, USSR Academy of Sciences, Moscow

[Abstract] An experimental study of the emission channels in $PbS_{1-x}Se_x$ injection lasers with diffused p-n junctions was made, a p-n junctions having been embedded in such a laser about 30 μm deep by diffusion annealing of an n-$PbS_{0.63}Se_{0.37}$ wafer with an $n_e = 5.10^{18}$ cm^{-3} concentration of free electrons in a sealed vial containing excess selenium and $Pb_{0.49}Se_{0.51}$. The cavity was almost 400 μm long and its width was varied over the 30-1200 μm range. The distance between contact tabs varied from 130 μm to 470 μm. Spalling on four sides completed the fabrication process. The laser diodes were pumped with pulses of up to 1 μs duration at a repetition rate of approximately 170 Hz, their emission spectra under these conditions being measured at temperatures covering the 4.2-77 K range. An analysis of the spectra, characterized by a dominant and several side modes, indicates that free-carrier concentration autowaves appear in such structures, the distance between the contact tabs determining their frequency and the latter in structures such as these experimental ones ranging up to 10 MHz. The authors thank G.A. Krasilnikova and Ye.G. Chizhevskiy for preparing the laser diodes. Figures 6; references 7.

UDC 621.373.826.038.824

Phase Modulation of Femtosecond Pulses in Dye Laser With Passive Mode Locking

907L0073D Moscow KVANTOVAYA ELEKTRONIKA in Russian Vol 16 No 12, Dec 89 pp 2486-2489

[Article by D.p Krindach and V.I. Novoderezhkin, Moscow State University imeni M.V. Lomonosov]

[Abstract] An experimental study of dye lasers with passive mode locking and intracavity pulse compression was made, of concern being the inevitable phase modulation of ultrashort light pulses generated by such lasers and the resulting chirp The latter has been shown to be made up of three components contributed respectively by gain saturation, the Kerr effect, and absorption in the dye solution. As the energy density per pulse increases from low levels, the chirp increment first increases proportionally to the energy density squared and then decreases fast owing to strong saturation so that the Kerr effect becomes the dominant contributor to a positive chirp The experiment was performed with ethanol solutions of rhodamine 6G or rhodamine 110 as amplifiers and solutions of various triphenylmethane dyes (methyl violet, malachite green, crystal violet, dahlia violet, basic fuchsin) as absorbers. The widths of amplifier and absorber jets were 400 μm and 200 μm respectively. The laser dyes were pumped by a continuous-wave Ar^+-laser with a power up to 6 W for all emission lines. The optical scheme included five spherical mirrors, three of them having 5 cm, 10 cm, 7.5 cm radii respectively and two of them having both either 5 cm or 2.5 cm radii. Two quartz prisms 29-30 cm apart were included for chirp suppression. The exit mirror had a T= 0.02 transmission

coefficient. Pulse duration was measured by the autocorrelation method with noncollinear second-harmonic generation, assuming a $sech^2$ envelope. With the rhodamine-110 and basic fuchsin combination (self-tuning to 565 nm wavelength) were recorded a 61 fs pulse duration on the basis of 95 fs half-width of the autocorrelation function, without any overlapping of pulses in the absorber. Figures 3; tables 1; references 5.

UDC 621.373.826

Quantum Compressed States in Optical Solitons

907L0073E Moscow KVANTOVAYA ELEKTRONIKA in Russian Vol 16 No 12, Dec 89 pp 2570-2572

[Article by A.V. Belinskiy and A.S. Chirkin, Moscow State University imeni M.V. Lomonosov]

[Abstract] A quantum theory is constructed to describe propagation of optical solitons through fibers and to establish the conditions under which they can exist in quantum compressed states. The theory is based on the continuous-integral form of the nonlinear Schroedinger equation and thus avoids use of the perturbation method. Propagation of an optical soliton through a fiber is accordingly described by the equation for slowly varying operators of positive and negative frequency-dependent parts the electric field in a traveling system of coordinates. The solution to this equation, after the latter has been normalized to dimensionless one, is retained in the form of a doubly-infinite integral. An analysis of this solution for a coherent soliton entering a fiber at $\zeta = z/L_d = 0$ (z-longitudinal space coordinate, L_d-group velocity dispersion length) in the $<\psi(\tau)> = e^{<j\varphi>}sech\tau$ form (φ-arbitrary constant phase, $\tau = t/T_0$, t-time coordinate, T_0-pulse duration) reveals that quantum fluctuations of its one quadrature component can be suppressed and high compression of quantum fluctuations thus is attainable. The authors thank S.A. Akhman and V.A. Vysloukh for helpful discussions. Figures 1; references 11.

UDC 621.373.826.038.823:537.874.7

Collisionless Laser Excitation of Vibrational Molecular Transitions With Intricate Structure of Rotational Spectrum

907L0072A Tomsk OPTIKA ATMOSFERY in Russian Vol 2 No 12, Dec 89 pp 1265-1272

[Article by S.V. Ivanov and V.Ya. Panchenko, Scientific Research Center for Technological Lasers, USSR Academy of Sciences, Tomsk]

[Abstract] Collisionless pulsed laser excitation of vibrational transitions with intricate structure of the rotational spectrum is analyzed on the basis of the Schroedinger equation for probability amplitudes and by statistically describing the vibrational-rotational spectra of air molecules of the asymmetric-top type. First is considered interaction of an infrared radiation pulse and an individual vibrational-rotational transition, assuming that the electric field of the infrared carrier wave whose intensity is a composite function of time $E(t) = \varepsilon f(t)\cos\omega t$ and that the spectral width of the pulse envelope is much smaller than the carrier frequency ω. The solution to the system of two equations for the probability amplitude pertaining to a nondegenerate two-level system then depends largely on the form of function f(t), f(t) oscillating in time upon a "fast" turn-on of the population field and f(t) remaining almost constant upon a "slow" turn-on. The analysis proceeds by consideration of real vibrational-rotational levels in molecules, these levels in the absence of an external magnetic field being (2J + 1)-fold degenerate with respect to the magnetic quantum number M. The probability of excitation of a vibrational transition divides $0 >$ - divides $1 >$ is then calculated as the sum of the probabilities of all vibrational-rotational transitions occurring within spectrum of incident radiation. The necessary integration is performed for the two extreme cases of "narrow" and "wide" dipole moment probability density distributions corresponding to weak and strong radiation fields respectively. The probability of excitation of vibrational transitions is found to depend differently on the intensity of incident radiation in a weak field and in a strong field and altogether differently in the intermediate case. Theoretical estimates are made on the basis of this analysis for ozone molecules and radiation of a CO_2-laser, the results indicating that collisionless excitation of vibrational transitions by infrared radiation pulses of longer than 10-100 ps is less efficient than when collisions upon radiation absorption take place. Figures 4; references 15.

UDC 535.317.2:535.393

Multipass Matrix Systems: Most Promising Systems for High-Resolution Long-Path Spectroscopy

907L0072B Tomsk OPTIKA ATMOSFERY in Russian Vol 2 No 12, Dec 89 pp 1310-1318

[Article by S.M. Chernin and Ye.G. Barsakay, Institute of Chemical Physics imeni N.N. Semenov, USSR Academy of Sciences, Moscow]

[Abstract] The authors have developed two new types of optical systems with multiple reflections for high-resolution laser spectroscopy, the most promising of them being use of a multipass matrix systems. The maximum number possible number of successive very stable reflections resulting in a compact rectangular matrix of images is attainable here with a limited number of mirrors. In the first variant a pair of spherical objective mirrors is rigidly and symmetrically fastened to a movable compound bracket at an angle to one another which makes the distance between their centers of curvature equal to half the horizontal space period on the image matrix, the bracket being rotatable on a vertical shaft between the mirrors and on a horizontal shaft under them. A square convex spherical field mirror mounted on a vertical disk faces both objective mirrors

symmetrically so that it reflects each onto the other. Adjacent to it on the same disk is mounted an auxiliary field mirror, a narrow convex strip not as high as the main field mirror so as to clear two round holes one above the other in the disk for letting a light beam in and out. This auxiliary field mirror reflects the objective mirror it faces back onto an auxiliary objective mirror mounted on the same bracket near nearby. In the second variant there are four identical square convex spherical objective mirrors mounted in a row on a panel rotatable about its horizontal axis and held in a bracket rotatable about its vertical axis. Both variants are designed to provide a long path for the light beam. The mechanism for regulating the number of passes is simpler in the second variant and thus ensures higher reliability as well as higher precision. Both variants were tested with a He-Ne laser, no distortions of images on the field matrices having been recorded after 306 passes of the light beam through the system. Both were also used with a spectrometer consisting of a semiconductor laser and a multipass matrix tray, vibrational-rotational absorption lines of SO_2 (30 ppm in a humid air under a pressure of 30 torr) having been recorded after 90 passes of the light beam through the system. Figures 4; references 16.

UDC 621.373.826.038.823

Frequency-Stabilized Dye Laser With Automatic Precise Wavelength Tuning for High-Precision Spectroscopy

907L0072C Tomsk OPTIKA ATMOSFERY in Russian Vol 2 No 12, Dec 89 pp 1319-1324

[Article by B.V. Bondarev, A.V. Karablev, S.M. Kobtsev, and V.M. Lunin, Novosibirsk State University imeni Lenin Komsomol]

[Abstract] A continuous-wave single-frequency dye laser with stable linear frequency tuning for high-resolution spectroscopy has been built which includes three frequency selectors: 1) a triple birefringent filter, 2) a 0.5 mm thick Fabry-Perot quartz etalon with a 10 cm base and an R = 0.4 reflection coefficient, 3) a radiation-absorbing aluminum film with a T = 0.7 transmission coefficient for traveling waves. The etalon is tuned by means of a special electromechanical drive. The aluminum film on a quartz substrate and the exit mirror are mounted on opposite sides of the same monoblock consisting of a PP-4 piezoceramic tiles cell held by adhesive bonding between two quartz disks with center holes. The aluminum film has no protective coating, inasmuch as it can perform without it for at least one year. The electronic laser controls include not only automatic tuning of the selector film to the node of the extracted radiation mode and automatic frequency trimming to a Fabry-Perot reference interferometer but also control of the etalon drive and four high-voltage amplifiers which excite four piezoceramic cells, one for controlling the base of the selective mirror and a stack of three for controlling the position of the collimating cavity mirror. The reference interferometer is a scanning confocal one with a 1.5 GHz dispersion range and a definition index of 3. Its controls consist of a thermostat and a capacitive transducer with a high-voltage amplifier. With rhodamine 6G as the active medium pumped by an Ar^+-laser with linearly polarized radiation at all its wavelengths with a total power of 3 W, this dye laser delivers up to 50 mW radiation power tunable over a 15 GHz range, the line width not exceeding 3 MHz over a period of 1 s with a drift rate not exceeding 60 MHz/h and with not more than 0.1% nonlinearity. Figures 3; references 14.

UDC 621.373.826.038.823

Thulium-Vapor Laser

907L0067A Moscow KVANTOVAYA ELEKTRONIKA in Russian Vol 16 No 12, Dec 89 pp 2387-2393

[Article by V.A. Gerasimov and B.p Yunzhakov, Institute of Atmospheric Optics, Siberian Department, USSR Academy of Sciences, Tomsk]

[Abstract] An experimental study of the Tm-vapor laser was made, for a determination of its spectral and energy characteristics. Metallic thulium was placed between two electrodes in gas-discharge tubes 15 mm in diameter with external heating, made of beryllia with a 150 mm long active space and of alundum with a 400 mm long active space. Either helium or neon were used as buffer gas. Excitation was provided by a TGI1-25—/50 hydrogen-filled thyratron with a 3,7 nF peaking capacitor along the 10 nF storing capacitor charged to 40 kV. Recording and measuring instruments included an MDR-23 monochromator with 1200 lines/mm and 600 lines/mm gratings, a set of FEU-83 optical radiation detectors, a Ge avalanche photodiode, and a programmable S7-17 two-channel stroboscopic oscillograph. The laser was tested at temperatures covering the 800-1250°C range, corresponding to the 0.004-6 mm Hg range of thulium vapor pressure as the helium pressure was varied over the 0.5-10 mm Hg range. In addition to the eight already known emission lines (589.95, 1101.11, 1310.06, 1338.01, 1433.97, 1448.51, 1637.9, 1958.4 nm) were also recorded two emission lines 1304.32 nm and 1499.51 nm near the two lines (130.4.0 nm and 1500.0 nm) corresponding to transitions already earlier detected but not identified as well as three new emission lines: 1069.39 nm 1453.04 nm, 1495.78 nm. All the recorded transitions within the infrared range of the spectrum occur between the two lowest even configurations ($4f^{12}6s^26p$, $4f^{13}5d6s$) and the two lowest odd configurations ($4f^{13}6s6p$, $4f^{12}5d6s^2$). A characteristic feature of all the infrared emission lines (not the 589.95 nm line) is that their upper laser levels are of the same parity as the ground state of a Tm atom, which precludes effective pumping of those levels by electron impact from the ground state. Rather, population inversion at these laser transitions in a Tm atom are evidently produced by excitation transfer from nearby resonance levels to upper laser levels. All transitions within the infrared range of the laser emission spectrum fall into three groups. The

first group comprises those (1069.39, 1101.11, 1304.06, 1448.51 nm) of emission with a pulse form independent of the Tm-vapor pressure, but these lines successively vanishing as the He pressure is lowered and only the last two ones remaining under a He pressure of 0.75 mm Hg. The second group com-prises those (1495.78, 1499.51, 1637.90 nm) which appear as the He pressure is lowered from 3.5 mm Hg with the pulse duration becoming longer as the temperature is raised from 1000°C to 1250°C. The third group comprises those (1338.01, 1433.97, 1453.04 nm) which have the characteristics of both other groups. The energy characteristics were measured with the laser in the self-heating mode with a 1 kHz repetition rate of pumping pulses. An average emission power of 520 mW was attained with 22 kV across a 1.65 nF storing capacitor before discharge, which corresponded to a specific energy output of 20 $\mu J/cm^3$ with 4 $\mu J/cm^3$ of 589.95 nm radiation and 16 $\mu J/cm^3$ of all infrared radiation. The authors thank V.M. Klimkin and V.Ye. Prokopyev for helpful discussion. Figures 6; references 16.

UDC 621.373.826.038.825.2

ZrO_2-Y_2O_3: Er^{3+} 3 m Laser

907L0067B Moscow KVANTOVAYA ELEKTRONIKA in Russian Vol 16 No 12, Dec 89 pp 2421-2423

[Article by V.I. Aleksandrov, M.A. Vishnyakova, V.p Voytsitskiy, Ye.Ye. Lomonova, M.A. Noginov, V.V. Osiko, V.A. Smirnov, A.F. Umyskov, and I.A. Shcherbakov, Institute of General Physics, USSR Academy of Sciences, Moscow]

[Abstract] Emission of 2.693-2.697 mm radiation was obtained from a ZrO_2-Y_2O_3: Er^{3+} crystal 3 mm in diameter and 55 mm long with a 2.5 x 10^{21} cm^{-3} concentration of Er^{3+} ions. The 15 cm long cavity was formed by a spherical high-reflectance mirror and a plane exit mirror. The crystal, in an elliptical silver-plated quartz monoblock, was optically pumped by 300 µs flashes from an INP-3/45 lamp The lamp was triggered by pulses from discharge circuit having a 200 µF capacitance and 50 µH inductance, for continuous-wave operation of the laser. For periodically-pulsed operation of the laser, the lamp was pumped by an LTIPCh laser. Pulse repetition rates up to 100 Hz were attained, the emission threshold for a 12.5 Hz pulse repetition rate being 3.5 J with a dielectric plane exit mirror and 5 J with a 90%-reflectance mirror. The laser crystal was cooled with a 0.1 wt.% $K_2Cr_2O_7$ solution in distilled water. Figures 2; references 1.

UDC 621.373.826

Feasibility of Light Pulse Compression by Stimulated Brillouin Scattering in Plasma

907L0067C Moscow KVANTOVAYA ELEKTRONIKA in Russian Vol 16 No 12, Dec 89 pp 2457-2460

[Article by A.A. Andreyev and A.N. Sutyagin]

[Abstract] The feasibility of compressing a high-intensity light pulse by stimulated Brillouin-Mandelshtam scattering in a plasma is demonstrated theoretically, following an analysis of nonsteady such scattering. First the process of stimulated Brillouin-Mandelshtam backscattering is described by a system of three coupled wave equations in the quasi-optical approximation for the complex amplitudes of pump wave, the sound wave, and a Stokes component of the scattered field, with heating of the plasma and longitudinal nonhomogeneity of light waves due to focusing taken into account. Next is considered amplification of a Stokes pulse from the thermal noise level, assuming a square pumping pulse and negligible plasma heating. The resulting expressions for logarithmic gain, obtained after Laplace transformation of that system of equations, is evaluated successively in quasi-steady, nonsteady, and ultranonsteady approximations, with subsequent correction for light absorption and plasma heating. Compression of a light pulse in the process of stimulated Brillouin-Mandelshtam scattering is found to require matching the duration of the pump pulse with its path length in the medium (from entry point to center of caustic surface, far behind the focus) and that the threshold scattering increment be exceeded. Minimizing the effect of plasma heating, which decreases the scattering increment, requires that the the time necessary for the plasma temperature rise to become equal to 5% of the electron temperature be longer than the duration of the pump pulse. The conditions ensuring smallness of two corrections to the increment of nonsteady scattering due to plasma heating, namely correction for sweeping and correction for detuning of the sound, are established in the form of inequalities. With the relation between the characteristic times stipulated accordingly, these conditions yield the dependence of laser emission and plasma parameters on the variable system design parameters. References 12.

UDC 621.375.826:535.544:66.085.3

Optical Breakdown of LiF Crystals Containing Radiative Color Centers

907L0067D Moscow KVANTOVAYA ELEKTRONIKA in Russian Vol 16 No 12, Dec 89 pp 2520-2523

[Article by O.M. Yefimov, A.M. Mekryukov, and V.M. Reyterov]

[Abstract] An experimental study of LiF crystals containing radiative color centers was made, for a determination of their resistance to optical radiation under simulated real conditions. Single crystals in the form of 30 mm thick slabs were grown under vacuum by the Stockbarger method. They were first treated with a 200 MR dose of γ-radiation from a ^{60}Cosource at a 0°C temperature, the radiation power not exceeding 600 R/s. They were then treated with light from a single-frequency (phosphate glass):Nd laser in pulses of 30 ns duration, with the laser radiation concentrated by a long-focus (1.6 m) lens within spots 0.47 mm or 0.02 mm

in diameter inside a crystal and the power of incident radiation being varied by means of light filters. The energy of incident radiation was measured with an acoustooptical calorimeter. A spark as well as scattering of radiation from a probing He-Ne laser served as indicators of fracture. For a correct comparison of breakdown thresholds in pure crystals and in crystals colored by γ-radiation, either one specimen was cut out from a pure single crystal for measurements before and after exposure to γ-radiation or two specimens were cut out from contiguous regions of a single crystal, one of them being then colored by γ-radiation treatments and the other remaining pure for breakdown tests. A statistical analysis of the data reveals a linear dependence of the probability of optical breakdown on the power density of incident laser radiation, this probability being slightly lower for γ-treated LiF crystals when the laser radiation is mildly focused (0.47 mm spot) but much lower when the laser radiation is sharply focused (0.02 mm spot). Figures 2; references 9.

UDC539.184.2+621.373.535

High-Resolution Laser Spectroscopy in Atomic GdI Beam

907L0046A Leningrad OPTIKA I SPEKTROSKOPIYA in Russian Vol 67 No 4, Oct-Dec 89 pp 779-784

[Article by Yu.p Gangrskiy, S.G. Zemlyanoy, B.K. Kuldzhanov, K.p Marionova, B.N. Markov, Hoang Thi Kim Hue, and Chang Kuong Tam]

[Abstract] Precision measurements of the hyperfine split and the isotopic shift were made by the method of laser resonance fluorescence in an atomic beam on 15 lines of GdI within the spectral range of a tunable rhodamine 6G laser, for information about the excitation levels of even Z^9F and z^9F terms of all stable Gd isotopes. The new data on the hyperfine split have been evaluated for the upper level, on the basis of a theoretical expression for the location of the component with the total momentum F relative to the center of gravity of the hyperfine structure in the approximation of negligible higher-order effects and with the aid available accurate data on the hyperfine structure of the lower level. The new data on the isotopic shift reveal its dependence on the total momentum J of the electron shell and a significant second-order crisscross effect, this shift consisting of a mass shift and a field shift which are each approximately equal for all levels of a given pure configuration but in the case of several rare-earth elements quite different for different terms or even for different levels in one term. The authors thank G.N. Flerov and Yu.Ts. Oganesyan for support and I. Pachev for helpful discussions. Figures 2; tables 3; references 15.

Raising Heterojunction-Laser Efficiency by Multiple Self-Absorption of Spontaneous Radiation

907L0043A Leningrad PISMA V ZHURNAL TEKHNICHESKOY FIZIKI in Russian Vol 15 No 23, 12 Dec 89 pp 18-22

[Article by pV. Adamson, Institute of Physics, ESSR Academy of Sciences, Tartu]

[Abstract] Lowering the excitation threshold and raising the efficiency of heterojunction lasers with the aid of multiple spontaneous self-absorption of radiation is considered, spontaneous self-absorption being technically feasible in a perfect heterostructure upon attainment of a nearly 100% quantum yield of internal luminescence. Theoretical calculations based on a given cavity loss factor and by the maximum laser efficiency being determined by the work function as well as on the parameter $p = R_s j_t/V$ (R_s-series resistance of diode per unit surface area, j_t-threshold current density, V-voltage across p-n junction) confirm the theoretical possibility of a high-efficiency heterojunction laser with multiple self-absorption, a pair of heterojunctions, after the common substrate has been removed and the interlayer has been replaced with a high-reflectance ohmic contact directly under each emitter. Owing to reradiation, the threshold current density will thus be lowered by a factor n equal to the ratio of radiative losses in the laser without and with reflective coatings respectively. Numerical calculations made for a GaAs heterojunction pair with intrinsic active regions at room temperature indicate that sufficiently thin active regions are required for avoidance of the amplification band and sufficiently reflective coatings are required attainment of high efficiency. The feasibility of high efficiency is thus limited, owing to the impossibility of producing such coatings by the conventional brazing method. Figures 1; references 12.

UDC 621.373.826.038.823

High-Pressure He-Cd Laser Pumped by Nanosecond Electror Beam

907L0032A Moscow KVANTOVAYA ELEKTRONIKA in Russian Vol 16 No 10, Oct 89 pp 2039-2046

[Article by F.G. Goryunov, V.I. Derzhiyev, A.G. Zhidkov, A.V. Karelin, D.Yu. Nagornyy, V.S. Skakun, V.F. Tarasenko, A.V. Fedenev, and S.I. Yakovlenko, Institute of General Physics, USSR Academy of Sciences, Moscow, and Institute of High-Current Electronics, Siberian Department, USSR Academy of Sciences, Tomsk]

[Abstract] An atmospheric-pressure He-Cd laser with a dense active medium in a cavity between dielectric mirrors lasing at not only 537 nm and 534 nm but also 442 nm and 325 nm wavelengths was built, with pumping by an electron beam 1.5 cm in diameter in pulses of approximately 10 ns duration. A pulsed magnetic field was used for turning and focusing the electron

beam, its current density being approximately 100 A/cm^2. The 40 cm long middle part of the 80 cm long laser cell was heated. Pure helium and He-Ar, He-Xe, He-N_2 mixtures were used as buffer gas, its pressure being varied over the 0.8-1.4 atm range. With the aid of appropriate light filters and a photodiode detector as well as an S8-12 oscillo-graph and an ISP-30 spectrograph were determined the temperature ranges for emission at each of the four wavelength and the pressure dependence of the emission power as well as of the pulse duration in each case. The results indicate that the temperature range for emission of green light (537 nm and 534 nm) is 360-530°C with maximum intensity within 450-490°C and the temperature range for emission of blue light (442 nm) is 330-450°C with maximum intensity within 360-380°C, the two green lines and the blue line thus appearing together within the 360-450°C range but green light becoming dominant above 400°C, while the temperature range for emission of ultraviolet light (325 nm, Cd-II) is 360-440°C but its intensity is an order of magnitude lower than that of the blue light. Addition of Ar, Xe, or N_2 was found to weaken the emission of green light and to cut off both blue and ultraviolet light. While the emission power of green light was maximum under a pressure of approximately 1 atm, its pulse duration being almost independent of pressure, the emission power of blue light increased monotonically and its pulse duration decreased monotonically with increasing pressure to respectively a maximum and a minimum under 1.4 atm. The emission power was found to depend strongly on the reflection coefficient of the exit mirror, with the reflection coefficient of the front mirror near unity. A reflection coefficient of 0.50-0.60 was optimum for green light and blue light in terms of maximum emission power, a reflection coefficient of 0.75-0.80 was optimum for ultraviolet light. The results are compared with theoretical calculations on the basis of a model which includes 42 plasmo-chemical reactions in a He-Cd mixture, 18 of them involving only He and 11 of them involving only Cd (13 of them involving both). Calculations are based on the PLA-ZER-1 computer program package covering the nonsteady kinetics in the "zero-dimensional" approximation. They yield a maximum efficiency of 0.8% and a maximum power of 100 W for the ultraviolet laser with respectively a 0.85 and a 0.75 reflection coefficient of the exit mirror, the pulse duration becoming shorter and the efficiency thus becoming lower as the reflection coefficient is decreased, while the experiment yielded a maximum power of 10 W only. A maximum power of 6 kW per liter was reached with the active medium as green laser, the highest power being attainable with the active medium as blue laser. Figures 6; tables 1; references 18.

UDC 621.373.826:612.054.44

Effect of Infrared Radiation on Cornea

907L0032B Moscow KVANTOVAYA ELEKTRONIKA in Russian Vol 16 No 10, Oct 89 pp 2136-2140

[Article by A.S. Podoltsev and G.I. Zheltov, Institute of Physics, BSSR Academy of Sciences, Minsk]

[Abstract] The action of infrared radiation pulses on the human cornea is evaluated by numerical solution of the equation of transient heat conduc-tion for a stack of four disks forming an axisymmetric cylinder 0.590 mm high and 12 mm in diameter, with homogeneous initial conditions and boundary conditions of the third kind at the frontal surface of the cornea. The latter consists of four layers: a 0.055 mm thick endothelium with a Bowman membrane under a 0.006 mm thick teardrop film, a 0.489 mm thick stroma, and a 0.60 mm thick Descemet membrane with endothelium on a 3.110 mm thick layer of moisture. The radius of the entire affected region sufficiently large so as to make the temperature at the lateral surface of this cylindrical stack at the end of the cooling period after a pulse equal to the physiological temperature of the cornea. The problem is solved by the difference factorization method on a nonuniform space-time grid with an economical locally-uniform approximating scheme of finite differences. The results of this solution for radiation pulses of 0.75 μs to 1.0 s duration from a CO_2-laser operating at the 10.6 μm wavelength are accurate within +/-28.3%. The temperature dependence of the rate constant of protein denaturation needed for calculations has been determined on the basis of "in vivo" measurements of the threshold energy density. That threshold energy density of laser radiation necessary for causing the smallest visible change in the cornea structure is found to depend exponentially on the pulse duration, with the temperature rise at the center of the spot under threshold conditions peaking later during longer pulses. A laser beam with a Gaussian radial intensity distribution was used in the experiments and assumed for the theoretical analysis. Calculations for pulses of 1.54 μm and 2.795 μm laser radiation agree closely with experimental data. Figures 3; tables 1; references 17.

UDC 621.373.826.038.823

SPER Laser a Recombination Laser ?

907L0034B Moscow KVANTOVAYA ELEKTRONIKA in Russian Vol 16 No 10, Oct 89 pp 2049-2053

[Article by V.V. Apollonov and A.A. Sirotkin, Institute of General Physics, USSR Academy of Sciences, Moscow]

[Abstract] The possibility of plasmochemical reactions taking place during segmented excitation of the plasma of a metal vapor in a buffer gas is examined, to establish the feasibility and the mechanism of population inversion for such a laser. Three reactions are considered involving Zn II and Cd II vapors with He or Ne as buffer gas. The first one is charge transfer by current pulses with attendant population of ionic levels in Zn II and emission of 384 nm, 492 nm, or 210.0 nm radiation. In this case both recombination and electron impact play the essential role. The second reaction is Penning ionization of Cd II or Zn II with attendant emission of 441.6 nm or

747.8 nm radiation respectively. This reaction intensifies the emission, while populating the levels by recombination weakens it. The third reaction involves metastable buffer gas and metastable metal vapor, Cd II but not Zn II. Theoretical interpretation of experimental data, the latter including oscillograms of emission line kinetics, indicates that the ionic levels of metal vapors are populated principally by these reactions rather than by recombination or electron impact. Recombination pumping takes place at transitions in metal atoms, while singly charged ions are produced by a plasmochemical reaction. It can be a viable mechanism, however, for singly charged ions not only of these two metals but also of metals whose doubly charged ions are produced by charge transfer and ionization. Figures 2; references 13.

UDC 621.375.9:535

Quantum Fluctuations in Laser With Intracavity Frequency Doubling

907L0029A Tomsk OPTIKA ATMOSFERY in Russian Vol 2 No 10, Oct 89 pp 1118-1120

[Article by A.I. Zhiliba, Institute of Atmospheric Optics at Siberian Department, USSR Academy of Sciences, Tomsk]

[Abstract] A source of light with a minimal quantum fluctuations of intensity for ultrasensitive laser spectroscopy is considered, namely one consisting of an active lasing medium and a frequency-doubling nonlinear crystal inside a common cavity. The ability of such a device to generate simultaneously compressed fundamental and second-harmonic radiation or, under the appropriate optimum condition, second-harmonic radiation only is demonstrated theoretically on the basis of a semiclassical description of the process by a system of two differential equations. Two successive integrations by parts solve this system of equations in the zeroth and then first approximation, sufficiently accurate for a second-harmonic generator. A subsequent quantum-electronic description of this device and analysis of its statistical characteristics on the basis of the Fokker-Planck equation, with positive-definite Glauber phase density and with adiabatic elimination of variables, indicates the feasibility of attenuating shot noise in the low-frequency range of the radiation power spectrum and thus in emission of fundamental radiation. The author thanks V.N. Gorbachev for helpful discussion and Ye.p Gordov for constructive comments. References 7.

UDC 534.511.4:621.373.826

Use of Traveling Acoustic Waves for Mode Locking in Lasers

907L0012A Moscow KVANTOVAYA ELEKTRONIKA in Russian Vol 16 No 11, Nov 89 pp 2231-2234

[Article by V.Ye. Nadtocheyev and O.Ye. Naniy, Scientific Research Institute of Nuclear Physics at Moscow State University imeni M.V. Lomonosov]

[Abstract] A new method of mode locking in a laser was tested in an experiment with an acoustooptic modulator on traveling acoustic waves. A continuous-wave garnet laser was placed inside a V-cavity between a convex spherical opaque mirror, a plane mirror with a center hole, and another plane mirror off the common optical axis at a slant to it. The mirror with a center hole was followed by another plane exit mirror on the common optical axis. The light, following its Bragg diffraction in the modulator, was not extracted from the cavity so that longitudinal modes became locked by mutual energy transfer on the ultrasonic traveling grating. The experiment confirmed the prediction based on theoretical analysis that, with the appropriate geometrical configuration and a symmetrically tuned cavity, stable mode locking in such a laser is feasible. In this case regular sequences of ultrashort 200 ps pulse were formed at a repetition rate of 10 ns. This stimulated mode locking retained its stability at frequency deviations of up to 300 kHz from the beat frequency, but the pulse duration increased to 400 ps at at that limiting frequency deviation. The authors thank N.V. Kravtsov for formulating the problem. Figures 2; references 8.

UDC 621.373.826

Interaction of Radiation Pulse and Aerosol as Active Medium in Lasers and Amplifiers

907L0012B Moscow KVANTOVAYA ELELEKTRONIKA in Russian Vol 16 No 11, Nov 89 pp 2297-2300

[Article by D.S. Bobucvhenko and V.K. Pustovalov, Belorussian Polytechnic Institute, Minsk]

[Abstract] Interaction of an optical radiation pulse pumping a laser and a fine dispersion of metal particles forming the active medium in the cavity is analyzed by the method of numerical simulation, assuming that the medium is an optically dense aerosol and taking into account several factors responsible for slowing down the evaporation process. These are the temperature dependence of optical and thermophysical properties as well as of heat and mass transfer coefficients, melting, diffusion, and convection. Calculations are made for the active medium of a DF-CO_2 laser with initial temperature and pressure 300 K and 1 atm respectively, into which spherical aluminum particles with an initial radius 0.25 μm are injected and spread over a 1 m thick layer with a uniform concentration of 3.10^7 cm^{-3}. A pulse of 10.6 μm radiation within a beam 5 cm in diameter is considered. Calculations cover the 300-1000 K temperature range. They include both scattering and absorption of radiation, scattering by thermal aureoles being treated in the Rayleigh-Gans approximation. Figures 2; references 13.

UDC 621.373.826.038.824

Emission of Tunable Ultrashort Light Pulses by Laser With Dynamic Distributed Feedback and External Ring Cavity

907L0011A Moscow KVANTOVAYA ELEKTRONIKA in Russian Vol 16 No 9, Sep 89 pp 1827-1831

[Article by A.A. Afanasyev, V.A. Zaporoshchenko, A.V. Kachinskiy, M.V. Korolkov, and O.V. Chekhlov, Institute of Physics, BSSR Academy of Sciences, Minsk]

[Abstract] Adding an external ring cavity to a dye laser with distributed feedback is considered, for the purpose of raising the efficiency of such a laser as source of tunable ultrashort light pulses and improving the characteristics of its output radiation. Theoretical analysis of this scheme is based on dimensionless quasi-classical equations for a four-level active medium with distributed feedback optically induced on a population inversion amplitude grating. The feasibility of this scheme has been established experimentally with an approximately 1.6 mmole/l rhodamine 6G solution in ethanol as active medium. Optical pumping in a Gnom-2 apparatus, with attendant formation of an approximately 5 mm long distributed feedback structure coaxial with the external ring cavity, was done by second-harmonic radiation pulses of 150-200 ps duration from a YAG:Nd^{3+} laser with active mode locking and intracavity frequency doubling periodically pulsed at a repetition rate of 100 MHz. Radiation emitted by the dye laser was extracted from the external cavity by a mirror with a 0.70 reflection coefficient and its wavelength was varied 568-602 nm range by varying the interference angle for the pumping light beams at the grating. The spectral characteristics of this radiation as well as its space, time, and energy characteristics were measured with the aid of an Agat-SF electron-optical spectrophotometric camera having a 2.7 ps time resolution. With a pumpingenergy of approximately 25 μJ energy, the efficiency of this laser emitting a narrow radiation band not wider than 0.08 nm under optimum conditions reached approximately 4%, while the efficiency of this laser without external ring cavity was only approximately 0.5% under the same conditions. The authors thank A.N. Rubinov and T.Sh. Efendiyev for helpful discussions and for supplying the Gnom-2 laser. Figures 2; references 9.

UDC 621.373.826.038.825.2

Formation of Tunable Giant Pulses in Corundum: Ti Lasers

907L0011B Moscow KVANTOVAYA ELEKTRONIKA in Russian Vol 16 No 9, Sep 89 pp 1853-1854

[Article by V.p Danilov, T.M. Murina, Ye.G. Novikov, and A.M. Prokhorov, Institute of General Physics, USSR Academy of Sciences, Moscow]

[Abstract] Formation of giant pulses in an Al_2O_3: Ti laser was achieved in an experiment which also established the feasibility of tuning such a laser without use of any dispersing device besides an electrooptic shutter in the cavity. An interference-polarization light filter with a voltage-dependent transmission coefficient served as a conventional electrooptic shutter, two transverse faces of a corundum crystal with a Brewster-angle slant serving as analyzer and polarizer respectively. A blocking constant voltage and a triggering pulse voltage were applied to the shutter with optimum time delays, for electrooptic Q-switching of the laser. The blocking voltage was regulated over the 0.5-4 kV range and the triggering voltage was regulated over the 2-5 kV range, selection of their difference or sum making it possible to smoothly tune the shutter to peak transmission over the 760-820 nm range of wavelengths with a fixed pumping energy of 40 J. Giant light pulses of 10-30 mJ energy and 50-70 ns duration with an only 10-15 nm spectral width were generated at pumping energy levels of 50-100 J. Figures 3; references 6.

Radiation and Nonequilibrium Population Relaxation in Quantum-Dimensional Semiconductor Lasers

18620162a Leningrad PISMA V ZHURNAL TEKHNICHESKOY FIZIKI in Russian Vol 15 No 3, Feb 89, pp 79-83

[Article by N. S. Averkiev, A. N. Imenkov, A. M. Litvak, Yu. p Yakovlev]

[Abstract] This study analyzes the comparative speed characteristics from the activation and deactivation of ordinary injection and quantum-dimensional lasers based on a heterojunction of the second kind (GaSb/GaAlSbAs). The analysis focuses on an investigation of the influence of the time to a quasie-quilibrium carrier distribution in the active region on laser speed. Numerical solution of provided equations made it possible to determine the time constants of the laser. The calculation was carried out by the Runge-Kutta method. It was determined that coherent radiation relaxation occurs more rapidly with diminishing RC. A comparison of the switching kinetics between a quantum-dimensional laser and an ordinary injection laser suggests that the speed of the former is an order of magnitude better, while the radiation flux drops by a factor of e for the quantum-dimensional laser over a period less than the laser characteristic operating time. The analysis also suggests that quantum-dimensional semiconductor heterolasers based on heterojunctions of the second kind are the fastest operating semiconductor lasers.

Magnetic Cooling Within Range of Room Temperatures

907L0102A Leningrad PISMA V ZHURNAL TEKHNICHESKOY FIZIKI in Russian Vol 16 No 2, 26 Jan 90 pp 12-16

[Article by A.M. Tishin, Moscow State University imeni M.V. Lomonosov]

[Abstract] In search of other materials besides gadolinium now in common use for magnetic refrigerators operating at room temperature on the basis of the magnetocaloric effect, the magnetic part of the change in entropy S_m serves as criterion. Its dependence on both temperature T and magnetic induction B is calculated for ferromagnetic rare-earth alloys of the Tb_xGd_{1-x} series in accordance with the molecular field theory. The change of entropy as a function of both is expressed as the difference between entropy in a magnetic field and entropy without a magnetic field, whereupon this expression is reduced to a single integral with respect to magnetic induction from 0 to B. Theoretical analysis is supplemented with experimental data on the magnetocaloric effect in polycrystalline gadolinium in magnetic fields of up to 6 T. The results of calculations indicate that Tb_xGd_{1-x} alloys are have a higher specific cooling capacity $(\Delta S_m \cdot gDT)_{max}/B$ (ΔT temperature drop from heat receiver to cold object) than pure gadolinium, up to 16 J/T.mole with x = 30 atom.% Tb in a magnetic field of 6 T. Figures 2; references 6.

UDC 621.313.17:537.856

Numerical Analysis and Experimental Study of Multistage Inductive Conductor Accelerator

907L0096A Novosibirsk PMTF: VSESOYUZNYY NAUCHNYY ZHURNAL PRIKLADNOY MEKHANIKI I TEKHNICHESKOY FIZIKI in Russian No 6, Nov-Dec 89 pp 37-41

[Article by I.A. Vasilyev and S.R. Petrov, Istra]

[Abstract] A model of a multistage inductive conductor accelerator is constructed which includes the propelled conductor and a series of n solenoids through which the conductor will pass, each solenoid being energized through a switch by a capacitor bank. The conductor material is characterized by its electrical conductivity, each inductor-solenoid has some resistance, each capacitor bank and the switch have some resistance and inductance. On the basis of this model are derived analytical expressions for the vector potential of a current-carrying circular "point" turn of a solenoid at any point within its magnetic field including points in other solenoid magnetically coupled to the given one and for the force driving the conductor. The electromechanical processes in this system are then described by a system of three equations: integrodifferential equation for the current density in the conductor as a function of time over the period of capacitor discharge, plain differential equation of motion for the conductor, and plain differential equation of the Joule effect. This system of equations is reduced to matrix form with a matrix of self-and mutual inductances [L], a column of currents [I], a column of voltage drops [RI], and a column of applied voltages [V]. This system is reduced to one of linear algebraic equations in unknown rates of change of current dI/dt, after the integrals have been replaced with finite sums according to the rule of rectangles and the inductors with equivalent "thin" solenoids of uniform cross-section. This system was solved numerically on a Yes-1061 computer for an accelerator with 20 solenoid stages, the conductor having been broken down into 8x8= 64 segments. A comparison of the results with experimental data indicates that the conductor velocity actually attainable with such an accelerator is equal to 78% of the theoretical upper limit determined by melting. Figures 5; references 5.

Transient Resonance Radiation in Multilayer Interference Structures

907L0058A Leningrad ZHURNAL TEKHNICHESKOY FIZIKI in Russian Vol 59 No 11, Nov 89 pp 18-21

[Article by A.p Apanasevich and V.A. Yarmolkevich, Scientific Research Institute of Problems in Nuclear Physics at Belorussian State University imeni V.I. Lenin]

[Abstract] Considering the wide use of transient resonance radiation occurring during uniform motion of a charged particle through a medium with a periodic structure for detection of charged high-energy particles, a technology of producing multilayer interference structures with space periods within the 5-50 nm range is being developed for the use of such structures in x-ray optics. In view of this, the feasibility of such x-ray sources generating by this mechanism 0.5-100 eV photons in slightly relativistic 2-5 MeV electron beam by this mechanism is examined and the parameters of a multilayer interference structure is optimized for maximum quantum yield. The design and performance analysis pertains to normal incidence of an electron beam on a stack of M binary composite layers, all consisting of the same two different dielectric materials. The two component layers have generally different thicknesses, the ratio of their thicknesses as well as their combined thickness and the effective structural period of the stack being the design variables. Absorption of radiation is accounted for by a reducing the geometrical stack period to an effective one. Numerical calculations have been made for Ni-Be, Ni-C, Ni-Si, Mo-Si, and C-Be layer pairs. The results indicate the feasibility of using a multilayer interference structure and a slightly relativistic electron beam as a narrow-angle high-intensity x-ray source for either pulsed or quasi-continuous operation. The authors thank Professor V.G. Baryshevskiy for stating the problem and O.T. Gradovskiy for helpful discussions. Tables 3; references 6.

Active Medium of Near-Ultraviolet Recombination Laser

907L0058C Leningrad ZHURNAL TEKHNICHESKOY FIZIKI in Russian Vol 59 No 11, Nov 89 pp 110-112

[Article by B.A. Bryunetkin, V.M. Dyakin, I.Yu. Skobelev, A.Ya. Fayenov, and S.Ya. Khakhalin]

[Abstract] An experimental study of a near-ultraviolet solid-state recombination laser involving spectroscopy of its active medium in the process of its formation was made, for the purpose of verifying the theoretical model of this process and determining the plasma parameters directly within the lasing region. Plasma was generated by focusing radiation of a neodymium laser in pulses of up to 20 J energy and 3 ns duration above the half-amplitude level onto the surface of a solid beryllium target with a power density of 3.10^{11} W/cm^2. The time-integral spectra of the plasma covering the 200-550 nm range of wavelengths were recorded in one of the two spectroscope channels with a space resolution of approximately 0.1 mm. The time characteristics of radiation at various transitions in Be^{I}, Be^{II}, Be^{III}, Be^{IV} ions were recorded in the other channel with a space resolution of approximately 1 mm and a time resolution of 3 ns. The data reveal an intricate space-time structure of the plasma flare consisting of groups of ions spreading with different velocities, the fastest three groups with velocities of $4x10^7$ cm/s, 1.3×10^7 cm/s, and 5×10^6 cm/s being the principal contributors to the 4f-5g line of Be^{IV}, the 4d,f-5f line of Be^{III}, and the 3d-4f line of Be^{II} respectively. Estimates of the average gain at the 4f-5g transition in Be^{IV} ions within the lasing region beyond the self-absorption region have been made on the basis of electron concentration and temperature measurements. These estimates agree, within a factor of 2, with the theoretical value of the average gain based on numerical analysis of a mathematical model: 0.05-0.10 cm^{-1}. Figures 2; references 5.

Entrance States for Fission

907L0056A Moscow YADERNAYA FIZIKA in Russian Vol 50 No 6 (12), Dec 89 pp 1546-1550

[Article by D.F. Zaretskiy and F.F. Karpeshin, Leningrad State University]

[Abstract] On the premise that pre-fission states of nuclei constitute a superposition of n surface-vibrational phonons, the width of their breakup into more intricate configurations is estimated for a determination of the lifetime of particle-hole states. A qualitative analysis of particle-hole interaction and entrance states with the aid of applicable Feynman diagrams is followed by quantitative calculations for a two-quasiparticle state and then for a multiparticle multiparticle compound-nuclear state, three states being possible for n = 8 phonons with a total momentum I = 2. The width of an n-phonon state is expressed as the imaginary part of the energy polarization operator, the magnitude of this operator being determined by the sum of amplitudes on the corresponding Feynman diagrams. The theoretically calculated widths are comparable with the widths of breakup obtained experimentally in photofission of ^{238}U at two near-threshold excitation levels of 5.0 MeV and 5.7 MeV respectively. The authors thank Yu.I. Kharitonov and G.A. Petrov for fruitful discussions. Figures 2; tables 1; references 15.

Thermodynamic Modl of Nucleus-Nucleus Collision Process

907L0056B Moscow YADERNAYA FIZIKA in Russian Vol 50 No 6 (12), Dec 89 pp 1583-1594

[Article by D.N. Voskresenskiy, Moscow Institute of Engineering Physics]

[Abstract] Following a review of the various thermodynamic fireball models which have been proposed to describe NN-collision, the Valecky model describing the

nucleon susbsystem in the relativistic mean-field approximation is modified by lowering the compressibility K from the overestimated 360 MeV to 210 Mev and increasing the effective nucleon mass m_N^* from the underestimated $0.5m_N$ to $0.85m_N$. The results of calculations for pions on the basis of this model, taking into account polarization of a hot nuclear medium, are compared with experimental on differential and integral cross-sections for collisions of nuclei with 0.1-2 GeV energy. The equation of state for a nuclear fireball at temperatures not exceeding 1 is then rigorously derived from the three equations of that Valecky model modification. These equations are the dimensionless one for the energy per mass of a particle in the baryonic subsytem, one for the energy of populating the lower branches in the spectrum of the excited system, disregarding the negligible contribution of quantum fluctuations, and one for the energy of virtual particles the softest of which have pion quantum numbers. Temperature-density iagrams have been plotted which depict expansion and compression of nuclear matter in the collision process. The author thanks O.V. Oreshkov for assistance. Figures 7; references 33.

Phase Transitions in Nuclear Matter: Metastability and Fluctuations

907L0056C Moscow YADERNAYA FIZIKA in Russian Vol 50 No 6 (12), Dec 89) pp 1747-1754

[Article by V.G. Boyko, L.L. Yenkovskiy, and V.M. Sysoyev, Institute of Theoretical Physics, UkSSR Academy of Sciences]

[Abstract] Phase transitions from hadronic matter to quark-gluon plasma are analyzed for possible depths of intrusion into the metastability range. The analysis is based on the Blaizot-Ollitrault equation of state P(T) for each phase according to this bag model, this equation being extended to also include metastable states. For the purpose of estimating the possible intrusion depths into this range and the stability of metastable stable states, a phase transition is assumed to occur under equilibrium conditions and a fluctuational seeding of the new phase is assumed to occur within a finite spherical volume. A critical radius is established, spherical seeds with a larger than critical radius being stable and capable of further growth so that subsequent merger of such seeds will results in a phase transition of the first kind. Surface tension coefficient $\sigma = \omega B^{3/4}$ is evaluated according to field-theory bag models, $B^{-1/4}$ having the dimension of length and the P_c/T_c ratio is roughly estimated in the Van der Waals approximation. The square of this ratio is entered into the criterion of possible intrusion depths and the latter is then compared with the Ginzburg criterion, which consists of a part depending only on properties of the original phase and a part depending on the thermodynamic state of the metastable phase. Further analysis reveals metastable states of superheated hadronic matter and of supercooled quark-gluon plasma. The authors thank participants of science seminar held by the Institute of Theoretical Physics at the UkSSR Academy of Sciences for helpful critique and advice. Figures 5; references 13.

UDC 537.533.3

Detection of Exchange-Induced Orthogonal State of Magnetic Impurity

907L0018B Moscow PISMA V ZHURNAL EKSPERIMENTALNOY I TEORETICHESKOY FIZIKI in Russian Vol 50 No 9, 10 Nov 89 pp 401-403

[Article by A.M. Balbashov, A.G. Berezin, Yu.V. Boryshev, pYu. Marchukov, I.V. Nikolayev, and Ye.G. Rudashevski, Institute of General Physics, USSR Academy of Sciences]

[Abstract] An experimental study of the $YFeO_3$ orthoferrite was made, a single crystal of this material having been grown by zone melting with radiative heating of a compact 1.00:1.00 mixture of Y_2O_3 and Fe_2O_3 which had been sintered at 1400°C. The weight fraction of magnetic impurity in the two oxides did not exceed 10^{-6} and 10^{-4} respectively. The single crystal contained also Mn, its weight fraction not exceeding 2.10^{-5} but no Co, Cu, and rare-earth elements. Annealing at 1400°C in an oxygen atmosphere under a pressure of 20 atm for 8 h minimized the number of defects as well as the Fe^{2+} and Fe^{4+} ion content. Ferromagnetic and antiferromagnetic resonance spectra of this single crystal, an orthorhombic one, were recorded at a temperature of 12 K in a magnetic field of up to 120 kOe parallel to the principal axis of the crystal, no field-induced spin reorientation having been found to occur. In addition to only one ascending antiferromagnetic resonance line representing a quasi-ferromagnetic mode, was also obtained a descending two to three times weaker and two to three times wider absorption line. This line disappeared at 77 K. It evidently corresponds to an impurity mode owing to presence of Fe^{3+} ions in 4R positions in the crystal with a magnetic moment opposing the weakly ferromagnetic moment and perpendicular to the axis of antiferromagnetism, its intensity being attributable to exchange amplification. The authors thank Academician A.M. Prokhorov for attentiveness. Figures 1; references 11.

Equilibrium Characteristics of Relativistic High-Current Electron Beam in Two Magnetostatic Fields Quasi-Uniform and Periodic Respectively

907L0050A Tomsk IZVESTIYA VYSSHIKH UCHEBNYKH ZAVEDENIY: FIZIKA in Russian Vol 32 No 11, Nov 89 pp 106-108

[Article by S.Ya. Belomyttsev, S.D. Korovin, and I.V. Pegel, Institute of High-Current Electronics, Siberian Department, USSR Academy of Sciences, Tomsk branch]

[Abstract] The equilibrium dimensions of a relativistic high-current electron beam in a wiggler with a sinusoidal

magnetostatic field and a quasiuniform one are calculated, assuming a short transport channel with no reflections at its edges and thus disregarding radiation effects. For an axisymmetric tubular beam, its characteristic equilibrium radius is determined from the equation of electron ballistics according to Busch's theorem without constraints on the intensities of both fields. A correction is added for small oscillations of electrons and small fluctuations of their trajectories about this radius. The equation describing them becomes, after linearization and averaging, a nonhomogeneous Mathieu equation describing parametric resonance buildup of oscillations at near bounce frequency or its multiples. The correction simplifies off resonance when the electron plasma frequency is low. References 3.

Giant Radio Detectors of High-Energy Particles Penetrating Ice Crust With Movement of Radio Modules Through Ice in High-Power Microwave Beams

907L0040A Moscow PISMA V ZHURNAL EKSPERIMENTALNOY I TEORETICHESKOY FIZIKI in Russian Vol 50 No11, 10 Dec 89 pp 446-447

[Article by G.A. Askaryan, Institute of General Physics, USSR Academy of Sciences]

[Abstract] The feasibility of constructing giant detectors of high-energy particles such as muons and neutrinos in large natural media masses such as an ice crust is examined, utilizing the high transparence of very cold ice for radio waves being considered being proposed here. Particles penetrating an ice crust vertically or nearly so being of particular concern and considering furthermore that they emit Cerenkov radiation at large angles, a detector with both transmitter and receiver modules movable not only over the ice surface but also through the ice mass is most desirable. The latter possibility can be achieved by melting the ice around the modules with microwaves. Asymmetric heating is very effective and so is superheating with attendant pressure buildup not only by the melting of ice but also by the formation of steam from boiling water, especially when heating is done with a periodically pulsed microwave beam. References 5.

Local Active Corpuscular Diagnostic Measurements of Poloidal Magnetic Field and Stability Margin Index q Near Discharge Axis in TUMAN-3 Tokamak

907L0040B Moscow PISMA V ZHURNAL EKSPERIMENTALNOY I TEORETICHESKOY FIZIKI in Russian Vol 50 No 11, 10 Dec 89 pp 453-457

[Article by V.I. Afanasyev, A.I. Kislyakov, S.V. Lebedev, S.Ya. Petrov, F.V. Chernyshev, and K.G. Makhovets]

[Abstract] Local measurements of the poloidal magnetic field and the stability margin index near the discharge axis in the TUMAN-3 tokamak were made made by the method of active corpuscular plasma diagnostics, a beam of neutral 10 keV hydrogen molecules being injected along vertical chords at some distances from the discharge axis. Such a molecular hydrogen beam became the source of atoms as a result of ionization by protons and of dissociation upon collision with electrons. The theory of such measurements is outlined, considering the geometry of the experiment with an injected molecular beam much thinner than the plasma filament. The measurements were made at two operating levels, with the plasma current 40 kA and 70 kA respectively. The results indicate no significant change in the current density near the plasma axis, a larger current possibly spreading wider and the internal inductance becoming smaller with a correspondingly smaller displacement of the plasma filament. Figures 3; references 5.

Possibility of Thermonuclear Fusion in Counterflowing Plasma Streams in Radio-Frequency Potential Wells

907L0043B Leningrad PISMA V ZHURNAL TEKHNICHESKOY FIZIKI in Russian Vol 15 No 23, 12 Dec 89 pp 69-71

[Article by A.I. Dzergach, Moscow Institute of Radio Engineering, USSR Academy of Sciences]

[Abstract] The possibility of thermonuclear fusion in r-f potential wells is examined, experiments having demonstrated the such wells are capable of localizing charged particles and thus confining a cold subcritical-density plasma. Considering that plasma electrons are localized by a high-frequency field with a focusing alternating gradient and plasma ions are localized by a polarizing field, the conditions are established necessary for counter-flowing clusters of a nonequilibrium plasma with cold ions to enter into a fusion reaction with the ions remaining cold and thus thermally isolated in the well. These conditions are a plasma density sufficiently high for collisions to take place and a longitudinal velocity of ions sufficiently high for overcoming the Coulomb barrier. Random relative motion of electrons and ion is necessary only for preventing recombination, which becomes in creasingly difficult at higher temperatures. References 5.

Amplification of Cerenkov Waves by Flow of Medium

907L0043C Leningrad PISMA V ZHURNAL TEKHNICHESKOY FIZIKI in Russian Vol 15 No 23, 12 Dec 89 pp 91-93

[Article by I.A. Kolmakov and N.N. Antonov]

[Abstract] The possibility of interfering Alfven and acoustic waves generating high-intensity Cerenkov radiation in a plasma when it flows in a constant parallel external magnetic field at a constant velocity relative to both sources of waves is examined, assuming a "cold" plasma with negligible energy dissipation and infinitely long beams of waves. The system of three differential

vector field equations describing flow with fluctuation of all parameters except the frequencies of Alfven and acoustic waves is solved for a parabolic distribution of "sources" of nonlinear sum-frequency waves and for time-invariant perturbations. The solution obtained with the aid of a Fourier-Hankel transformation, after an appropriate change of coordinates, yields Cerenkov cones whose surfaces vary harmonically in space. The intensity of Cerenkov radiation drops fast as the condition for diffraction is reached, but the effect of diffraction remains minimal when the primary Alfven and acoustic beams are equally divergent. References 2.

Destruction of Metal Plate by Pulsed Proton Beam

907L0038A Leningrad PISMA V ZHURNAL TEKHNICHESKOY FIZIKI in Russian Vol 15 No 22, 26 Nov 89 pp 39-43

[Article by S.L. Leshkevich, V.A. Skvortsov, and V.Ye. Fortov, Institute of High Temperatures, USSR Academy of Sciences, Moscow]

[Abstract] Use of high-power ion beams for controlled inertial thermonuclear fusion and for monitoring extreme states of matter is considered, preliminary theoretical analysis of anticipated processes being necessary for minimizing the high cost of experimentation. Such an analysis was performed numerically on the basis of a mathematical model for a flat aluminum plate as target and a normally incident monoenergetic proton beam: plate thickness 0.2 cm, beam diameter 0.2 cm, kinetic energy of particles 15 MeV, maximum beam current 10 kA, total duration of sinusoidal pulse 100 ns, total beam energy within a pulse 15 kJ. Transient motion of the target medium upon its heating by the ion beam was analyzed on the basis of a two-dimensional hydrodynamic model and the equation of heat conduction, the target medium being treated as a continuous one. The hydrodynamic model was built with Euler's divergence equations representing the laws of mass, energy, and momentum conservation on a grid of coordinates fixed in space. The equations of motion were integrated by the large-particle method with first-order precision in both time and space. The equation of heat conduction was solved by the local iteration method. The semiempirical equation of state relating density and internal energy to pressure covered a broad range of states through melting to evaporation, also ionization, compression under high pressures, and decompression processes. This equation was formulated so as to not only avoid ill-conditioned asymptotic behavior, by including the results of quantum-mechanical calculations based on the band theory of metals as well as on the theoretical Thomas-Fermi and Debye-Hueckel models for extreme concentrations of internal energy, but also ensure a close agreement with experimental data on shock-wave compression under megabar pressures and subsequent isentropic decompression as well as on the thermophysical properties of the material under low pressures and at low temperatures. Figures 2; references 6.

UDC 539.17

Effect of Relaxation of Gamov-Teller Resonances on Force Function and Delayed-Neutron Yield of β-Decay Function and Delayed-Neutron Yield

907L0027A Kiev UKRAINSKIY FIZICHESKIY ZHURNAL in Russian Vol 34 No 11, Nov 89 pp 1646-1650

[Article by V.G. Guba, M.A. Nikolayev, and M.G. Urin, Moscow Institute of Engineering Physics]

[Abstract] The force function of β-decay is described on the basis of an optical-shell model, this description being more accurate than earlier ones based on circuit theory of giant resonances or accounting for Gamov-Teller transitions in the Tamm-Dankov approximation but ignoring decay of high-excitation states. The force function is, according to this model, determined by the imaginary part of the mean nuclear polarizability corresponding to the external field. Both half-life period and probability of delayed-neutron emission are calculated on this basis, considering that allowed Gamov-Teller transitions with $J^{\pi} = 1^{+}$ are the dominant contributors to the force function for nuclei with a large number of excess neutrons. Both these principal characteristics of β-decay have been calculated accordingly for ^{93,95,97,99}Rb, ^{81}Ga, ^{80}Zn, and ^{96}Kr nuclei, their thus obtained theoretical values agreeing closely with the experimentally determined ones. Figures 1; tables 1; references 18.

Study of Spin-Electron Exchange Interaction at Any Temperature by Bogolyubov-Tyablik Method. Change in Characteristics of Magnetic Subsystem

907L0026A Moscow TEORETICHESKAYA I MATEMATICHESKAYA FIZIKA in Russian Vol 81 No 2, Nov 89 pp 230-238

[Article by A.A. Trushchenko, Kiev Polytechnic Institute]

[Abstract] The method of approximate second quantization, improved by Bogolyubov and Tyablik, is applied to the problem of spin-electron exchange interaction in ferromagnetic or paramagnetic semiconductors with weak coupling of the magnetic subsystem to the electronic one of either conduction or impurity-center electrons. The energy of elementary excitations in the magnetic subsystem and its magnetization at any temperature except very low ones are calculated accordingly, using the Hamiltonian of an electronic subsystem and Green's retarding temperature function. An appropriate correction proportional to the magnetic field intensity is included in the form of two terms proportional to exchange (s-d or s-f) interaction energy and to a power series of the latter respectively, taking into consideration the width of the conduction band. This

method is thus shown to be suitable for tracking changes in both exchange interaction energy and magnetization. References 23.

UDC 539.163

Additional Evidence Proving Existence of Intermediate Structure in Cu Isotopes

907L0023A Moscow IZVESTIYA AKADEMII NAUK SSSR: SERIYA FIZICHESKAYA in Russian Vol 53 No 10, Oct 89 pp 2055-2057

[Article by V.M. Sigalov]

[Abstract] Additional experimental evidence proves the existence of an intermediate structure in Cu isotopes, this structure being characterized by a systematic deviation from the statistical model. The evidence is based on γ-decay of resonances in ^{59,61,63}Cu isotopes into the ground state, depending on their energy, during pγ-reactions and the attendant angular distribution of γ-quanta attenuating these resonances. The A_2 coefficient characterizing this distribution in $3/2^-$ to $3/2^-$ transitions was found to be positive in only five out of 16 such transitions in ^{59}Cu, in only two out of 12 such transitions in ^{61}Cu, and in only seven out of 38 such transitions in ^{63} Cu. The probability of a γ-quanta multipolarity distribution conforming to the statistical model is correspondingly lower than 7% (^{59}Cu), 2% ^{61}Cu, and 0.005% ^{63}. The thus evidently asymmetric γ-quanta multiplicity distribution confirms the existence of an intermediate structure. Figures 2; references 6.

Currents of Second Kind and Mass of Neutrino in β-Decay Processes ^{19}Ne into ^{19}F + Positron + Neutrino and n into Proton + Electron + Antineutrino

907L0022A Moscow IZVESTIYA AKADEMII NAUK SSSR: SERIYA FIZICHESKAYA in Russian Vol 53 No 11, Nov 89 pp 2110-2115

[Article by N.V. Samsonenko, A.L. Samgin, M.I. Suvorov, and Ye.V. Brilev]

[Abstract] Both the $1/2^+$-to-$1/2^+$ transition from one of the mirror nuclei ^{19}Ne and ^{19}F to the other and the β-decay of a free neutron with arbitrary polarization are analyzed without models from a phenomenological approach, using the current-current interaction Hamiltonian and taking into account the isotopic structure of strong interactions as well as the Lorentz invariance. The object of this analysis is evaluating the dependence of these two processes on the magnitude of the neutrino mass and the effect on them of currents of the second kind. An expression is derived for the differential probability of β-decay which, together with the experimentally determined electron-neutrino correlation coefficient and with form factors included, will yield the other relevant correlation coefficients and the polarization coefficients as well as the rest mass of a neutrino The results of this theoretical evaluation are supplemented by those of numerical analysis. References 21.

UDC 538.935

Soliton Conductivity of Randomly Nonhomogeneous One-Dimensional Systems

907L0020A Leningrad FIZIKA TVERDOGO TELA in Russian Vol 31 No 10, Oct 89 pp 256-259

[Article by B.A. Malomed, Institute of Oceanology, USSR Academy of Sciences, Moscow]

[Abstract] Soliton conductivity of randomly nonhomogeneous onedimensional systems such as a long Josephson junctions with randomly modulated maximum supercurrent density and specifically a randomly nonhomogeneous SNS junction with strong dissipation is considered, nonlinear conductivity of one-dimensional metals being generally attributed to commensurability of a charge density wave and charged particles acting on it with phase deviation evolving as a consequence. A model is constructed from the standpoint of perturbation theory, on the basis of kinks released by an electric field from entrapment in a random potential relief. The current-voltage characteristic is calculated accordingly and compared with that for a homogeneous system, its hysteresis loop is plotted, the frequency dependence of the dynamic conductivity according to this model being compared with that according to the commensurability and phase deviation model. The proposed model is evidently applicable to long Josephson junctions, with f denoting the density of lateral current and j representing the voltage across the junction. The author thanks A.R. Bishop A.F. Volkov, I.V. Kriva, A.A. Nepomnyashchev, and A.S. Rozhavskiy for helpful discussions. Figures 3; references 8.

UDC 538.945:535.343

Ceramic and Thin-Film Tl-Ba-Ca-Cu-O high-Tc Superconductors

907L0020B Leningrad FIZIKA TVERDOGO TELA in Russian Vol 31 No 10, Oct 89 pp 295-297

[Article by O.V. Kosogov, A.I. Akimov, M.V. Belousov, S.V. Bogachev, V.Yu. Davydov, V.A. Ilin, S.F. Karmanenko, A.L. Karpey, O.V. Kornyakova, V.N. Makarov, and L.p Poluchankina, Institute of Engineering Physics imeni A.F. Ioffe, USSR Academy of Sciences, Institute of Electrical Engineering imeni V.I. Lenin (Ulyanov), and Scientific Research Institute at Leningrad State University, Leningrad]

[Abstract] An experimental study of ceramic and thin-film Tl-Ba-Ca-Cu-O superconductors was made, the ceramic specimens having been produced by solid-phase synthesis of Tl_2O_3 + $BaCO_3$ + $CaCO_3$ + CuO powder mixtures. Approximately 0.5 μ thick film specimens

were produced by magnetron sputtering of ceramic targets onto 500-600°C hot Al_2O_3, ZrO_2, and MgO substrates and subsequent annealing in an oxygen atmosphere. All specimens were found to have a polyphase content. Three ceramic specimens were selected for x-ray spectrum microanalysis, after superconducting transition had been established on the basis of their d.c. resistance dropping to zero at the transition temperature In specimen 1 was predominant the1-2-1-2 phase and its critical temperature was 109 K (transition ending at 107 K). In specimen 2 was predominant the 1-5-4-7 phase and its critical temperature was 130 K (transition ending at 120 K). In specimen 3 was predominant the 1-2-2-4 phase and its critical temperature was 122 K. The critical temperature for two film specimens was 126 K and 124 K respectively. Evidently, the critical temperature is higher for a material with a higher (Ca+Cu):(Tl+Ba) content ratio. The temperature dependence of a weak-field EPR signal was tracked in a Radiopan EPR spectrometer at 9.8 GHz frequency, for detection of superconductivity contactlessly on the basis of change in absorption of microwave power in a weak field. Measurement of Raman scattering spectra was done at room temperature in air with a DFS-24 diffraction photospectrometer, incident 514.5 nm light from an argon laser covering a spot 30 μ in diameter. All spectra contained a principal peak in the vicinity of 520 cm^{-1}, characteristic of $TlBa_2 Ca_{n-1}Cu_nO_{2n+3}$ compounds. Companion peaks appeared in the spectrum of specimen 2 (435 cm^{-1}, 555 cm^{-1}) and in the spectra of both film specimens (435 cm^{-1}, 585 cm^{-1}, 635 cm^{-1}), indicating the presence of foreign inclusions. The films, structurally imperfect, were found to contain a substantial amount of the $BaCuO_2$ phase. Figures 2; references 6.

UDC 537.32:546

New CeM_2(M=Fe,Co)X_8(X=Al,Ga) Kondo Lattices

907L0020C Leningrad FIZIKA TVERDOGO TELA in Russian Vol 31 No 10, Oct 89 pp 297-299

[Article by M.D. Koterlin, B.S. Morokhivskiy, R.V. Lapunova, and O.M. Sichevich, Lvov State University imeni I. Franko, Lvov]

[Abstract] An experimental study of CeM_2(M=Fe,Co)X_8(X=Al,Ga) compounds and their solid solutions was made involving the density of states and the fine structure near the Fermi level in these new materials of the rhombic crystal class with the Pbam space group Measure-ments of their electrical resistivity, thermo-e.m.f., and magnetic susceptibility were made over a temperature range from below 77 K to 400 K. They revealed that the magnetic component of electrical resistivity equal to the difference $\rho(CeM_2X_8 - \rho(LaM_2X_8)$ has maxima at approximately 40 K for $CeCo_2Al_8$, 120 K for $CeFe_2Ga_8$, and 150 K for $CeFe_2Al_8$, but remains almost constant at a high metallic residual level of 0.240 mohm.cm for $CeCo_2Ga_8$. While the Seebeck coefficient was found to be a negative one monotonically becoming more so with rising temperature for $CeCo_2Ga_8$, to cross over from negative to positive at about 50 K and to remain so after peaking to a maximum at about 120K for $CeFe_2Ga_8$, to be a positive one peaking at about 40 K for $CeCo_2Al_8$ and at about 150 K for $CeFe_2Al_8$ and then dropping into the negative range at respectively higher temperatures. The temperature of maximum Seebeck coefficient for solid solutions such as $CeCo_2$ $Al_{8-x}Si_x$, $CeCo_{2-x}Fe_xAl_8$, $CeFe_{2-x}Co_xAl_8$ was found to be quite sensitive to change of x and to thus depend on the composition. Magnetic susceptibility measurements revealed a deviation of only $CeFe_2Al_8$ from the usual trivalent state of Ce. The results indicate a magnetic state of Ce in $CeCo_2Ga_{8_2}Al_8$, an intermediate valence of Ce in $CeFe_2Al_8$, and a critical state of Ce within the range of transition from intermediate valence to Kondo lattice in $CeFe_2$ Ga_8 with pronounced coherent effects in the temperature dependence of the Seebeck coefficient. Figures 3; references 5.

UDC 539.12.01

Heavy Solitons in Generalized Spinor Electrodynamics

907L0019A Tomsk IZVESTIYA VYSSHIKH UCHEBNYKH ZAVEDENIY: FIZIKA in Russian Vol 32 No 10, Oct 89 pp 97-100

[Article by Ye.N. Magar and Yu.p Rybakov, 'Amity of Nations' University imeni Patrice Lumumba]

[Abstract] An extension of spinor electrodynamics to curved momentum spaces, specifically the de Sitter space, was proposed by V.G. Kadyshevskiy in 1980. Its model was constructed according to the gauge principle, with an 8-spinor Ψ and a 4-potential A_μ of the electromagnetic field projected into the physical four-dimensional space as initial objects. Soliton solutions to the equations of motion in Lagrangian model density are sought by application of the Cowlman-Palais symmetry principle and formulations are sought invariant after any transformation among all possible groups of transformations admissible by the equations of motion. Successive reductions of the initial model yield then the structure of an admissible soliton which describes motion of a heavy charged particle with a ½ spin whose mass and magnetic moment can be numerically estimated. The authors thank Professor V.G. Kadyshevskiy for interest. Figures 1; references 2.

Ternary Fision of Neutron-Excited Uranium Fissioning Isomers

907L0017a YADERNAYA FIZIKA in Russian Vol 50 No 4, Oct 89, pp 928-935

[Article by V. Ye. Mararenko, Yu. D. Molchanov, G. A. Otroshchenko, and G. B. Yan'kov]

[Abstract] This study describes an experiment producing ternary fision of uranium fissioning isomers in the reactions $^{236, 238}U(n, n')$ at a mean neutron energy of 4.5

MeV. The results reported from this study cover the two known fissioning isomers of uranium. The measurements were carried out on the electrostatic accelerator of the Kurchatov Institute of Atomic Energy. The pulsed fast neutron flux was produced in a D(d, n)^{3}He reaction by deuterium ion bunches with a pulse repetition frequency of 2 MHz. The spontaneously fissioning isomers of uranium were identified in this study by measuring the half-decay period and the relative probability of nuclear fission through the isomer state. The reported values for the relative probability of nuclear fission through the SFI state for the mean neutron energy cited above are (1.30 +/- 0.01) times 10^{-4} for ^{236}U and (1.48 +/- .02) times 10^{-4} for ^{288}U. The study establishes that the relative probability of ternary fission of the spontaneously fissioning isomers of uranium grows significantly compared to the case of ternary fission of the nucleii in nonisomeric states. The analysis attributes this to the peculiar nucleon configuration of the isomer states.

Generalized Shock Adiabats and Relativistic Nuclear Collisions

907L0017b YADERNAYA FIZIKA in Russian Vol 50, No 4, Oct 89, pp 1172-1182

[Article by K. A. Bugaev, M. I. Gorenstein, V. I. Zhdanov, B. Kampfer]

[Abstract] This study carries out a consistent analysis of possible relativistic shock-wave compression configurations in a medium containing regions with anomalous thermodynamic properties. The decay of a random discontinuity is analyzed and a generalized shock compression adiabat is constructed for the case of relativistic nuclear collisions with a two-phase equation of state. The study considers the case where there is a first order phase transition between the hadron and quark-gluon matter. This analysis reveals stable shock-wave configurations consisting of several shock waves and simple waves traveling in the same direction. The thermodynamic properties of the state are described by a general shock adiabat and it is found that this adiabat may consist of Taub, Poisson, and wave adiabats. A generalized compression adiabat is also found for nuclear-nuclear collisions.

New Metastable Structure in Amorphous 85 Fe - 15 B Alloy After Ion Bombardment

907L0014A Moscow PISMA V ZHURNAL EKSPERIMENTALNOY I TEORETICHESKOY FIZIKI in Russian Vol 50 No 10, 25 Nov 89 pp 420-421

[Article by A.L. Pivovarov, S.p Chenakin, and V.T. Cherepin, Institute of Metal Physics, UkSSR Academy of Sciences]

[Abstract] Ion bombardment of an amorphous alloy, 85 Fe-15 B, was found to result in formation of a metastable amorphous structure first and a crystalline phase next upon breakdown of the latter. Specimens of 30 μm thick tape had been produced for the experiment by quenching the alloy melt on a rotating disk. With the back surface coated with varnish, they were bombarded with a 5 keV AR'-ion beam 2 mm in diameter at a 30°glancing angle, at room temperature under an oilless vacuum of 40 μPa. The temperature of the bombarded surface spot did not exceed 60°C. After bombardment with an ion dose of 10^{19} cm^{-3} at a current density of 0.3 mA/cm^2, the structure of specimens was examined in an EMR-100 transillumination electron diffractograph. The new amorphous structure featured a high degree of disorder with an interatomic distance almost 23% larger than in the original one, the latter having evidently been either split into two different ones in a varying volume ratio or completely transformed into the new one. The authors thank I.Ye. Kotenko for assistance in the experiments. Figures 2; references 2.

Noncommensurate Structures in Crystals of High-Temperature Superconductors

907L0014B Moscow PISMA V ZHURNAL EKSPERIMENTALNOY I TEORETICHESKOY FIZIKI in Russian Vol 50 No 10, 25 Nov 89 pp 428-430

[Article by V.V. Zaretskiy, V.A. Zaretskaya-Eliashberg, and M.B. Kosmyna, Institute of Solid-State and Semiconductor Physics, BSSR Academy of Sciences]

[Abstract] A microstructural examination of $Bi_{2.2}Sr_{1.8}CaCu_2O_{8+x}$ single crystals was performed in an x-ray diffractometer with FeKα_1-radiation source, in search of properly noncommensurate structures besides quasi-noncommensurate superstructures combining commensurate periods in such a high-temperature superconductor. The pattern of satellite reflections on tails of Bragg reflections besides additional reflections and diffuse scattering recorded in the reciprocal lattice reveals such heretofore unknown truly noncommensurate structures and confirms the authors' hypothesis about their existence. Accordingly, Bi-Sr-Ca-Cu-O crystals belong in the class of noncommensurate ones. The authors thank A.p Levanyuk and Ye. Kolomeyskiy for discussion. Figures 3; references 5.

Possibility of Verifying Mikheyev-Smirnov-Wolfenstein Effect With Neutrino Beams from Accelerator

907L0005A Moscow YADERNAYA FIZIKA in Russian Vol 50 No 5, Oct 89 pp 1357-1364

[Article by pI. Krystev, Institute of Nuclear Research, USSR Academy of Sciences]

[Abstract] The possibility of verifying the Mikheyev-Smirnov-Wolfenstein effect, namely resonant amplification of neutrino oscillation in matter, and explaining the results of the Davis experiment measuring the solar neutrino flux is considered, an experiment being proposed which would involve scanning a neutrino beam for oscillations as it passes through earth. Such a neutrino beam would be produced with the aid of a proton accelerator boosting the energy of about 10^{14} protons per pulse to a final energy of several TeV, with 1-2 min time intervals between pulses. These protons would strike a target followed by a focusing device and an about 1 km long decay channel for passage of neutrinos downward through an earth "tunnel" to a detector at the other end. The channel should be off vertical by an angle of approximately 6.5° for

a 500 km long "tunnel" and approximately 19.5° for a 4300 km long "tunnel". After extraction of charged pions and kaons from the decay channel, pure neutrino and antineutrino beams will pass through earth. Evaluation of the detector readings must take into account muon fluxes generated by interaction of muon neutrinos and nucleons in the ground mass, including the effect of neutrino oscillations on those muon fluxes. The author thanks E.V. Bugayev, I.M. Zheleznykh, S.p Mikheyev, S.T. Petkov, R.A. Rzayev, A.Yu. Smirnov, and V.A. Chechin for discussions, suggestions, and comments, also V.A. Tsarev for discussing the partial overlap and the overall agreement with his reports on such an experimental research program. Figures 2; references 29.

The Soliton Dynamical Structural Factor of a Classical Easy-Axis Single-Dimensional Antiferromagnet

18620185B Kiev UKRAINSKIY FIZICHESKIY ZHURNAL in Russian Vol 34 No 3, Mar 89, pp 429-434

[Article by A. K. Kolezhuk]

[Abstract] This study investigates the contribution of nonlinear excitations in the form of 180° domain boundaries and localized solitons in the dynamical structural factor of a classical one-dimensional antiferromagnet with easy axis anisotropy. The study limits the analysis to neutron scattering by magnetic induction inhomogeneities. The study demonstrates that it is necessary to account for the contributions of the 180° domain boundaries as well as the small-amplitude localized solitons. Both these contributions produce the socalled central frequency peak with the first contribution significant near the spin flop-transition point only where it determines the integral peak intensity. The second contribution determines the peak width. The study also concludes that in analyzing the magnetic scattering of neutrons the kinks in antiferromagnets with easy axis anisotropy behave in the same manner as bions in ferromagnets. This is because the kinks in antiferromagnets are not topologic solitons in the vector field.

The Statistical Character of the Topologic Cross-Sections of Electron-Positron Annihilation Into Hadrons

18620161A Moscow YADERNAYE FIZIKA in Russian Vol 49 No 3, Mar 89, pp 834-839

[Article by A. S. Liventsova, L. A. Sanko, p A. Usik]

[Abstract] This study determines the specific form in which a statistical interpretation of the properties of topologic electron-positron annihilation cross-sections is applicable. The analysis focuses on two distributions of electron-positron annihilation events over the total number of hadrons in the final state, specifically: a truncated Poisson distribution and a truncated normal distribution. The results of the statistical analysis and parametrization of experimental data on the topologic cross-sections of electron-positron annihilation into hadrons indicate that the topologic electron-positron annihilation cross-sections in the range 14-34 GeV follow statistical (probability) laws. They are described by a truncated normal distribution of annihilation events over the total number of generated hadrons n and with a fixed n the formation probabilities satisfy a binomial distribution. It is also determined that the ratio of the average total number of hadrons to the square root of the distribution variance is a constant in the interval under analysis. This could possibly indicate the existence of KNOscaling for the event distribution over the total number of hadrons. The study also determines that the distribution of events over the number of charged hadrons cannot be reduced to a scale-invariant form.

Pulsed Excitation of Solitons in Easy-Plane Ferromagnetics

18620159a Leningrad FIZIKA TVERDOGO TELA in Russian Vol 31 No 2, Feb 89 pp 209-212

[Article by Yu. S. Kivshar, B. A. Malomed]

[Abstract] This study provides a consistent solution to the problem of pulsed soliton excitation using a light-plane ferromagnetic. The study first considers the linear excitation of a $CuRb_2Cl_2.2H_2O$ quasi-one-dimensional light-plane ferromagnetic by an inhomogeneous pulsed field. The solution of this problem is then used to derive functions as initial conditions for the sineGordon equation: the direct scattering problem is then solved and the socalled scattering data for the inverse scattering method are obtained. Exact analytic results are also obtained in other limiting cases. The study also focuses on spin waves described within the framework of the inverse scattering problem by the so-called continuous spectrum. The energy contained in nonsoliton excitations is determined from the solution of the direct scattering problem within the framework of the inverse scattering problem. It is determined that only a relatively small fraction of pulse energy is expended in soliton generation, while all remaining energy is contributed to spin waves. It is demonstrated that this approach is also useful to account for the influence of dissipation on the threshold excitation conditions of magnetic solitons.

Recording Time Intervals Between Optical Picosecond Pulses

907L0075A Leningrad PISMA V ZHURNAL TEKHNICHESKOY FIZIKI in Russian Vol 15 No 24, 26 Dec 89 pp 6-10

[Article by A.V. Selishchev and A.S. Shcherbakov, Leningrad Polytechnic Institute imeni M.I. Kalinin]

[Abstract] An instrument for recording the actual time intervals between individual ultrashort optical pulses in a sequence has been developed in which cross-correlational responses are obtained by the method of a second-harmonic beam. A plane 50%-reflectance mirror splits the beam of pulsed radiation incident at a 45° angle into two, one being transmitted to a plane high-reflectance mirror which sends it through an adjustable prismatic delay line to a $LiIO_3$ at angles which correspond to phase synchronism for second-harmonic generation in a noncollinear geometry and the other beam being reflected into plane another high-reflectance mirror which sends it directly to that same crystal. The second-harmonic pulses generated in this nonlinear crystal by interaction of the two partial beams proceed to a linear recording photodetector and, when both beams are much wider than the ultrashort pulses, then the time of entry of pulses into the crystal will determine the location of the interaction space as well as the position of the energy peak in the space distribution of the second-harmonic field. The instrument was tested on pulses of 5.2 ps duration from a source of 1.06 μm radiation, departures from the regular pulse repetition period being simulated with a delay line. Densitograms of the correlation function representing the photodetector response along the time scale were compared with that corresponding to zero time shift between interacting beams and thus to perfect balance of the two transmission channels. The results indicate that this instrument will measure time shifts in a binary optical data flux transmitted at a 10^{10} bits per second or higher rate or even higher bit rate. Figures 2; references 6.

Tunable LiF:F_2^+OH-Crystal Laser With Pumping by Cathodoluminescence

907L0075B Leningrad PISMA V ZHURNAL TEKHNICHESKOY FIZIKI in Russian 26 Dec 89 pp 21-24

[Article by I.I. Kulak, A.I. Mitkovets, and V.P Morozov, Institute of Physics imeni B.I. Stepanov, BSSR Academy of Sciences]

[Abstract] Tunable lasing of LiF:F_2^+ crystals was realized, for the first time, by pumping them with radiation from a cathodoluminescent $CdS_{1-x}Se_x$ semiconductor crystal. Wafers of 100-200 μm thickness were cut from single crystals of these semiconductor materials and cemented with an optical adhesive to 3 mm thick quartz substrates. After a surface treatment by a special technological process for maximum emissivity, these semiconductor crystals were bombarded with a 200 keV electron beams from an accelerator with a current densities up to 1 kA/cm^2 in pulses of 1.5 ns duration above the half-amplitude level. The anode, made of foil, was 1.4 cm in diameter. Luminescence spectra were recorded with a B & M Spektronik OSA analyzer. Semiconductors emitting 529 nm, 585 nm, 619 nm radiation with a 11.8 nm, 14.2 nm, 15.6 nm line width respectively were used for pumping 11.5x13x27 mm^3 large LiF crystals with a $1.2x10^{16}$ cm^{-3} concentration of F_2^+ radiative color centers. The maximum absorption coefficient of the color centers was 2.5 cm^{-1}, for 600 nm radiation, and the lifetime of the excited state was 29 ns. The lasers were pumped transversely, with the active medium contiguous to the cathodoluminophor inside an 85 mm long cavity formed by two plane mirrors. Pulses of up to 1.05 mJ energy were emitted by the laser with optimum intracavity feedback, this maximum energy corresponding to 12% of the pump energy and to 0.03% of the electric excitation energy. The authors thank G.p Yablonskiy for supplying the cathodoluminophors and for helpful discussion of the results. Figures 2; tables 1; references 4.

Amplification of Cerenkov Waves by Flow of Medium

907L0043C Leningrad PISMA V ZHURNAL TEKHNICHESKOY FIZIKI in Russian 12 Dec 89 pp 91-93

[Article by I.A. Kolmakov and N.N. Antonov]

[Abstract] The possibility of interfering Alfven and acoustic waves generating high-intensity Cerenkov radiation in a plasma when it flows in a constant parallel external magnetic field at a constant velocity relative to both sources of waves is examined, assuming a "cold" plasma with negligible energy dissipation and infinitely long beams of waves. The system of three differential vector field equations describing flow with fluctuation of all parameters except the frequencies of Alfven and acoustic waves is solved for a parabolic distribution of "sources" of nonlinear sum-frequency waves and for time-invariant perturbations. The solution obtained with the aid of a Fourier-Hankel transformation, after an appropriate change of coordinates, yields Cerenkov cones whose surfaces vary harmonically in space. The intensity of Cerenkov radiation drops fast as the condition for diffraction is reached, but the effect of diffraction remains minimal when the primary Alfven and acoustic beams are equally divergent. References 2.

UDC 530.145

Method of Generating New Exact Solutions to One-Dimensional Schroedinger Equation

907L0050B Tomsk IZVESTIYA VYSSHIKH UCHEBNYKH ZAVEDENIY: FIZIKA in Russian Vol 32 No 11, Nov 89 pp 114-116

[Article by V.G. Vagrov, A.V. Shapovalov, and I.V. Shirokov, Institute of High-Current Electronics, Siberian Department, USSR Academy of Sciences, Tomsk branch]

[Abstract] A method is proposed for generating new exact solutions to the one-dimensional generally nonsteady-state Schroedinger equation $[i\delta_t + \delta_x{}^2x - u(x,t)]$ $\varphi(x,t) = 0$, namely solutions which will yield infinitely large families of essentially new exactly resolvable potentials. An operator kernel $K(x,y;t) = \Phi(x,t)\Phi$ divides $(y,t)/A(x,t)$ is constructed where $A(x,t) = a +$ integral from x to infinity of $\Phi(z,t)\Phi$ divides $(z,t)dz$ with a = constant. Then function $\psi(x,t) = \varphi(x,t) -$ integral from x to infinity of $K(x,y;t)\varphi(y,t)dy$ is the solution to the equation $[i\delta_t + \delta_x{}^2 - V(x,t)]\Psi(x,t) = 0$ with potential $V(x,t) = u(x,t) + v(x,t)$ and $v(x,t) = 2\delta_x K(x,y,t) = -2\delta_x{}^2$ the log of the absolute value of A(x,t). The procedure can be repeated any number of times. Generating a steady-state potential $u(x,t) = u(x)$ and a steady-state solution is demonstrated on an infinitely deep rectangular potential well and a harmonic oscillator. References 13.

UDC 621.7.068

Magnetooptical Interaction in Fiber-Optics

907L0012C Moscow KVANTOVAYA ELEKTRONIKA in Russian Vol 16 No 11, Nov 89 pp 2310-2316

[Article by S.N. Antonov, A.N. Bulyuk, and Yu.V. Gulyayev, Institute of Radio Engineering and Electronics, USSR Academy of Sciences, Moscow]

[Abstract] An initially isotropic single-mode optical fiber wound into a helical coil with radius R and pitch p is considered, winding into such form giving rise to a magnetic field as well as to optical anisotropy characterized by linear and circular birefringence. The magnetooptic effect, namely modulation of the dielectric permittivity of the material by the magnetic field according to Faraday's law, is analyzed theoretically with changes in the polarization of light along its propagation through a fiber taken into account. The corresponding system of equations is solved analytically by the perturbation method, first for weak magnetooptic interaction in a short fiber and the for longer fibers. An experiment was performed with a stepped-index isotropic quartz fiber, its core having a 5 μm diameter and its shell having a 100 μm diameter. The cutoff wavelength for the LP_{11}-mode in a straight fiber segment was 670 nm. Segments 6 m in length were wound into helical coils on circular cylindrical bobbins made of a nonmagnetic material with radii ranging from 3.5 to 4.5 mm. The magnetooptic effect was measured and found to depend on the wavelength of transmitted light, with a narrow high center peak within the 600-620 nm range and a series of much smaller lateral peaks on each side of this range. Its magnitude of the magnetooptic effect was found to be proportional to the magnetic field intensity. The radiation wavelength corresponding to the strongest magnetooptic effect became shorter with a larger coil diameter. Additional optical losses were found to first peak slightly within the 560-10 range of wavelengths and then rise steeply with wavelengths exceeding 800 nm. The authors thank pM. Vetoshko for assisting in the experiment and Yu.K. Chamorovskiy for supplying the optical fibers. Figures 6; table 1; references 10.

UDC 621.373.826

Interaction With Self-Conjugation of Counterpropagating Waves in $BaTiO_3$ Crystal

907L0011C Moscow KVANTOVAYA ELEKTRONIKA in Russian Vol 16 No 9, Sep 89 pp 1863-1869

[Article by A.B. Mamayev and V.V. Shkunov, Institute of Problems in Mechanics, USSR Academy of Sciences, Moscow]

[Abstract] Interaction of counterpropagating light waves in $BaTiO_3$ crystals was studied with a continuous-wave He-Cd laser as source of 440 nm light. High-grade crystals in the form of 0.7-1 mm thick triangular plates had been grown by the Remeika method from solution in a KF melt at the Dnepropetrovsk Industrial Institute's Department of Physics. The important feature of these crystals was a high density of structural microdefects, which facilitated reading into the crystal lattice electric fields with a very small space period by interaction of counterpropagating waves, this feature overriding the drawback of strong light absorption and consequent limitation of the effective interaction space to a not more than 1 mm length. The dark conductivity of such crystals was, moreover, comparable with their photoconductivity under illumination of 1-10 W/mm^2 intensity. The small-signal gain due to interaction of a weak signal wave with a counterpropagating reference pump wave having a Gaussian form and with one having speckle structure was measured without and with bias illumination, either the pump intensity or the ratio of bias intensity to pump intensity being held constant in the latter case. The signal gain was found to be linearly dependent on whichever was varied and stimulated diffuse backscattering was found to be weak as long as the angle of pump wave incidence remained sufficiently smaller than 50°. The data are evaluated for feasibility of discriminatory self-conjugation of signal wave under steady-state conditions as well as during stimulated diffuse backscattering, which requires that the steady-state gain be locally dependent on the amplitude of the wave to be conjugated. The discrimination factor is calculated following a theoretical analysis of the process, whereupon self-conjugation of a signal wave during stimulated diffuse backscattering in a $BaTiO_3$ crystal is evaluated. Within a 0.1 Hz accuracy, measurements by interferometry revealed no frequency shift upon reflection. The authors thank V.G. Taran, Ye.Ye. Sheyko, and A.T. Kugay for growing and supplying the crystals, B.Ya. Zeldovich and N.F. Pilipetskiy for support. Figures 6; references 14.

Control of Liquid-Crystal Correctors in Adaptive Optical Systems

907L0066A Leningrad ZHURNAL TEKHNICHESKOY FIZIKI in Russian Vol 59 No 12, Dec 89 pp 35-41

[Article by V.A. Dorezyuk, A.F. Naumov, and V.I. Shmalgauzen, Department of Physics, Moscow State University imeni M.V. Lomonosov]

[Abstract] Electric feedback control of liquid-crystal correctors in an adaptive optical system is considered for compensating phase distortions in monochromatic light occurring as it propagates through a turbulent medium and through that optical system. The basic method is amplitude control, namely varying the voltage across the liquid crystal so as to produce the necessary phase delay for the extraordinary beam and to minimize the amplitude of its fluctuations. For liquid crystals with low-frequency sign reversal of dielectric anisotropy it is possible to attain higher response speed by pulse control, namely by varying the ratio of low-frequency voltage pulse and high-frequency voltage pulse duration to match the error signal. An experiment was performed with a ZhK-999 nematic liquid crystal in an electrooptic Stark-effect cell having one degree of freedom, for stabilization of the path difference between reference beam and object beam in a Twyman-Green-Williams interferometer: audio-frequency oscillator, spherical reference mirror, laser, microobjective and microdiaphragm, beam-splitting cube, collimating lens, liquid-crystal cell backed by a plane mirror, beam-splitting plate, two diaphragms, one photomultiplier followed by with a spectrum analyzer, one photomultiplier for feedback to the liquid-crystal cell. The feedback loop included a comparator with input from the photomultiplier and from a reference-voltage generator, a square-pulse voltage generator, a NAND gate, a transistor switch, and an RC-circuit preventing dissociation of liquid-crystal molecules. Both methods can be combined, high-frequency modulation of the phase delay being effected by a periodic sequence of low-frequency and high-frequency voltage pulses while global control is effected by varying the amplitude of these pulses. The feedback loop for experimental implementation of this method included a filter following the photomultiplier, a phase detector with an input from that filter and from a sine-wave voltage generator, an integrator making the system more nearly astatic, a control unit, and also an RC-circuit protecting the liquid-crystal cell. Figures 5; references 6.

Scale Effects in Kinetics of Fracture and Explosion of Solid Bodies by Impact and Problem of Simulating Far Off-Equilibrium Processes

907L0066B Leningrad ZHURNAL TEKHNICHESKOY FIZIKI in Russian Vol 59 No 12, Dec 89 pp 102-105

[Article by A.S. Balankin, A.A. Lyubomudrov, and I.T. Sevryukov]

[Abstract] Scale effects during fracture of a solid body by impact and explosion of a chemically active charge is analyzed by covering kinetic phase transitions accompanied by internal self-adaptation with attendant formation of dissipative structures and kinetic transitions from one state to another with different dissipative structures, considering also that in every system with finite dimensions there occur scaled phase transitions when critical dimensions are reached. The system of generalized Ginzburg-Landau equations describing kinetic phase transitions which occur upon impact are solved with the aid of the S-theorem, an analysis of the problem in the "laser scheme" formulation revealing three fundamentally different mechanisms of scaled phase transitions based respectively on: 1) dependence of the conditions for stability of dissipative structures on the body dimensions, shape, and constraints, 2) dependence of the characteristic scales of dissipative structures on the body dimensions, this dependence determining whether or not the conditions for self-adaptation within elements of a dissipative structure are attainable when its characteristic scales exceed the critical dimensions, 3) characteristic scales of dissipative structure independent or only weakly dependent of the body dimensions so that the conditions for internal self-adaptation are attainable when those scales exceed the critical dimensions and larger-scale dissipative structures are formed. A helical detonation spin wave can be generated and helical cracks can be formed in a cylindrical charge inside a rigid cylindrical shell made of a material acoustically stiffer than the charge material. Figures 1; references 25.

UDC 535.338

Production and Study of Metal Dimers in Supercooled Dense Plasma Flare

907L0062A Moscow TEPLOFIZIKA VYSOKIKH TEMPERATUR in Russian Vol 27 No 6, Nov-Dec 89 pp 1047-1052

[Article by S.V. Baranov, p.A. Sankevich, and S.S. Sulakshin, Scientific Research Institute of Nuclear Physics at Tomsk Polytechnic Institute]

[Abstract] Metal dimers were experimentally produced by bombardment of Fe, Cu, Mo, Pb targets with a 500 keV and 400 A/cm^2 ion beam in pulses of 80 ns duration above the half-amplitude level, this ion beam containing mostly protons having been generated in a long diode with magnetic shielding and ballistically focused onto an up to 3 x 30 cm^2 large rectilinear spot. The characteristics of the resulting plasma flare were found to depend on those of the ion beam, its energy and current density, as well as on the target material such as heat of sublimation and mean free micropath for protons. The electron concentration and the electron tempera-ture were measured for the Cu target and for the Pb target with a Cu-film coating, measurement of the electron concentration being based on the Stark widening of the 406.2 nm Cu-I line and measurement of the electron temperature being based on the ratio of 510.7 nm Cu-I line intensity to 515.3 nm Cu-I line intensity. Spectroscopy of the plasma flare revealed presence of metal dimers, the emission spectrum containing molecular dimer bands with atomic and ionic lines. Evidently, of the total ion (proton) beam energy 25-75% can be spent on vaporization of the target material with correspondingly 75-25% spent on ionization and excitation of the vapor. The

authors thank C.A. Chistyakov, V.S. Pak, and M.S. Arteyev for assisting in the experiments. Figures 5; tables 2; references 21.

UDC 536.423

Speed of Ultrasound in and Thermophysical Properties of Superheated (Metastable) Alcohols

907L0062B Moscow TEPLOFIZIKA VYSOKIKH TEMPERATUR in Russian Vol 27 No 6, Nov-Dec 89 pp 1078-1085

[Article by V.N. Chukanov and I.L. Kostromin, Uralsk Polytechnic Institute]

[Abstract] An experimental study of superheated alcohols was made, for a determination of their thermophysical properties in this metastable state on the basis of ultrasonic measurements under temperature and pressure control. The upper part of the test cell made of Pyrex glass was an acoustic cell with with a 5:1 ratio of diameter to wall thickness and split by a planeparallel partition. Several acoustic cells of different sizes were used, their volumes covering the 1-2 cm^3 range so that the length of the acoustic path could be varied over the 0.4-0.8 cm range. The test cell was equipped with thermostatic control within 0.01 K, the temperature inside was measured with either a platinum resistance thermometer accurate within 0.02 K or with a Chromel-Copel thermocouple accurate within 0.05 K. Pressure was measured with a mechanotropic gage and an analog-digital transducer, an electromagnetic valve dumping the pressure fast while a contactor simultaneously connected the instruments for measurements under no load. The time taken by ultrasound to travel through the cell walls, the fluid (alcohol) inside, and then through a sound guide was measured with an electroacoustic system consisting of sound radiator and a sound receiver ($LiNbO_3$ plates), and an audio-frequency oscillator generating a square pulse for excitation of the sound radiator. The speed of ultrasound in the fluid was measured along isotherms under various pressures. Measurements were made with methanol along seven isotherms covering the 374.0-444.3 K range, with ethanol along nine isotherms covering the 373.3-463.1 K range, with n-butanol along ten isotherms covering the 403.6-502.9 K range, and with n-pentanol along eight isotherms covering the 433.9-513.8 K range. The measurements along each isotherm were made under pressures from atmospheric to saturation, in 0.1 MPa steps in the metastable region: for methanol from 0.382 MPa down to 0.1 MPa at 374.0 K and from 2.21 MPa to 0.1 MPa at 444.3 K, for ethanol from 2.14 MPa down to 0.3 MPa at 463.1 K. On the basis of the data were determined both adiabatic and isothermal compressibilities and the Poisson constant of these alcohols at each temperature-pressure point within the metastability region, their density at each point being known and the speed of ultrasound at each point also having been measured. An analysis of the data reveals that the speed of ultrasound in each of these substances remains a continuous function of pressure upon crossover through the equilibrium line farther and farther into the metastability region, this being an experimental confirmation of the continuity of the second derivatives and of some third derivatives of thermodynamic potentials during transition from the stable to metastable state. Figures 4; tables 2; references 14.

UDC 517.9:538.5

Analyzing Resonance Absorption of Electromagnetic Waves by Method of Discrete Sources

907L0057B Moscow VESTNIK MOSKOVSKOGO UNIVERSITETA, SERIYA 3: FIZIKA, ASTRONOMIYA in Russian Vol 30 No 6, Nov-Dec 89 pp 7-11

[Article by Yu.A. Yeremin and A.G. Sveshnikov, Chair of Mathematics]

[Abstract] A methodology is developed for estimating the amount of electromagnetic energy which live tissue has absorbed upon its interaction with electromagnetic radiation, the mode of this interaction depending on the wavelength and on the polarization of incident radiation. The methodology of absorption dosimetry utilizes the phenomenon of resonance absorption by biological scatterers and involves its mathematical simulation by the method of discrete sources. As the mathematical model is selected diffraction of a linearly polarized external electromagnetic field by a homogeneous dielectric body of revolution. An approximate solution to this problem of diffraction is obtained in the form of a linear combination of elementary functions which satisfies the applicable Maxwell equations at the dielectric surface and the condition of radiation at infinity. A plane incident wave is then expanded into a series which satisfies the boundary condition at the scatterer surface. A recursive system of linear algebraic equations is thus obtained for calculating the unknown amplitudes of discrete sources. Each space harmonic can be analyzed upon collocation of the fields on the generatrix of the body of revolution. This methodology facilitates the determination of the total crosssection for absorption, which only requires calculating the cross-section for scattering. Both cross-sections depend on the wavelength of incident radiation and on the angle of incidence. This is demonstrated on radiation of 3-300 cm wavelengths incident at $0\text{-}\pi/2$ angles on a spheroidal body such as a laboratory mouse. The numerical calculations, based on diffraction of plane waves by oblong spheroids, have been programmed so as to yield the dependence of the total cross-section for scattering on the characteristic dimension of the body (major axis of large ellipse) relative to the radiation wavelength. Figures 3; tables 1; references 7.

Spatial Behavior of Compressed States of Light and Quantum Noise in Optical Images

907L0035A Moscow ZHURNAL EKSPERIMENTALNOY I TEORETICHESKOY FIZIKI in Russian Vol 96 No 6 (12), Dec 89 pp 1945-1956

[Article by M.I. Kolobov and I.V. Sokolov, Leningrad State University]

[Abstract] Multimode compression of light is considered from the theoretical standpoint of quantum electrodynamics and from the practical standpoint of producing a regular photon flux to impinge on a detectorcounter. The possibility of compressed light generating photon count statistics regular not only in time but also in space and thus suitable for optical heterodyning is examined along with the necessary conditions for it. Analysis of the problem begins with a description of photon count and light intensity fluctuations in both space and time domains, as the basis for calculation first of their time-frequency and space-frequency spectra and then of the quantum noise in the produced image. Suppression of natural fluctuations in a heterodyne receiver of compressed light is evaluated next, the degree of their suppression and the heterodyne efficiency depending not only on the form of mode locking but also on the free propagation and the focusing of compressed light. On the basis of this analysis and known experiments is considered the physical feasibility of optical measurements and data transmission with low quantum noise in both space and time domains. Figures 5; references 30.

Nonlinear Generation of Sound in Metals Carrying Current

907L0035B Moscow ZHURNAL EKSPERIMENTALNOY I TEORETICHESKOY FIZIKI in Russian Vol 96 No 6 (12), Dec 89 pp 2149-2162

[Article by N.M. Makarov, F. Perez-Rodriguez, and V.A. Yampolskiy, Institute of Radiophysics and Electronics, UkSSR Academy of Sciences, and Kharkov State University imeni A.M. Gorkiy]

[Abstract] Generation of longitudinal sound waves in a metal by the nonlinear electromagnetic mechanism is analyzed theoretically, the metal being in a constant external magnetic field parallel to its surface which has been excited by an incident monochromatic plane electromagnetic radio wave. Both deformation and induction mechanisms of electron-phonon interaction are taken into account, only the quasi-static state with the sound frequency much lower than the electron relaxation frequency and a correspondingly anomalous skin effect being considered. The equation of elasticity is solved first generally for longitudinal acoustic vibrations in a metallic half-space. Asymptotic solutions in both acoustic long-wave and short-wave limits are obtained for the case of a weak nonlinearity, namely a weak constant magnetic field and a weak alternating magnetic field of the incident radio wave. Next is considered a strong nonlinearity with the metal in the currentcarrying state owing to a strong alternating magnetic field and thus a strong induction mechanism. In the latter case the acoustic field contains a series of sharp spikes and its dependence of its distribution on the magnitude of the constant external magnetic field is found to be hysteretic. Figures 6; references 18.

UDC 535.56

Rotation of Light Polarization Plane in Isotropic Dispersive Medium

907L0046B Leningrad OPTIKA I SPEKTROSKOPIYA in Russian Vol 67 No 4, Oct-Dec 89 pp 873-876

[Article by S.V. Cherepitsa]

[Abstract] The possibility of rotation of the polarization plane in anisotropic dispersive medium and resulting birefringence by it is demonstrated theoretically for light with two nondegenerate intrinsic polarization states characterized by a different energy and a different magnitude of the wave vector each. It is demonstrated on the basis of the Maxwell wave equation for light beam propagating through a dielectric nonmagnetic medium and with the aid of the Pauli matrix. As a specific example is considered a light beam with dextrorotary circular polarization and thus a nondegenerate helicity in an electric field oscillating at resonance frequency. As the beam penetrates deeper into such a medium whose dielectric permittivity varies parametrically in time, its circular polarization oscillates periodically between a dextrorotary and a levorotary one. The light beam circularly polarized before entering the medium will thus exit from the medium as a linearly polarized one with two wave numbers and two frequencies, the linear polarization representing an equipollent superposition of the two circular ones, if the thickness of the traversed layer is $L=(\pi/2 + 2N\pi)/(k_+^+ - k_+^-)$ with N denoting a positive integer. This effect is called r-f polarization flipping of light, in analogy to spin flipping of polarized particles with magnetic momentum by combined action of a rotating r-f magnetic field and a constant one. For correct analysis of the resulting birefringence, the latter is described in terms of wave packets. References 5.

Optical Discharge in Fused Quartz

907L0024A Moscow TEPLOFIZIKA VYSOKIKH TEMPERATUR in Russian Vol 27 No 5, Sep-Oct 89 pp 833-837

[Article by N.Ye. Kask, Ye.G. Leksina, G.M. Fedorov, and D.B. Chopornyak, Scientific Research Institute of Nuclear Physics at Moscow State University imeni M.V. Lomonosov]

[Abstract] Optical discharge was for the first time obtained in the bulk of fused quartz, by excitation with millisecond laser pulses. In the experiment was used a Nd-glass laser emitting pulses of 10 ms duration at the

1.06 μm wavelength with a power density of approximately 1 MW/cm^2 on the target. The instrumentation included a shutter for cutoff at the appropriate instants of time, a high-speed camera for recording the propagation of optical-discharge plasma, a displacement interferometer, an ILM 120 probing Ar-Kr laser, an SI-8-200U ribbon flash lamp as source of a standard continuous spectrum, and a photoelectric apparatus for recording glow as well as laser radiation. The threshold temperature for initiation of optical discharge was determined with the aid of a tungsten foil touching the quartz surface, the beginning of optical discharge being indicated by a change in the intensity of its glow at a temperature within 3100-3500 K. The evolution of the plasma state was tracked with the camera, optical discharge in the quartz having been initiated by focusing the laser radiation either onto a spot inside with a high thermal absorption coefficient or onto the surface in thermal contact with a heat absorber (graphite, metal). The experimental data on plasma glow kinetics in quartz or quartz glass are evaluated analytically in terms of light absorption by the material around the discharge path, energy balance, and structurization during fast plasma cooling. They are also compared with available data on optical discharge in silicate glass. Figures 5; references

Examination of Energy Superstructure in Lithium

907L0007A Moscow PISMA V ZHURNAL EKSPERIMENTALNOY I TEORETICHESKOY FIZIKI in Russian Vol 30 No 7, 10 Oct 89 pp 323-324

[Article by Yu.M. Kobzar, N.N. Bodnar, V.Ya. Kozych, and V.G. Kovtun, Institute of Physical Mechanics, UkSSR Academy of Sciences]

[Abstract] The spectrum of photon emission by excess electrons in light metals during transition of excited energy states to lower ones was studied, such a transition following intraband and interband transitions during bombardment of such a metal by slow electrons. The experiment was performed with a lithium thick-film target on a Si(111) single-crystal substrate. The film had been deposited by the vacuum evaporation process from a batch of 99.999% pure Li. Measurements were made first at room temperature, with the target inside a high-vacuum chamber (70 nPa) and radiation extracted through a sapphire window. Visible radiation was recorded with an FEU-84 photomultiplier in the photon count mode and infrared radiation was recorded with a cold photoresistor in the synchronous detection mode. The energy spectrum was found to contain three anomalous intensity peaks, two of them within the visible range at E_1= 2.85 eV and at E_2= 1.85 eV respectively predicted theoretically on the basis forward interband transitions near points N and F in the energy band structure of lithium. The third peak at E_3= 0.23 eV within the infrared range, attributable to charge density waves and attendant formation of a superstructure containing various energy gaps between bands, should correspond to a photon energy equal to twice the energy gap at the band boundary (which is characteristic of the recombination radiation spectrum of electrons pulled into these bands by an external energy source. Subsequent measurements with lithium film on a substrate cooled to 77 K yielded the same results, but cooling the film to 77 K altered the form of the emission spectrum and cooling it to 4.2 K raised the E_3-peak as a result of a martensite transformation in the lithium lattice with attendant stabilization of charge density waves. Figures 2; references 9.

Nonlinear Theory of Relativistic Emitters on Rectilinear Free-Electron Beams

907L0003A Moscow ZHURNAL EKSPERIMENTALNOY I TEORETICHESKOY FIZIKI in Russian Vol 96 No 3 (9), Sep 89 pp 865-877

[Article by M.V. Kuzelev, V.A. Panin, A.P Plotnikov, and A.A. Rukhadze]

[Abstract] A nonlinear theory of stimulated scattering of electromagnetic waves by dense relativistic electron beams is constructed, for analysis of possible mechanisms causing instability of such beams in the field of two, incident and reflected, electromagnetic waves. A strong longitudinal magnetic field inhibiting transverse motion of electrons is assumed to be present. A system of dimensionless nonlinear equations describing the dynamics of stimulated scattering by free electrons in such a beam is derived on this basis from the equation of one-dimensional relativistic electron motion. Calculations yield a new mechanism of stimu-lated scattering, namely energy phasing stabilizable by full electron momentum modulation, in addition, depending on the density of the electron beam and its degree of relativity, to Raman collective scattering stabilized by lock-in with a Langmuir beam wave or with a nonlinear frequency shift and Thomson one-frequency scattering stabilized by lock-in with a combination-frequency wave. Figures 3; tables 1; references 15.

Scattering of Light in Gyrotropic Media

907L0003B Moscow ZHURNAL EKSPERIMENTALNOY I TEORETICHERSKOY FIZIKI in Russian Vol 96 No 39), Sep 89 pp 926-937

[Article by A.Yu. Valkov, V.P Romanov, and A.N. Shalaginov, Leningrad State University]

[Abstract] Scattering of light in media with spatial dispersion is analyzed on the basis of electrodynamic theory and Onsager's symmetry principle. The material equation containing the dielectric permittivity tensor is derived first for a medium with a weak spatial dispersion and then for a spatially homogeneous gyrotropic one. Scattering of light attending fluctuation of the dielectric permittivity in an isotropic gyrotropic medium is considered next, then in liquid mixtures, in cholesteric liquid crystals, and in ferroelectric crystals with isotropic-to-ordered phase transition. Relations are obtained

for the scattering intensity in each case, its magnitude depending on the direction and on the polarization. Figures 1; references 28.

UDC 535.375.5:551.51

Measurement of Cross-Sections for Spontaneous Raman Scattering by Some Atmospheric Gases Excited by KrF-Laser Radiation

18620237B Leningrad OPTIKA I SPEKTROSKOPIYA in Russian Vol 66 No 5, May 89 pp 1043-1045

[Article by M. A. Buldakov, I. I. Ippolitov, V. M. Klimkin, I. I. Matrosov, and V. M. Mitchenkov]

[Abstract] An experimental study of spontaneous Raman scattering (SRS) by four constituent gases of the atmosphere (O_2, H_2O, CO_2, O_3) was made, their cross-sections for such scattering being measured relative to the Q-branch of N_2 upon excitation of their molecules by a KrF-laser. Radiation scattered by O_2 molecules and H_2O molecules at a 180° angle and at a 90° angle was measured with an SRS-lidar and with a conventional SRS-spectrometer respectively. Only radiation scattered by CO_2 molecules and O_3 molecules at a 90° angle was measured, with the conventional SRS-spectrometer. A statistical analysis of the differential cross-sections, after they had been normalized to that of N_2, reveals a wide variance of the H_2O scattering cross-section and resonance increases of O_2 and O_3 scattering cross-sections. The data are compared with known data on spontaneous Raman scattering of fourth-harmonic YAG:Nd-laser radiation (wavelength 266 nm) and Kr-laser radiation (wavelength 337 nm) by these gases. Tables 1; references 13: 7 Russian, 6 Western.

UDC 535.375+621.373:535

Conformational Analysis in Liquid by Active Polarization Spectroscopy of Raman Scattering: Experimental Implementation of Principle of Holographic Spectroscopy

18620237C Leningrad OPTIKA I SPEKTROSKOPIYA in Russian Vol 66 No 5, May 89 pp 1046-1051

[Article by A. A. Ivanov, N. I. Koroteyev, R. Yu. Orlov, and A. I. Fishman]

[Abstract] The theory of conformational analysis by active polarization spectroscopy of Raman scattering is reviewed, the high resolution of this method facilitating separation of contiguous resonance lines. This method is analogous to holographic spectroscopy, inasmuch as a change of the polarization angle is equivalent to a change in the viewing angle. The principle of holographic spectroscopy was, accordingly, applied to conformational analysis by active polarization spectroscopy of Raman scattering in liquid n-pentane over the 150-300 K temperature range, of particular interest being the 800-960 cm^{-1} frequency range. Measurements were made with an automatic spectrometer aided by a DZ-28 minicomputer, molecules of the liquid specimen being excited by Ar-laser radiation (wavelength 488 nm) and spontaneous Raman scattering being recorded through a DFS-24 dual monochromator. The analysis has confirmed that liquid n-pentane is a mixture of three isomers (trans-trans, trans-levo, levo-levo) and has quantitatively identified the parameters of their six vibrational resonances (840.5, 841, 863, 868, 910, 920 cm^{-1} at four temperatures (153, 193, 233, 293 K). The authors thank S. A. Akhman for support and for discussion of the results. Figures 2; tables 1; references 10: 7 Russian; 3 Western.

UDC 535.33+535.375.5:546.811

Coherent Anti-Stokes Scattering of Light by Excited Sn Atoms in Flare of Laser Plasma

18620237D Leningrad OPTIKA I SPEKTROSKOPIYA in Russian Vol 66 No 5, May 89 pp 1182-1185

[Article by S. B. Bunkin, S. M. Gladkov, A. M. Zheltikov, N. I. Koroteyev, V. B. Morozov, M. V. Rychev, and A. B. Fedorov]

[Abstract] An experiment with coherent anti-Stokes scattering of light by excited Sn atoms has established the feasibility of analyzing Sn vapor by this method, provided the vapor has been excited into the J = 1 state (transition from J = 0 ground state to J = 1 state is forbidden). A YAG:Nd laser was used for boosting the vaporization process as well as for excitation of the vapor. A tunable dye laser (rhodamine 6G) was used for mixing so that anti-Stokes scattering with a difference-frequency (f_1-f_2) resonance could be recorded upon excitation at combination frequency $2f_1$-f_2 (f_1-frequency of second-harmonic YAG:Nd-laser radiation, f_2-frequency of dye-laser radiation). The depolarization coefficient and components of the cubic susceptibility tensor were measured by the method of polarization spectroscopy. A comparison of the results with theoretical estimates of depolarization at the given Sn-vapor line reveals a discrepancy, indicating presence of an antisymmetric component in the Raman scattering tensor. The authors thank S. A. Akhmanov for support and attentiveness. Figures 2; references 9: 6 Russian, 3 Western.

UDC 535.34:548.0

Transient Absorption Spectra of Bleachable Cr-Centers in Rare-Earth Garnets

18620237E Leningrad OPTIKA I SPEKTROSKOPIYA in Russian Vol 66 No 5, May 89 pp 1189-1190

[Article by Ye. N. Karnaukhov, A. V. Lukin, L. G. Popov, E. E. Penzina, L. I. Ruzhnikov, and V. A. Sandulenko]

[Abstract] The electronic structure of phototropic centers in rare-earth garnets (Y-Al, Y-Sc-Ga, Gd-Sc-Al, Gd-Sc-Ga) was for the first time studied experimentally

by the method of picosecond laser absorption spectroscopy. Specimens of these garnets, having been doped with Cr and an alkali-earth metal, were excited with radiation pulses of 2 mJ energy ND 30 ps duration from a YAG:Nd laser (wavelength 1,060 nm) covering a spot 1 mm in diameter. The initial transmission coefficient of all garnets was within the 0.50-0.60 range. The transient absorption spectra were measured with probing pulses of 460-1,100 nm radiation, with zero time delay. The spectra of Y-Sc-Ga and Gd-Sc-Al were found to be almost identical to that of Gd-Sc-Ga, except for slight differences in the longwave region. A comparison with known reabsorption spectra of these garnets indicates that all three absorption bands belong to the same center, namely the Cr^{4+} ion, and are associated with its transitions from the ground state $^3A_2$ to the excited states $^3T_2$, $^3T_1$, $^1T_2$ respectively. Figures 1; references 4: Russian.

UDC 535.2

Doubling the Frequency of Compressed Light

18620237F Leningrad OPTIKA I SPEKTROSKOPIYA in Russian Vol 66 No 5, May 89 pp 1190-1192

[Article by A. V. Belinskiy and A. S. Chirkin]

[Abstract] Conversion of compressed coherent light into second-harmonic radiation is analyzed theoretically, this nonlinear conversion being necessary when the source of compressed light such as an efficient degenerate parametric amplifier converts the pumping light into second-subharmonic radiation. The analysis is based on the two equations of motion for the photon generation operator and the photon annihilation operator respectively, both slowly varying, in the Heisenberg representation of a fundamental wave and a harmonic wave propagating in the same direction. References 12: 2 Russian, 10 Western.

UDC 535.33.34:539.19(047)

Eighth All-Union Symposium on High-Resolution Spectroscopy

18620237G Leningrad OPTIKA I SPEKTROSKOPIYA in Russian Vol 66 No 5, May 89 pp 1193-1195

[Article by Yu. N. Ponomarev and V. I. Zakharov]

[Abstract] The Eighth All-Union Symposium on High-Resolution Spectroscopy, organized by the Institute of Atmospheric Optics (Siberian Department, USSR Academy of Sciences) and held on 3-5 June 1987 in Krasnoyarsk, was split into five sections. Section 1 dealt with latest theoretical research on the spectra of molecules and radicals, including effects of intramolecular interactions and of external fields. Section 2 dealt with experimental research on high-resolution spectra of molecules, the main object of both theoretical and experimental research having been absorption spectra, fluorescence spectra, and Raman scattering spectra. Section 3 dealt with spectroscopy of intermolecular interactions in the gaseous phase. Section 4 dealt with spectroscopy of intensity fluctuations, including its practical application to data gathering and its orientation toward quantum optics. Section 5 dealt with technical problems of high-resolution spectroscopy such as limitations on resolution and sensitivity of instruments, feasibility of wideband tunable solid-state lasers, development of an automatic $BeAl_2O_4$(alexandrite)-laser spectrometer, development of new nonlinear crystals to serve as efficient frequency converters for high-resolution infrared spectroscopy, construction of an atomic-absorption mercury analyzer with Zeeman correction of background noise, and construction of a third-generation microwave spectrometer.

Scanning Tunnel Microscope for Analysis of Film Growth Processes

18620164C Leningrad PISMA V ZHURNAL TEKHNICHESKOY FIZIKI in Russian Vol 14 No 24, Dec 88, pp 2273-2277

[Article by Yu. A. Bityurin, D. G. Volgunov, A. A. Gudkov, M. G. Kuzevanov, V. L. Mironov, A. A. Petrukhin

[Abstract] This study provides a brief description of a scanning tunnel microscope design for use in conjunction with a high-vacuum film deposition set, and its capabilities are illustrated based on an investigation of the surface relief of film structures. The microscope installation is used in conjunction with an automation system which is required to control microscope operation, as well as data acquisition and processing. The system utilized in the present article consists of an LSI 11/23 HYTEC computer, a 40 megabyte Winchester disk and CAMAC interface equipment. The lower resonant frequency of the microscope design was determined to be approximately 4 kHz. This made it possible to achieve a scanning rate of approximately 1000 points per second and to recover a standard 128 by 128 element frame in 30 seconds. This system was used to investigate pyrolitic graphite surfaces and various metallic films. Regions with good periodicity on atomic scales were detected on the pyrolitic graphite surfaces, making it possible to achieve angstrom resolution in the X, Y plane. It was established from a series of measurements that plane drift did not exceed 3 angstroms per minute. The experiments revealed that this microscope assembly has good resolution and temperature stability.

UDC 533.95

Role of Space Charge in Nonlinear Theory of Plasma Interaction With Relativistic High-Current Electron Beam

907L0087A Moscow FIZIKA PLAZMY in Russian Vol 16 No 1, Jan 90 pp 19-26

[Article by Ye.A. Galstyyan and N.I. Karbushev, Moscow Institute of Radio Engineering, USSR Academy of Sciences]

[Abstract] Nonlinear steady-state interaction of a relativistic monoenergetic high-current electron beam and a cold electronic plasma in a strong magnetic field is analyzed, principally for the role of the space charge in such a process. The theory which describes this interaction is, in the approximation of a plasma with a linearly frequency-dependent dielectric permittivity and assuming a linear motion of the plasma electrons, reduced to a system of two nonlinear equations describing the motion of beam electrons in the electric fields of the space charge and of the synchronous plasma wave respectively plus an equation for the amplitude of the longitudinal component of that latter field. This system of equations includes the integral law of energy conservation and its characteristic equation yields the range of frequency deviation within which a plasma wave can be exponentially amplified. The electron beam is assumed to enter the interaction space with both charge and current compensation and with neither density nor velocity modulation. Plasma and beam are assumed to have equal equilibrium electron concentrations. The system of equations has been solved numerically for an infinitely wide relativistic electron beam and an wave of magnetized plasma obliquely intersecting it. The results indicate how the frequency deviation, the longitudinal coordinate of the first maximum of the wave field amplitude, and the maximum fraction of kinetic energy extracted from the electron beam depend on the normalized beam current strength, also how the maximum fraction of kinetic energy extracted depends on the frequency deviation. The role of the beam space charge in beam-plasma interaction increases with higher beam electron concentration, especially when the beam current is high and when the frequency deviation is small. Figures 4; references 22.

UDC 533.9

Double Stimulated Mandelshtam-Brillouin Scattering in Plasma in Field of Two Light Waves

907L0087B Moscow FIZIKA PLAZMY in Russian Vol 16 No 1, Jan 90 pp 46-55

[Article by V.P Silin, V.T. Tikhonchuk, and M.V. Chegotov, Institute of Physics imeni pN. Lebedev, USSR Academy of Sciences]

[Abstract] Pumping of a plasma with two plane electromagnetic waves having generally different amplitudes, frequencies, and wave vectors is considered, a homogeneous plasma layer of uniform thickness reflecting them specularly and thus finding itself in the field of four waves: electromagnetic waves: the two incident ones and the corresponding two reflected ones. Scattering of two waves by a common sound wave propagating along the plasma layer is analyzed and the distance at which such a scattering can occur is established in accordance with the theory of double stimulated Mandelshtam-Brillouin scattering, assuming the two pumping waves have the same frequency and direction. The problem is solved for scattering of one incident wave and the corresponding reflected wave with generally different frequency and wave vector. Their scattering can be coherent with each wave scattered separately, or the resultant pump field of the two incident waves can be that of a plane wave whose amplitude and phase are smoothly modulated in time and space. Depending on the wave vector of the sound, two processes are possible in the former case: only two Stokes components are generated in the SS-mode, a Stokes component and an anti Stokes component are generated in the SA-mode. The threshold gain is found to be twice as high for the SA-mode than for the SS-mode when the scattering gain is the same or nearly the same for both incident and reflected waves. The analysis of double stimulated M-B scattering in a plasma under conditions of two-wave pumping is extended to conditions of pumping by two laser beams with the same frequency which intersect within a spot in the plane of the of the target surface, with emphasis on the differences between this process and other modes of stimulated M-B scattering or backscattering. Figures 2; references 7.

UDC 533.9

Acceleration of Ion Cluster by Phase-Modulated Slow Cyclotron Wave in Relativistic Electron Beam

907L0087C Moscow FIZIKA PLAZMY in Russian Vol 16 No 1, Jan 90 pp 91-94

[Article by I.V. Bachin, V.G. Dorofeyenko, and V.B. Krasovitskiy, Rostov State University]

[Abstract] The possibility of accelerating a solitary ion cluster along a relativistic electron beam which propagates through a homogeneous wave system in a strong constant longitudinal magnetic field is demonstrated theoretically, the phase velocity of the driving wave being raised by time modulation of the electron beam and acceleration of the cluster then being effected by raising the frequency at the entrance to the wave system. With only one ion cluster on the acceleration path, continuous acceleration requires a sequence of accelerating pulses at the entrance. A relativistic electron beam of finite width in vacuum is considered, the cyclotron frequency of its electrons being much higher than its Langmuir frequency. First is solved the nonlinear equation for the beam radius as a function of the longitudinal coordinate and of time. Subsequent solution of the

equation of motion for an ion in this system reveals that the mechanism of ion acceleration is phase modulation of the cyclotron wave, which produces in the electron beam a wave whose frequency and wave vector vary in time. Figures 3; references 7.

Possibility of Focusing Flux of Expanding Laser Plasma With Magnetic Lens

907L0058B Leningrad ZHURNAL TEKHNICHESKOY FIZIKI in Russian Vol 59 No 11, Nov 89 pp 94-96

[Article by D.V. Strelnikov and G.A. Sheroziya]

[Abstract] The possibility of focusing an expanding laser plasma with a magnetic lens was studied in an experiment in which 1.06 μ radiation from an LTI-403 neodymium laser was focused on an aluminum target so as to ensure a power density of 2.10^9-10^{10} on the target surface. The target was being rotated so as to prevent formation of a crater while the same amount of material was sputtered by each laser radiation pulse. A short solenoid with 13,500 turns of copper wound around a 1 m long drift tube served as magnetic lens focusing the ionic aluminum plasma into a collector, a Faraday cylinder, through the approximately 0.1 mm in diameter center hole in a diaphragm in front of it. A vacuum of 5.10^{-6} mm Hg was maintained inside the drift tube so as to ensure recombinationless passage of ions from the target to the collector. The tube as well as all lens components and the collector diaphragm were made of conducting materials and were grounded so as to shield the plasma beam from external electrostatic fields. The lens (solenoid) current was varied from 0 to 100 mA and the magnitude of the collector output signal served measure of the focusing effect. Its magnitude was found to be maximum and the radial profile of the plasma beam in the plane of the diaphragm to have the sharpest single peak, within a 1 mm radius around the center, when the lens current was 3 mA. The focusing power of the lens was found not to depend on the direction of the magnetic lines of force. The resultant focal length, geometrical mean of the focal lengths for ions and for electrons respectively when all move at the same velocity, is therefore evidently proportional to their velocity squared and inversely proportional to the lens current squared. The dependence of the optimum lens current on the ion mass was studied with C, Al, Fe, Cu, Mo, and Ta targets, taking into account that dependence of the focal length of the lens on the ion velocity. The results of this experiment indicate that that focal length is directly proportional to the ion mass, the experimental error not exceeding 30%. Figures 2; references 4.

UDC 533.951

Oscillating Light-Activated Detonation in Laser Plasma

907L0082A Moscow FIZIKA PLAZMY in Russian Vol 16 No 2, Feb 90 pp 203-208

[Article by R.A. Liukonen, I.V. Kurnin, and A.M. Trofimenko]

[Abstract] An experimental study of transient processes occurring behind the shock wavefront in a cold plasma produced by a CO-laser beam was made, under conditions of low radiation intensity within the 10^6-10^9 W/cm^2 range corresponding to light-activated detonation. The laser emitted radiation within the 5-6 μm range of wavelength in pulses of up to 0.9 kJ energy and 50-100 μs duration with a 15 μs rise time. A plasma was produced on the surface of a target in the focal plane of a lens with a focal length of 50 cm. The plasma dynamics were recorded by a highspeed camera in either the schlieren or the shadowgraph mode. Two infrared detectors and two calorimeters were provided for respectively recording and measuring the parameters of incident laser pulses and of infrared radiation reflected by the target plasma. X-ray emission by the plasma was recorded by a NaCl scintillation detector with fiber-optic coupling to a photomultiplier. The experiment revealed oscillatory detonation by laser radiation and specular reflection of laser radiation by the plasma, the reflection coefficient being anomalously high. Formation of a plasma under the given conditions evidently occurs in an avalanche mode, as the intensity of laser radiation at the focus of the lens had reaches the level just sufficient for optical breakdown. A shock wave is then generated which propagates into the neutral gas around the plasma which compresses it and heats it up, but keeps its absorption coefficient low so that it remains transparent to the laser radiation and the latter becomes effectively absorbed by the plasma within the region where the electron concentration continues to rise. This causes overheating and spherical expansion of the plasma, but the attendant compression of the surrounding gas tends to slow down the expansion and to cool the overheated plasma so that it becomes more transparent to the laser radiation and the latter will be more effectively absorbed somewhere else. There the same sequence of events is repeated and so the detonation front jumps from spot to spot behind the shock wavefront. An explanation of this phenomenon on a theoretical basis is found by reference to the self-focusing of laser radiation in a nonhomogeneous plasma. The equation for the amplitude of the electric field of a converging laser beam propagating through such a plasma in the direction of its density gradient includes a term which contains the second derivative with respect to the corresponding coordinate. The equation thus describes a laser beam whose self-focusing length is comparable with its initial diameter and thus reflects the actual condition of the experiment. Figures 5; references 11.

UDC 533.951

Transport Model of Canonical Electron Temperature and Pressure Profiles in Tokamak

907L0082B Moscow FIZIKA PLAZMY in Russian Vol 16 No 2, Feb 90 pp 216-224

[Article by Yu.N. Dnestrovskiy, S.Ye. Lysenko, and K.N. Tarasyan, Institute of Atomic Energy imeni I.V. Kurchatov]

[Abstract] A transport model of radial electron temperature and pressure profiles in tokamaks is constructed which considers deviation of these profiles from their canonical form. This model is adequate for analysis of T-10 experiments with high-power electron-cyclotron-resonance pumping and JET experiments with ion-cyclotron-resonance pumping after pellet injection, also for description of the L → H transition which improves the plasma confinement in the DIII-D tokamak. The simplest model of canonical profiles is a system of two transport equations in which the thermal flux being expressed as the sum: neoclassical flux Γ_{neo} + convective flux $\Gamma_{conv} + \Gamma_{T-11} + \Gamma_{PC} + \Gamma_{mix}$, where $\Gamma_{conv} = 5\Gamma_n T_e/2$ (Γ_n is the particle flux known from the experiment, T_e is the electron temperature) and Γ is the thermal flux component which appears when the the radial $T_e(r)$ profile deviates from its canonical form. This model is not adequate for those experiments and, therefore, has been expanded into a transport model which allows a canonical profile to be "forgotten" so that the actual radial pressure profile is more adequately described by inclusion of a "forgetting" factor. The new model is based on the hypothesis that a plasma with a pressure profile deviating from its canonical form "forgets" the canonical pressure profile and the thermal flux component Γ_{PC} then becomes negligible. The farther the actual profile $p_e(r)$ deviates from the canonical one $p_{ec}(r)$, the less influential will the latter remain and beyond some critical deviation it will be completely "forgotten". On the basis of this new model are, for illustration, the H-mode of plasma confinement with a peaking plasma density profile and experiments with electron-cyclotron-resonance pumping. The authors thank Yu.V. Yesipchuk and K.A. Razumova for providing the experimental data, V.S. Mukhovatov and S.V. Neudachin for discussing the results. Figures 11; references 14.

UDC 533.591.8

Autowave Transfer in Plasma

907L0041A Moscow FIZIKA PLAZMY in Russian Vol 15 No 12, Dec 89 pp 1479-1483

[Article by I.p Zavershinskiy, Ye.Ya. Kogan, A.S. Mikhaykov, S.S. Moiseyev, and A.B. Samokhin, Kuybyshev State Pedagogical Institute imeni V.V. Kuybyshev]

[Abstract] Heat transfer by an ignition autowave triggered in a comionized nonhomogeneous plasma and propagating through it is analyzed theoretically, assuming that the heat transfer from an ohmic source takes place through a medium where the electron temperature relaxation time is much longer than the period of the external electric field. Considering that a standing autowave produces a temperature distribution in the plasma which depend only on the distribution of heat sources and on neither initial nor boundary conditions, the corresponding equation of heat conduction is formulated for an isotropic magnetized plasma with the electronic thermal conductivity reflecting all these plasma characteristics. The temperature dependence of the electronic thermal conductivity and of the frequency of electron-ion collisions at an electron temperature equal to the ion temperature is disregarded, as are also the usually slow variations of the ion temperature. The solution to this equation for the steady-state electron temperature reveals an unstable steady state within a bounded temperature range, the steady state being stable at temperatures below and above that range. On the basis of this result is considered the possibility of autowave relaxation of perturbations in the steady-state plasma temperature profiles. With the aid of the Kolmogorov-Petrovskiy-Piskunov equation for the velocity of an autowave in a temperature field with a slowly varying steady-state profile, this possibility is established for weakly nonlinear perturbations of the temperature profile within the lower temperature range of stable steady state. Figures 3; references 6.

UDC 533.932

Kinetics of Argon Beam Plasma in Electric Field Induced by Both Beam and Plasma Currents

907L0041B Moscow FIZIKA PLAZMY in Russian Vol 15 No 12, Dec 89 pp 1508-1512

[Article by K.S. Gochelashvili, V.I. Klimov, and A.M. Prokhorov, Institute of General Physics, USSR Academy of Sciences]

[Abstract] Experimental data on interaction of argon and an electron beam are interpreted on the basis of a semiempirical model which accounts for the influence of the electric field induced by both the electron beam current and the argon plasma current. In the experiments a nearly relativistic approximately 1 MeV electron beam with a 2.3 cm radius, the current at its periphery being approximately 8 kA, was injected in pulses of approximately 80 ns duration axially into a cylindrical argon chamber where the pressure was varied over the 1-750 torrs range. The distribution of the electric field in space and time is calculated on the basis of the appropriate Maxwell equation. The concentration and the temperature of plasma electrons are calculated as functions of time on the basis of six equations describing the kinetics of processes which involve plasma electrons, Ar^* (lower metastable state), Ar^+ (monoatomic ion), Ar_2^+ (diatomic ion), Ar_3^+ (triatomic ion), Ar_2^* (excimer) in 20 possible plasmochemical reactions and two equations for the internal energy of plasma electrons and argon gas respectively. Calculations are made first ignoring ionization and excitation of argon by plasma electrons, then including them. The results are in each case compared with those of calculations where the electric field was not included. One of the programs in the PLASER package was used for calculating the concentrations of plasma components. The authors thank G.p Mkheidze and A.A. Savin for supplying the experimental data and discussing the results, S.S. Vygran and A.V. Koval for assisting in the numerical calculations, V.I. Derzhiyev, A.A. Rukhadze, and S.I. Yakovlenko for discussing the results

at various stages, and N.V. Suyetin for reading the manuscript and for the several helpful comments. Figures 4; tables 1; references 10.

Multifrequency High-Power CO_2-Laser Radiation Pulse

907L0102B Leningrad PISMA V ZHURNAL TEKHNICHESKOY FIZIKI in Russian Vol 16 No 2, 26 Jan 90 pp 26-29

[Article by V.M. Akulin, N.p Datskevich, N.N. Kononov, and G.p Kuzmin, Institute of General Physics, USSR Academy of Sciences, Moscow]

[Abstract] Multifrequency pulse emission by a CO_2-laser has been achieved in the LAD-2 laser facility at the Institute of General Physics owing to its 30 cm large aperture, simultaneous autocollimation of several lines being made possible by use of a plane diffraction grating with a large aperture and a spherical mirror with a large radius of curvature in a configuration which creates several independent resonators within one volume. The concave spherical mirror had a 2000 radius of curvature and the diffraction grating was a 200 mm square aluminum echelette with 75 lines/mm. The latter was placed 550 cm away from the mirror at an angle allowing extraction of radiation modes at small angles relative to one another. It was oriented for extraction of the P20 line in the rotational 00°-10°0 band of a CO_2 molecule along the optical axis of the cavity, with the resonators for the P18, P16, ... lines on one side and the resonators for the P22, P24,...lines on the other side of that axis. The angular dispersion of the grating for frequencies of the fundamental CO_2 band was approximately 1 mrad/cm^{-1} and the angle subtended by the mirror was approximately 13 mrad. The frequency interval between rotational lines in the fundamental CO_2 band being 2 cm^{-1} or smaller, 13 or more lines could be extracted from that cavity. Successive emission lines were shifted in time by up to 200 ns. The rise time of an emission pulse was 20-50 ns. The duration of the leading peak was 50-150 ms above half-amplitude level. Each line carried at an energy of at least 10 J energy per pulse, with a peak power of 10-45 Mw. Figures 2; references 3.

Retention of Metastable High-Pressure Phases Formed During Impact Compression

907L0102C Leningrad PISMA V ZHURNAL TEKHNICHESKOY FIZIKI in Russian Vol 16 No 2, 26 Jan 90 pp 53-54

[Article by S.S. Batsanov, L.G. Bolkhovitinov, and A.I. Martynov, All-Union Scientific Research Institute of Physical and Radio Engineering Measurements]

[Abstract] A method of impact compression is proposed for ensuring retention of the metastable high-pressure phases without use of a cryogenic liquid for cooling during or after impact, subsequent confinement of the compact between two massive metal plates, and addition of water. The alternative is to ensure soft annealing and a lower final temperature by maintenance of a high pressure over a rather long period of time and by slowdown of the stress relief, this being achievable by use an explosive charge with a large diameter and by detonating it underground, in water, or inside a heavy metal shell, or, as proposed here, by utilization of the high residual pressure. Then, under the appropriate thermodynamic conditions, injection of a gas or heat will cause the compact to expand so that a high static pressure will be maintained while the dynamic pressure drops. This technique was tested on the hexagonal phase of BN in a cylindrical loading scheme, with a shock wave propagating at a velocity of 7.4 km/s following detonation of an explosive charge so that a dynamic pressure above 80 GPa was maintained for a period of 1-2 μs and a static pressure of approximately 1.5 GPa was maintained for a period of 100-1000 s. The monolithic product of this treatment contained 98% wurtzitic BN having a density of 3.2 g/cm^3 and a Vickers hardness 4000 under a 120 kgf/mm^2 indentation pressure. References 1.

UDC 533.6..011.72:534.222.2

Formation of Shock Waves With Explosion-Type Profile in Shock Tube

907L0096B Novosibirsk PMTF: VSESOYUZNYY NAUCHNYY ZHURNAL PRIKLADNOY MEKHANIKI I TEKHNICHESKOY FIZIKI in Russian No 6, Nov-Dec 89 pp 51-56

[Article by M.K. Berezkina, I.V. Smirnov, and M.p Syshchikova, Leningrad]

[Abstract] Formation and propagation of plane shock waves with a variable pressure profile in a shock tube with uniform cross-section upon instantaneous removal of the diaphragm are analyzed on the basis of the physical model describing and experiment and a mathematical model of gas dynamics. Experiments were performed in a 12 m long tube with a rectangular 50 x 150 mm^2 cross-section, the 9 m long expansion chamber consisting of several separate compartments with steel walls and the compression chamber being interchangeably 85 mm, 1 m, or 2 m long. Three different diaphgrams were used, all made of copper foil 0.15 mm, 0.25 mm, and 0.4 mm thick respectively, with an intentional notch. The initial conditions were varied in terms of four parameters: ratio of pressures p_c/p_e on diaphragm from compression side and from expansion side respectively, ratio of acoustic velocities a_c/a_e in compression chamber and in expansion chamber respectively, adiabatic exponent k in compression chamber, and adiabatic exponent γ_0 in expansion chamber. The velocity of a shock wavefront was measured by the base-line method and the pressure profile behind it was measured with piezoelectric transducers. The experimental data correlate closely with the results obtained by numerical simulation of a real shock tube, but not with calculations based on the ideal shock wave theory with "point" explosion. The theory, while it fairly accurately predicts the time at

which the head of a rarefaction wave appears at any tube section, predicts appearance of its tail much later than it actually does and consequently also underestimates the pressure in the cold zone. Figures 7; references 11.

UDC 539.89

Theoretical Determination of Temperature in Problems of Shock-Wave Interaction of Metals

907L0036A Novosibirsk FIZIKA GORENIYA I VZRYVA in Russian Vol 25 No 6, Nov-Dec 89 pp 104-112

[Article by I.I. Kostenko and L.I. Shakhtmeyster, Tomsk]

[Abstract] The temperature in shock waves produced by interaction of metals is calculated theoretically on the basis of the Mie-Grueneisen equation of state, this equation being valid for pressures and temperatures up to 2 Mbar and 5000 K respectively. The electronic term is omitted from this equation, inasmuch as it contributes not more than 5-7%. First, using the Debye theory along with the properties of both Hugoniot and Poisson functions for an adiabatic shock process, is formulated the thermodynamic potential of cold compression and are determined all the material constants needed for solving the system of equations derived from the equation of state. Density and pressure, also the thermal component of pressure, are calculated assuming either a Morse potential or a Born-Mayer potential, in which cases the results agree closely with experimental data. Calculations based on a Burch-Murnahan potential yield quite different results. The theoretical values thus obtained for Al, Cu, Pb, and In are compared with those obtained experimentally by other authors. Temperatures on the adiabatic line and on the isentropic line are then calculated for the same metals, using either of those two potentials. Tables 6; references 18.

UDC 662.215.4

Spontaneous Explosion of Hexamethylene Triperoxiddiamine

907L0036B Novosibirsk FIZIKA GORENIYA I VZRYVA in Russian Vol 25 No 6, Nov-Dec 89 pp 129-131

[Article by A.Ye. Fogelzang, V.V. Serushkin, and V.p Sinditskiy, Moscow]

[Abstract] An experiment with large crystals of hexamethylene triperoxiddiamine has revealed that, contrary to earlier predictions, there is a danger of their spontaneous explosion. The experiment was performed according to the Taylor-Rinkenbach method. Dry crystals weighing 12 g were dissolved in 1 liter of boiling chloroform and the resulting solution then passed through an accordion filter into a Dewar flask preheated to 65C. Into the flask, through the stopper, were suspended cotton threads serving as crystallization hosts during slow cooling to room temperature over a period of 48 h with the flask inside a thermostat initially at 60°C. Larger crystals were grown similarly in a Dewar flask, the latter not placed directly inside the thermostat but inside a larger Dewar flask containing 10 liters of water preheated to 60°C and shut with a penoplastic stopper. This one was placed inside the thermostat initially at 60° for slow cooling to room temperature. After removal of the threads from the flask, some crystals still attached to a thread exploded while a few were being separated from it. More crystals on a thread exploded subsequently one by one over a 10 min period while the thread holding them was resting freely on filter paper without any external action applied. Crystals taken off the threads and thrown into a beaker with cold water exploded spontaneously one by one over a period of 1-2 min, faint clicks being followed by a loud final bang. This phenomenon cannot yet be explained, except that cracking of the crystals is caused by internal stresses. References 6.

UDC 533,951

Production and Focusing of High-Power Ion Beam in Magnetically Shielded Diode

907L0025A Moscow FIZIKA PLAZMY in Russian Vol 15 No 11, Nov 89 pp 1337-1345

[Article by V.M. Bystritskiy, Institute of Electrophysics at Ural Department, USSR Academy of Sciences, V.I. Boyko, V.N. Volkov, Ya.Ye Krasik, and I.B. Shamanin, Scientific Research Institute of Nuclear Physics at Tomsk Polytechnic Institute]

[Abstract] An experiment was performed involving production of a highpower ion beam in a magnetically shielded diode and using the VERA accelerator together with the attendant test facility. Two concentric 0.2 mm thick and wide rings made of stainless steel served as cathodes. A spherical ring made of aluminum. 21-33° wide with a 150 mm radius and a 100 cm^2 large plasma-forming surface area served as anode. The plasma source was a 2 mm thick epoxy layer adjacent to the anode, with a 5x5 array of holes 1 mm in diameter. The interelectrode gap, equally wide for both cathodes, was varied from 6 mm to 10 mm. The shielding magnetic field was produced by two coaxial coils with a total inductance of 35 μH connected in series and inserted into a 0.2 mm thick shield made of stainless steel, is thickness being smaller than the penetration depth for a 14 kHz or 8 kHz fundamental harmonic of the magnetic field. The cylindrical gap between the two ring cathodes was covered by a neutralizing grid with a 0.85 high transmittance. The instrumentation included an active voltage divider, two Rogowski loops, four collimated multiaperture Faraday cylinders for measuring the amplitudetime characteristic, their apertures covered with 0.38-1.2 mg/cm^2 thick terylene films for measurement of the energy spectrum, and a movable multiaperture camera obscura with aerial-photography film for tracking the ion beam trajectory. The parameters of the ion beam were determined on the basis of trajectory

measurements, nuclear activation measurements on an intercepting polyethylene target using the $^{12}C(p,\gamma)^{13}N$ reaction, calorimetric measurements, in addition to measurements made with the Faraday cylinders. Interaction of a dense high-power ion beam and various targets (Al,Fe,Cu,W,Pb) was measured in a separate series of tests, with a spring-loaded pendulum, electron-optical recording of plasma expansion, and solitary plasma probes. The results of this experiment are analyzed with theoretical support and they indicate a still inadequate focusing of a thus produced ion beam, mainly owing to incomplete charge neutralization and azimuthal electron drift in the imperfectly aligned inter-electrode space. Figures 5; tables 1; references 11.

UDC 533.6.011.92

Study of Acceleration of Thin Foils dUring Laser Treatment on Basis of Shock Wave Dynamics in Rarefied Media

907L0006A Moscow FIZIKA PLAZMY in Russian Vol 15 No 10, Oct 89 pp 1164-1174

[Article by I.N. Burdonskiy, A.L. Velikovich, A.Yu. Goltsov, and M.A. Liberman, Institute of Problems in Physics, USSR Academy of Sciences]

[Abstract] An experimental study was made concerning ablative acceleration of thin flat foils during their laser treatment in a low-pressure gaseous atmosphere, the problem being identified as one of shock wave dynamics in rarefied media. Measurements were made by the methods of multiframe interferometry and schlieren photography in a Mishen("Target")-II test facility during treatment of 6 μm thick aluminum foils with a neodymium laser in a residual nitrogen atmosphere under a pressure not higher than 10 torrs. The intensity of laser radiation was varied over the 10-50 TW/cm ^{2} range. Interferograms were recorded by heating radiation and probing radiation at the target surface, an optical delay line having split the probing beam of 530 nm radiation into five and these arriving at the surface one after another with a time delay in pulses of 3 ns or 0.3 ns duration. For schlieren photography, a similar optical delay line split the probing beam into only two and shadowgrams were recorded through high-resolution high-speed objective lenses. The process of foil acceleration during such a treatment is analyzed theoretically, considering the dynamics of an accelerated center of mass under compression in a shock wave and the dynamics of plasma corona expansion in rarefied gas. The parameters of the plasma corona in the experiment are then calculated on the basis of self-similar solutions to the applicable equations and shock wave parameters characterizing the experiment. Figures 6; references 17.

Electromagnetic Tunnel Interference in Metal Films

907L0054C Leningrad PISMA V ZHURNAL TEKHNICHESKOY FIZIKI in Russian Vol 15 No 21, 12 Nov 89 pp 34-37

[Article by V.V. Sidorenkov and V.V. Tolmachev, Moscow Higher Technical School imeni N.E. Bauman]

[Abstract] An experiment with a plane-parallel metal films has confirmed the theoretically predicted phenomenon of electromagnetic tunnel interference in metal films. The experimental apparatus included a He-Ne laser and a twobeam interferometer with a light-beam amplitude modulator in one arm between the metal plate and the semiconductor beam-splitting mirror, this modulator consisting of a ferrite garnet film orthogonally magnetizable by an electric audio-frequency current and glued to a polarizing (Polaroid) film. A photodetector behind the metal plate was followed by an instrument amplifier and an oscillograph. Specimens of 20-80 nm thick titanium films for this experiment had been produced vacuum deposition on 0.15 mm thick glass substrates. The results of measurements validate the theoretical formulas for both plain transmission and interference transmission coefficients, considering not only normal but also oblique incidence of optical electromagnetic waves. Figures 2; references 4.

UDC 538.945

Alternating-Current Josephson Effect in $Tl_2Ca_2Ba_2cu_3O_{10+x}$ Ceramic

907L0091C Kharkov FIZIKA NIZKIKH TEMPERATUR in Russian Vol 15 No 11, Nov 89 pp 1213-1215

[Article by B.A. Aminov, A.I. Akimov, N.B. Brandt, Nguen Min Thu, M.V. Sudakova, Yu.A. Pirogov, and Ya.G. Ponomarev, Moscow State University imeni M.V. Lomonosov]

[Abstract] An experimental study of $Tl_2Ca_2Ba_2Cu_3O_{10+x}$ ceramic was made concerning the effect of an external microwave field on the current-voltage characteristics of Josephson microbreak junctions in this high-temperature superconductor material with a critical transition temperature of 106-108 K. Square bars 3 mm long and 0.8 mm thick were glued with epoxy cement to a glass-fiber plate, with a set of 0.1 mm thick copper-foil current and potential electrodes soldered to each end. After polymerization of the epoxy cement, each bar was ground down to 0.1 mm thickness and a 0.1-0.2 mm wide slot was cut with leather cloth across the center leaving 0.1-0.2 mm wide bridge. The plate was mounted on a brass spring so deflection of the latter by a micrometer screw caused the plate to bend. After a microcrack had been produced in each bridge by bending of the plate, the current-voltage characteristics of Josephson junctions across them was measured at temperatures covering the 4.2-104 K range, first without and then in a microwave field at 52-75 GHz frequencies. In the latter case there appeared a series of Shapiro on the I-V curves and in some also subharmonic steps, the latter indicating departure from a sinusoidal phase-current characteristic. The height of all steps was found to decrease with rising temperature, the height of subharmonic steps faster than that of Shapiro steps. The charge of superconducting electrons, based on the width of Shapiro steps, was found to be (1.95-2.05)e. The effective bridge diamater, determining the weak link across the microcrack and determined from the dependence of the critical supercurrent on the magnetic field in the plane of the microcrack, was found to be 10-20 μm and thus comparable with the size of superconducting grains. The critical supercurrent I_c was found to decrease with rising temperature according to the (3/2)-power law from maximum at 4.2 K to zero at the critical superconducting transition temperature, the product I_cR_N (R_N denoting normal-state resistance) spreading over the 1-10 mV range. The authors thank K.K. Likharev for extremely helpful discussions. Figures 3; references 6.

UDC 538.945

Ginzburg-Landau Equations for Two-Band Superconductors

907L0051A Kharkov FIZIKA NIZKIKH TEMPERATUR in Russian Vol 15 No 12, Dec 89 pp 1251-1260

[Article by Yu.M. Poluektov and V.V. Krasilnikov, Kharkov Institute of Engineering Physics, UkSSR Academy of Sciences]

[Abstract] The properties of two-band superconductors at temperatures near the critical are analyzed in accordance with the Ginzburg-Landau theory, assuming an overlap of two conduction bands whose properties including critical temperature and order parameter are different. From the corresponding analogous for both bands Ginzburg-Landau equations and expression for the supercurrent, obtained on a phenomenological basis by equating to zero the variation of the order parameter and the vector potential of free energy, are derived expressions for the entropy and for the jump change in thermal capacity. A relation is obtained for calculating the critical temperature. The behavior of the order parameter near the boundary in plane x= 0 is analyzed, fist assuming that no interband transitions occur and then with interband transitions occurring. The supercurrent density is then expressed in terms of superfluid velocity, whereupon the criterion for quantization of magnetic flux is established. An expression is obtained for the field penetration depth and an expression is obtained for the surface energy of the normal-superconductor interface, assuming a plane interface in the intermediate state perpendicular to the x= 0 plane. Special consideration is given to thin two-band superconductor films. An expresssion for the critical magnetic field is obtained, assuming an internal magnetic field equal to the external one and a negligible variation of the

order parameter over the film thickness. An expression for the critical current is then obtained, assuming a uniformly distributed concentration of superconducting electrons. References 21.

UDC 538.22

New Structural Phase Transition and Magnetic Ordering in $1C_2Mn$ Perovskite $(C_2H_5NH_3)_2MnCl_4$

907L0051B Kharkov FIZIKA NIZKIKH TEMPERATUR in Russian Vol 15 No 12, Dec 89 pp 1289-1295

[Article by S.V. Zherlitsyn, A.A. Stepanov, V.D. Fil, and V.p Popov, Institute of Low-Temperature Engineering Physics, UkSSR Academy of Sciences, Kharkov]

[Abstract] An experimental study of the perovskite $1C_2Mn$= $(C_2H_5NH_3)_2MnCl_4$ was made, of interest being its magnetic structure formed by monoclinic layers of Mn^{2+} ions inside octahedral chlorine shells separated by alkyl-ammonia groups. Single crystals were grown by slow vaporization of a saturated aqueous solution of $(C_2H_5NH_3)_2Cl_2$ and $MnCl_4.4H_2O$. The magnetic structure was analyzed by the method of antiferromagnetic resonance. The magnetic susceptibility was measured with an a.c. bridge at a frequency of 18 Hz. In addition were determined the coefficient of thermal expansion as well as the velocities of longitudinally and transversely propagating sound. Their temperature dependence over the 40-55 K range was obtained in two different ways: thermal expansion was measured precisely at discrete temperatures and the sound velocities were recorded during continuous heating. Measurements were made without an external magnetic field and in a longitudinal one. The coefficient of thermal expansion was found to depend neither on the intensity of the external magnetic field within the 0-40 kOe range nor on the frequency within the 54-258 MHz range, but to have a sharp anomaly near the critical temperature. At about 47 K, within the range of superconducting transition, the velocity of longitudinal sound was found to dip and the velocity of transverse sound was found to peak. The results indicate that at the critical temperature there occurs an improper ferroelectric transition, possibly caused by freezing of the transfers of hydrogen bonds in the NH_3 from axial to equatorial Cl-atoms and evidently preceding antiferromagnetic ordering at a Neel point of about 42 K. Two states were found to coexist below 10 K, characterized by different domain structure configurations with nearly the same energy, differently influencing the moduli of elasticity near the spin reorientation temperature. The frequency-dependent anomalies of acoustic properties within the 2-8 K temperature range indicate a relaxational interaction of sound and crystal inhomogeneities. Figures 7; tables 1; references 10.

UDC 537.533.35+539.211+539.216.2

Secondary-Electron Emission From Oxide Superconductors

907L0042A Leningrad FIZIKA TVERDOGO TELA in Russian Vol 31 No 11, Nov 89 pp 26-28

[Article by Yu.Ya. Tomashpolskiy, M.A. Sevostyanov, N.V. Sadovskaya, N.V. Kolganova, and N.G. Shirina, Scientific Research Institute of Physical Chemistry imeni L.Ya. Karpov, Moscow]

[Abstract] Secondary-electron emission by oxide superconductors is evaluated on the basis of a theoretical model and experimental data pertaining specifically to $YBa_2Cu_3O_{7-d}$ ceramic at and above room temperature. The secondary-electron emission current at temperatures above superconducting transition is calculated according to Sternglass' hypothesis, considering that the depth from which secondary electrons are emitted is much smaller than the depth at which they are excited. Their emission was examined under a scanning electron microscope with a fine probe covering a range not wider than 10-30 μm and thus individual large grains or clusters of small ones. It was measured with a detector feeding signals to an amplifier. The temperature dependence of the secondaryelectron emission current over the range from room temperature to 500 K was determined with temperature measurements accurate within 10 K. The results indicate a metal-like current-temperature characteristic of the orthorhombic phase (d= 0.1) and a semiconductor-like one of the tetragonal phase (d= 0.5) semiconductor-like current-temperature characteristic, to a degree which depends on the impurity content ($BaCuO_2$, Y_2BaCuO_5, CuO_x) and thus on the ceramic production process. Figures 1; references 7.

UDC 537.312

Effect of Hydrogen on Superconductivity of $Bi_2Sr_2Ca_3Cu_4O_{12+e}$

907L0042B Leningrad FIZIKA TVERDOGO TELA in Russian Vol 31 No 11, Nov 89 pp 275-276

[Article by V.V. Sinitsyn, I.O. Bashkin, Ye.G. Ponyatovskiy, V.I. Rashchupkin, S.F. Kondakov, and V.M.Prokopenko, Institute of Solid-State Physics, Chernogolovka (Moscow oblast)]

[Abstract] An experimental study of $Bi_2Sr_2Ca_3Cu_4O_{12+e}$ superconductor material was made, its critical temperature expected to be 131 K, not only for the purpose of verifying this but also for determining the effect of hydrogen on the superconducting transition. A ceramic specimen synthesized from a mixture of Bi_2O_3, $SrCO_3$, $CaCO_3$, CuO powders was annealed at 850-865°C in air for 30-35 h total, having been pulverized after the first installment and reconstituted before the second one, then additionally annealed in an oxygen stream. A batch of ceramic powder was, after this heat treatment,

degassed for 30 min by continuous scavenging at 50-60°C temperature to a residual gas pressure of 10 μm Hg and then cooled inside a vacuum reactor, whereupon hydrogen from a TiH_2 generator was admitted under a pressure of 400 mm Hg and its absorption facilitated by heating the reactor to 120-125°C. The superconducting transition temperature was determined not later than 1 h after hydrogenation and on the basis of magnetic susceptibility measurements by the induction method in a magnetic field alternating at a frequency of 113 Hz with an amplitude of at least 1 Oe. The results reveal two diamagnetic anomalies in the behavior of the original ceramic with an approximately 97% volume fraction of the superconducting phase, one at T_c= 78.5-79.5°C characterizing that phase and one at 112-114°C characterizing the impurity phase. They also indicate that the effect of absorbed hydrogen depends on its concentration x= 2(number of H atoms/number of Bi atoms). In small concentrations up to x= 0.5 it enters into a solid solution and raises both temperaures T_{co} (beginning of diamagnetic anomaly) and T_{cm} (middle of diamagnetic anomaly) slightly without significantly changing the volume fraction of the superconducting phase. In concentrations of x= 0.50.6 it raises the T_{cb} temperature by an approximately 7 K step and the T_{cm} temperature by only approximately 2 K. As its concentration continues to increase above 0.6, it does not raise these two temperatures further but decreases the volume fraction of the superconducting phase and a multiphase structure forms with likely amorphization of the ceramic. Figures 2; references 6.

UDC 538.958

Raman Scattering of Light by Exciton Mechanism in Two-Dimensional Electronic System

907L0042C Leningrad FIZIKA TVERDOGO in Russian Vol 31 No 11, Nov 89 pp 127-134

[Article by L.I. Korovin, S.T. Pavlov, and B.E. Eshpulatov, Institute of Engineering Physics imeni A.F. Ioffe, USSR Academy of Sciences, Leningrad]

[Abstract] Scattering of light by a quantum well in a semiconductor at a frequency corresponding to its fundamental absorption band by an exciton mechanism is analyzed theoretically, the mechanism involving formation of two-dimensional excitons and subsequent transitions between excitons or between dimensionally quantized states with attendant emission of secondary light in each case. The analysis is based on the triple-heterostructure model, narrow-band semiconductor containing Vanier-Mott excitons and sandwiched between two wideband dielectrics. Expressions for the exiton wave function and energy within the continuous spectrum are derived in the approximation of a narrow infinitely deep rectangular potential well, whereupon the differential cross-section for scattering is calculated with the aid of the scattering tensor and Fresnel coefficients for incident light. The frequency dependence of this differential cross-section indicates formation of a discrete scattering spectrum in accordance with the law of energy conservation, with a series of exciton lines corresponding to each level of dimensional quantization. The angular distribution of scattered light is different depending on its polarization, only transitions between excitons within the same quantization level contributing in the case of s-polarization and transitions of both kinds contributing in the case of p-polarization. Numerical estimates of the integral cross-section for scattering of normally incident light by a $GaAs/Al_{0.37}Ga_{0.63}As$ structure into S-polarized light made on the basis of this theory indicate their experimental verifiability. References 18.

Superconductor-Type Quark Model and Nondiagonal P-A Transitions

907L0039A Moscow TEORETICHESKAYA I MATEMATICHESKAYA FIZIKA in Russian Vol 81 No 3, Dec 89 pp 354-368

[Article by M.K. Volkov, Joint Institute of Nuclear Research, A.N. Ivanov and N.I. Troitskaya, Leningrad Polytechnic Institute, and M. Nad, Institute of Physics at Central Institute of Experimental Physics, Slovak Academy of Sciences, Bratislava/CZECHOSLOVAKIA]

[Abstract] A superconductor-type quark model based on quantum chromodynamics, quark version of the Nambu and Jona-Lasinio model, is constructed for describing low-energy interactions of hadrons by an effective chiral Lagrangian. The effective chiral Lagrangian which describes low-energy interactions of mesons is expressed as the sum of three Lagrangians, one of them including the kinetic components of mesons as well as the local vertices in their interaction and containing exclusively all the information about spontaneous breaking of chiral symmetry with attendant appearance of nondiagonal P-A transitions so that P-A diagonalization becomes necessary. The other two Lagrangians describe the vertices in strong low-energy interaction of mesons, which appear as a consequence of chiral anomalies in quark loops. The problem of P-A diagonalization in this quark model is solved first by expanding the effective chiral Lagrangian into an infinite series each term of which has the form of a one-loop quark diagram and defines the corresponding vertex in low-energy interaction. This method ofcalculating the quark diagram of interaction vertices is demonstrated on $\pi^0\gamma\gamma$-interaction, equivalent to $\omega\rho\pi$-interaction, and shown to require regularization for removal of ambiguity in the description of vertices due to P-A diagonalization. Most convenient is the Pauli-Willars regularization algorithm, but an additional regularization is required for removal of nonphysical vertices by a shift which effects transition to physical states. Using another effective chiral Lagrangian already regularized according to the Pauli-Willars algorithm and thus not containing nonphysical interaction vertices makes this additional regularization unnecessary. Figures 2; references 29.

UDC 538.945:535.343

Ceramic and Thin-Film Tl-Ba-Ca-Cu-O High-Tc Superconductors

907L0020B Leningrad FIZIKA TVERDOGO TELA in Russian Vol 31 No 10, Oct 89 pp 295-297

[Article by O.V. Kosogov, A.I. Akimov, M.V. Belousov, S.V. Bogachev, V.Yu. Davydov, V.A. Ilin, S.F. Karmanenko, A.L. Karpey, O.V. Kornyakova, V.N. Makarov, and L.p Poluchankina, Institute of Engineering Physics imeni A.F. Ioffe, USSR Academy of Sciences, Institute of Electrical Engineering imeni V.I. Lenin (Ulyanov), and Scientific Research Institute at Leningrad State University, Leningrad]

[Abstract] An experimental study of ceramic and thin-film Tl-Ba-Ca-Cu-O superconductors was made, the ceramic specimens having been produced by solid-phase synthesis of Tl_2O_3 + $BaCO_3$ + $CaCO_3$ + CuO powder mixtures. Approximately 0.5 μ thick film specimens were produced by magnetron sputtering of ceramic targets onto 500-600°C hot Al_2O_3, ZrO_2, and MgO substrates and subsequent annealing in an oxygen atmosphere. All specimens were found to have a polyphase content. Three ceramic specimens were selected for x-ray spectrum microanalysis, after superconducting transition had been established on the basis of their d.c. resistance dropping to zero at the transition temperature. In specimen 1 was predominant the1-2-1-2 phase and its critical temperature was 109 K (transition ending at 107 K). In specimen 2 was predominant the 1-5-4-7 phase and its critical temperature was 130 K (transition ending at 120 K). In specimen 3 was predominant the 1-2-2-4 phase and its critical temperature was 122 K. The critical temperature for two film specimens was 126 K and 124 K respectively. Evidently, the critical temperature is higher for a material with a higher (Ca+Cu):(Tl+Ba) content ratio. The temperature dependence of a weak-field EPR signal was tracked in a Radiopan EPR spectrometer at 9.8 GHz frequency, for detection of superconductivity contactlessly on the basis of change in absorption of microwave power in a weak field. Measurement of Raman scattering spectra was done at room temperature in air with a DFS-24 diffraction photospectrometer, incident 514.5 nm light from an argon laser covering a spot 30 μ in diameter. All spectra contained a principal peak in the vicinity of 520 cm^{-1}, characteristic of $TlBa_2$ $Ca_{n-1}Cu_nO_{2n+3}$ compounds. Companion peaks appeared in the spectrum of specimen 2 (435 cm^{-1}, 555 cm^{-1}) and in the spectra of both film specimens (435 cm^{-1}, 585 cm^{-1}, 635 cm^{-1}), indicating the presence of foreign inclusions. The films, structurally imperfect, were found to contain a substantial amount of the $BaCuO_2$ phase. Figures 2; references 6.

Composite Superconductors Produced by Rapid Coating With Ba-Sr-Ca-Cu-O Metal Oxide

907L0037A Leningrad PISMA V ZHURNAL TEKHNICHESKOY FIZIKI in Russian Vol 15 No 19, 12 Oct 89 pp 1-5

[Article by A.D. Grozav, L.A. Konopko, and N.I. Leporda]

[Abstract] Thin dense coatings of fused Bi-Sr-Ca-Cu-O ceramic were experimentally deposited on various metal and alloy substrates melting at temperatures above 1000°C. All those compatible with this ceramic were found to intensely interact with it chemically, which made it necessary devise a method of weakening this catastrophically detrimental interaction. Deposition of thin buffer layers between ceramic and metal was rejected in favor of shortening the duration of contact between liquid ceramic and solid metal by drawing flexible metal substrates through the liquid ceramic bath at a high velocity and, after solidification of the ceramic, heat treating the composite for a short time at a high temperature within 800-840°C. Copper wires (melting point 1085°C) 0.100-0.410 mm in diameter and 0.51.0 m long were coated with $BiSrCaCu_2O_x$ ceramic (melting point 880°C) by drawing them through the bath at a temperature of 900-1000°C at various constant velocities ranging from 5 to 150 mm/s. Refinement of this method yielded black coatings of uniform thickness ranging from 0.005 to 0.100 mm, uniform coating ensuring maximum flexibility and continuity of the deposition process being attained by coating wires not larger than 0.100 mm in diameter. Coatings deposited by drawing wire through the bath at a velocity of at least near 100 mm/s were found to have a lamellar structure oriented parallel or at a small angle to the direction of drawing. Those deposited by drawing the wires slower were found to have an irregular structure with intergrown crystals forming randomly distributed clusters of various sizes. These coatings were found to behave either like semiconductors or like metals, the temperature dependence of their electrical resistance indicating no superconducting transition above 4.2 K. Recovery of their superconductivity required heat treatment at 800°C in air for 10 min, superconducting transition afterwards beginning at 90 K and ending at 45 K as in the case of coatings with regular structure. Modification of the composition of the ceramic to $Bi_{1.5}Pb_{0.5}Sr_2Ca_2Cu_3O_x$ narrowed the temperature range of superconducting transition by raising the end point to 65 K. Figures 2; references 7.

Fractal Geometry of High-Temperature Superconductors

907L0037B Leningrad PISMA V ZHURNAL TEKHNICHESKOY FIZIKI in Russian Vol 15 No 19, 12 Oct 89 pp 64-68

[Article by A.B. Mosolov, Institute of Problems in Mechanics, USSR Academy of Sciences]

[Abstract] The fractal geometry of high-temperature superconductor ceramics is analyzed on the basis of the size distributions of pores and particles in $YBa_2Cu_3O_x$ ceramic, these power-law dependence of the volume fraction on the size in the $La_{2-x}Sr_xCuO_4$ series of ceramics being known and reducing to a linear one when plotted in log-log coordinates. Specimens of ceramic for this analysis were produced by sintering cryochemically produced $YBa_2Cu_3O_x$ powder without and with up to 60% Ag at 910-930°C in an oxygen stream for 90 min, followed by annealing and then slow cooling in an oxygen atmosphere. With the aid of data thus obtained, the analysis has yielded the fractal dimensionality data

needed for constructing the 2D-scale in iteratively in three steps. The fractal dimensionality was found to increase linearly with the Ag content: $d_f = 1.1 + 0.9c_{Ag}$. The analysis yields a dimensionality $d_f = 1.7$ rather than 2 as the limit of pure Ag is approached, which is consistent with the dimensionality of a percolation cluster. The author thanks M.V. Yelashkin, A.V. Luzhkov, and V.p Shabatin for producing and supplying specimens of the ceramic-Ag composites. Figures 3; references 9.

Recording Fast Neutrons With Dielectric Track Detectors in Electrolytic Pd-(D+T) Water Cell

907L0037C Leningrad PISMA V ZHURNAL TEKHNICHESKOY FIZIKI in Russian Vol 15 No 19, 12 Oct 89 pp 9-13

[Article by V.D. Rusov, T.N. Zelentsova, M.Yu. Semenov, I.V. Radin, Yu.F. Babikova, and Yu.A. Kruglyak, Odessa State University imeni I.I. Mechnikov]

[Abstract] Dielectric track detectors recorded fast neutrons during saturation of palladium with deuterium in an electrolytic Pd-(D+T) water cell, only such detectors being capable of this on account of their thresholdtype discrimination characteristic and their ability to correlate events in the case of a low neutron fluence or in the presence of many weakly ionizing particles. Other characteristics of such detectors favorable for recording rare events are high speed of response and long retention of recorded data, also high radiation immunity. In the experiment deuterium water containing at least 98% D and dilute tritium water with an activity of 10^9 Bk/ml were mixed in various volume ratios. A corrugated 0.2 mm thick plate of the 72 Pd 25 Ag 3 Au alloy served as the cathode under a voltage of 200 V, the current density being held at the 10 mA/cm^2 level throughout the experiment. The integral neutron flux from the likely occurring nuclear reactions (d,d), (d,t), (t,t) was recorded with an MAND/p Hungarianmade polyethylene track detector, which was also used for "zero level" experiments involving simultaneous exposition of some in the polyethylene envelope and some without it in D+T water for 2.5 h. The recorded tracks reveal two "wyes" produced by splitting of nuclei according to the $^{12}C(n,n')3\alpha$ reaction and indicating the presence of neutrons with higher than 10 MeV energy. The authors thank V.L. Ginzburg and participants in the all-Moscow seminar on theory for discussing the results. Figures 2; references 7.

The Role of the Energy Gap in Non-Josphson Generation S_xSe1-_x Semiconductor Solid Solutions S_xSe_{1-x} Semiconductor Solid Solutions

907L0016a FIZIKA NIZKIKH TEMPERATUR in Russian Vol 15 No 10, Sep 89 pp 994-997

[Article by G. Ye. Churiolv, D. A. Dikin, V. M. Dimitriev, V. N. Svetlov]

[Abstract] This study examines the rule of the energy gap in non-Josephson generation, as the energy gap is the most characteristic parameter of a superconductor. The tests are carried out on tin films approximately 1 mcm in width, 40 to 100 mcm in length, and approximately 100 Angstroms thick. The study focuses on the effect of certain external parameters such as temperature, and transport current as well as an applied longitudinal magnetic field on the non-Josephson generation conditions. The study identifies a strong dependence of the oscillation frequency on current in the specific non-Josephson process suggesting that the mechanism behind this effect is related to characteristics of a superconductor that are opposite in sign such as the temperature dependences. Other factors that diminish with increasing temperature such as the energy gap, H_c and I_c are mong such properties. It is determined that in the final analysis all these parameters of a superconductor can be expressed through the energy gap and each will have a different functional relation to the energy gap

A Possible Role of Condensed Oxygen in Internal Friction of Metal-Oxide High-Temperature Superconductors

907L0016b FIZIKA NIZKIKH TEMPERATUR in Russian Vol 15 No 10, Sep 89 pp 992-994

[Article by A. V. Leont'eva, G. A. Marinin, V. M. Svistunov, B. Ya. Sukharevskiy]

[Abstract] This study analyzes the possibility of attributing the behavioral irregularities of metal oxide high-temperature superconductors to the internal friction anomalies occurring in lanthanum-strontium and yttrium-barium specimens at various temperatures. The observation underlying this analysis is that a number of internal friction peaks in the specimens appear to be distributed near the reference points of oxygen. The study provides a table indicating the internal friction peaks identified by a variety of authors on LaSr-Cu-O and Y-Ba-Cu-O high-temperature superconducting specimens. The primary element of interest in this analysis is that the position of the internal friction peaks remains unchanged at different frequencies, suggesting that the internal friction anomalies are in fact attributable to phase transitions. This analysis is only valid when oxygen is present in the specimens in its condensed phases.

The Effect of Uniaxial Pressure on the Superconducting Transition Temperature in Niobium Diselenide

907L0016c FIZIKA NIZKIKH TEMPERATUR in Russian Vol 15 No 10, Sep 89 pp 984-988

[Article by M. A. Obolenskiy, Kh. B. Chashka, V. I. Beletskiy, V. M. Gvozdikov]

[Abstract] This study analyzes the effect of a minor uniaxial pressure applied along the axis of easy compressibility on the superconducting transition temperature in 2H-$NbSe_2$ and 2H$Nb_{0.9}Sn_{0.1}Se_{02}$ specimens. The

$Nb_{0.9}Sn_{0.1}Se_2$ single crystals were grown from chemical gas-transport reactions and specimens approximately 6 by 1.007 mm^3 were cleaved from these crystals. Electrical resistance measurements were carried out by the standard four-contact technique. The uniaxial pressure was applied by means of weights with the pressure calculated by the level rule. The design used in the study made it possible to carry out measurements over a temperature range of 4.2 to 300 K and a pressure range of 0 to 6 times 10^8 Pa. The results from this analysis suggest that the peak in the plot of the superconducting transition temperature as a function of pressure is independent of the pressure-induced degradation to the charge density wave. The study attributes this behavior to a change in the interlayer interaction. The study also provides a mechanism for a qualitative explanation of the nonmonotonic behavior of the dependence of the superconducting transition temperature on pressure with increasing applied pressure along the c axis.

Torons and Breaking of Chiral Symmetry in Quantum Chromodynamics and in Supersymmetric Quantum Chromodynamics

907L0004A Moscow ZHURNAL EKSPERIMENTALNOY I TEORETICHESKOY FIZIKI in Russian Vol 96 No 4 (10), Oct 89 pp 1167-1180

[Article by A.R. Zhitnitskiy, Institute of Nuclear Physics, Siberian Department, USSR Academy of Sciences]

[abstract] Existence of torons, self-dual solutions with fractional topological charge in SU(2) gauge theories and its physical consequences are analyzed, a gapless Dirac-operator spectrum for fermions with small mass being an inherent feature of such solutions. Its determinant, in the fundamental representation with the additional factor Z_{SQCD}, is expressed through Green's function of the appropriate operator and in this form yields the toron measure in supersymmetric quantum chromodynamics (SQCD). Next are considered chiral condensates in supersymmetric quantum chromodynamics and in quantum chromodynamics (QCD), a mechanism involving self-dual configurations being responsible for spontaneous breaking of chiral symmetry in gauge theories. In supersymmetric quantum chromodynamics with any number of light flavors the torons retain their individuality, but in quantum chromodynamics with any number of flavors except $N_f = 2$ they tend to merge. The author thanks A.I. Vaynshteyn, D.I. Dyakonov, V.Yu. Petrov, and V.L. Chernyak for helpful discussions. Figures 3; references 27.

Nonlocal Magnetoresistance of Bismuth Films Placed in Nonuniform Abrikosov Vortex Field

907L0002A Moscow PISMA V ZHURNAL EKSPERIMENTALNOY I TEORETICHESKOY FIZIKI in Russian Vol 50 No 8, 25 Oct 89 pp 359-362

[Article by A.K. Geym, Institute of Problems in Microelectronic and Extra-Pure Materials Technology, USSR Academy of Sciences]

[Abstract] An experimental study of thin bismuth films was made concerning their nonlocal magnetoresistance when placed in a transverse magnetic field at the surface of a type-II superconductor (Nb + 5% Mo), a magnetic field penetrating such a superconductor in the form of Abrikosov vortices. The bismuth film was 20 nm thick and separated from the 10x10 mm^2 large surface of a 0.2 mm thick superconducting single crystal by a 20-30 nm thick insulating interlayer of an anodic oxide. Its magnetoresistance was measured over the 0-300 G range of magnetic field intensity, also with the field reversed, at two temperatures: 4.2 K and 1.3 K. At both temperatures was the field dependence of the magnetoresistance found to be linear below 50 G and above 200 G. At the higher temperature its behavior was found to be similar to that in a uniform magnetic field in the local limit. At the lower temperature it increased faster than at 4.2 K within the weak-field range and then less than linearly with further increasing field intensity. All this is evidence of a departure from the local limit owing to a nonlocal effect of a transverse magnetic field on the electrical resistance of such a film. The author thanks L.I. Glazman, I.B. Levinson, and participants of the seminar conducted by V.F. Gantmakher for discussing the results. Figures 2; references 5.

The ε to σ Phase Transition in $TiH_{0.71}$ Hydride: Superconductivity and Electrical Resistance

18620159b Leningrad FIZIKA TVERDOGO TELA in Russian Vol 31 No 2, Feb 89 pp 91-96

[Article by V. M. Teplinskiy, I. O. Bashkin, V. Yu. Malyshev, Ye. G. Ponyatovskiy]

[Abstract] This study employs low-temperature annealing of $TiH_{0.71}$ specimens to generate and identify the various intermediate states occurring in the samples from the ε to δ irreversible transformation and to conduct measurements for each such state. The superconducting transition temperatures and the temperature dependences of the resistance in a normal state were measured for the $TiH_{0.71}$ specimens. The annealing routine consisted of slow heating of the sample from 4.2 K to the annealing temperature followed by rapid cooling. The temperature dependence ρ(T) was measured while the superconducting transition was recorded following annealing. These investigations revealed that as long as the irreversible structural transformations of the specimen were far from complete their rate would grow with rising temperature. Different annealing durations in the series of exposures would correspond to different successive stages in the process of irreversible structural changes. There was also an insignificant growth of the electrical conductivity identified in the initial stages, while the identical nature of the temperature dependence at low temperatures most likely indicates that the specimen is a monophase specimen in these stages with the relaxation processes attributable to the high mobility of hydrogen. Certain unexpected aspects of this problem were also revealed, specifically

the fact that all the conductivity relations at low temperatures could be approximated by the single function $AT^2 + BT^3$ and, second, the behavior of the coefficients A and B during the irreversible structural changes in the specimen. The coefficient B varied little during all stages of this transformation and even after the rearrangement of the metallic sublattice. It is determined that the BT^3 component could be attributed to scattering by vibrations in the metallic sublattice.

Superconductivity Induced in Ti_6O From Hydrogen Doping

18620159c Leningrad FIZIKA TVERDOGO TELA in Russian Vol 31 No 2, Feb 89 pp 240-248

[Article by I. O. Bashkin, V. Yu. Malyshev, S. I. Morozov, B. V. Sumin, V. M. Teplinskiy, Ye. G. Ponyatovskiy]

[Abstract] This study measures the superconducting properties of ordered phase Ti_6O specimens doped by hydrogen or deuterium. The initial Ti_6O specimen is obtained by repeated melting of titanium iodide with TiO_2 in an argon-arc furnace followed by homogenizing vacuum annealing at 600°C. The superconducting transitions were observed by electrical resistance measurements at T is greater than or equal to 1.15 K and inductively above 0.35 K. The measurements were carried out on specimens with an H/O atomic ratio of .53 and a D/O atomic ratio of .50, .63, and .80. Magnetic measurements indicated a superconducting transition in $Ti_6OD_{0.80}$ beginning at T_{c0} equals .64 plus or minus .02 K with at least 90 percent complete by T equals 0.35 K. No superconducting transition characteristics were observed up through .35 K in alloys with a D/O ratio of .50 and .63. The data for the deuterium samples suggests the absence of any anomalous isotope effect typical of existing superconducting phases in Me-H systems. A comparison of the superconducting transition temperatures in Me-H and the vibration energies of hydrogen in these systems indicate a correlation between T_c and $\hbar\omega_H$. The T_c is higher the lower the hydrogen vibration energy in the corresponding lattice.

Crystalline Lattice Deformations to Bi-Ca-Sr-Cu-O Ceramics by Heating an Thermal Desorption of Volatile Components

18620162C Leningrad PISMA V ZHURNAL TEKHNICHESKOY FIZIKI in Russian Vol 15 No 3, Feb 89, pp 23-26

[Article by S. K. Filatov, V. V. Semin, O. F. Byvenko, V. B. Trofimov, A. V. Nazarenko, V. T. Seregin]

[Abstract] This study carries out an investigation of various Bi-Ca-Sr-Cu-O compositions in order to find a method of reducing the extended range of superconducting transition temperatures. The behavior of the materials fabricated in this study was investigated under heating by thermal radiography and mass spectrometry. The best combination achieved in the study was $Bi_{1.05}Sr_{0.94}Ba_{0.18}Ca_{0.47}Cu_1O_x$. The temperature dependence of the electrical conductivity of this compound measured by the four-probe method shows a temperature transition to the superconducting state in the 91-94 K range (for different specimens) and a transition width of less than 3 K. Thermal radiography analysis revealed that the $Bi_{1.05}Sr_{0.94}Ba_{0.18}Ca_{0.47}Cu_1O_x$ specimen contains traces of an extraneous undiagnosed phase, which remains throughout the test temperature range and which does not interact with the primary phase. This compound remained stable up through 1150 K and at this temperature incongruent melting was initiated and the extraneous phase vanished. The parallel thermal radiography and massspectrometry analyses made it possible to attribute the anomalous progression of the temperature dependence of the parameters of the crystalline lattice in the 473-573 K range to the loss of the OH groups from the $Bi_{1.05}Sr_{0.94}Ba_{0.18}Ca_{0.47}$ $Cu_{Bi1}O_x$ ceramic structure.

UDC 517.977.58

Validation of Gradient Methods for Distributed Problems of Optimal Control

907L0097A Moscow ZHURNAL VYCHISLITELNOY MATEMATIKI I MATEMATICHESKOY FIZIKI in Russian Vol 30 No 1, Jan 90 pp 3-21

[Article by V.I. Sumin, Gorkiy]

[Abstract] Application of gradient methods to numerical solution of distributed problems of optimal control is scrutinized, L_2-type spaces being commonly used on account of the steepest descent corresponding to the Frechet derivative even though existence of this derivative imposes stringent constraints on the right-hand sides. Nonlinear systems with L_2-perturbations of admissible controls are considered first, even slightly nonlinear systems such as systems bilinear in control or state variables shown to become unstable under arbitrarily small L_2perturbations of admissible controls. Next are considered controllable systems of Volterra functional-operator equations such as $z(t)= f(t,A[z](t),v(t))$, where $A[.]:L_{infinity,m} \rightarrow L_{infinity,l}$, is a linear bounded operator. First are formulated three conditions which this operator and its majorant $B[.]:L_{infinity,l} \rightarrow L_{infinity,l}$ must satisfy, in addition to the K-condition that function f(t,p,u) be differentiable with respect to p, and then are proved two theorems regarding uniqueness of local solutions z. The operator A[.] is subsequently further constrained and two theorems pertaining to global solutions are proved with the aid of three lemmas, the first theorem establishing the sufficient conditions for stability of such solutions and the requirement that function f(t,p,u) be differentiable with respect to u following from it as a corollary. Next is analyzed differentiation of functionals in $L_{infinity,s}$ space, a fifth theorem being proved which establishes the condition for functional J[v] having a regular Freshet derivative in that space. The proof this theorem is based on the Scortz-Dragoni theorem and aided by a lemma. As examples are considered three optimization problems: a boundary-value problem for a controllable semilinear hyperbolic equation, first boundary-value problem for a controllable semilinear parabolic equation, and the Gours-Darboux control problem. References 21.

UDC 519.85

Exact Auxiliary Functions in Optimization Problems

907L0097B Moscow ZHURNAL VYCHISLITELNOY MATEMATIKI I MATEMATICHESKOY FIZIKI in Russian Vol 30 No 1, Jan 90 pp 43-57

[Article by Yu.G. Yevtushenko and V.G. Zhadan, Moscow]

[Abstract] The concept of an exact auxiliary function is introduced and defined for solution of nonlinear programming problems

$$f_* = \min_{x \in X} f(x), \qquad X = \{x \in E^n \mid g(x) \leqslant 0\}.$$

First are considered addi- tive exact auxiliary functions $R(x,y)= A(f(x),y)+ B(g(x))$, A(f,y) being an arbitrary continuous function of two arguments and B(g(x)) being the penalty function continuous and non-negative everywhere in space E^n (zero when and only when x is member of set X). Three theorems are proved pertaining to nonlinear programming problems where the Lagrange function $L(x^*,w^*)$ has a saddle point. The first theorem establishes R(x,y) as an exact auxiliary function in the PxY set (P- part or all of space E^n) for such a problem when B(g(x) is a strictly external penalty function. The other two theorems establish the sufficient condition for R(x,y) to be an exact auxiliary function for such a problem when B(g(x) is an internal penalty function and when it is a strictly mixed one. Next are considered nonlinear exact auxiliary functions $R(x,y)= H[(A(f(x)-,y),B(g(g(x))]$, $H(t,\tau)$ being a continuous nondecreasing function of two arguments and B(g(x)) being the penalty function. Three theorems establish the sufficient condition for R(x,y) to be an exact auxiliary function for the same nonlinear programming problems when A(f,y) is a convex monotonically increasing function of f(x) and B(g(x)) is 1) a strictly external penalty function, 2) an internal penalty function, 3) a strictly mixed one. The proof of these theorems is followed by exact modification of the Lagrange function and construction, with the aid of the Minkowski-Mahler inequality, of a whole class of exact auxiliary functions on the basis of the Lagrange function L(x,w). Two more theorems are then proved which establishes $R(x,y)= A(L(x,w),v)+ B(g(x))$ as an exact auxiliary function in the PxY set for the same nonlinear programming problems when B(g(x)) is a strictly external penalty function and when it is a internal one. References 11.

UDC 517.5

Development of Research Concerning Exact Solution of Extremal Problems in Best Approximation Theory

907L0095A Kiev UKRAINSKIY MATEMATICHESKIY ZHURNAL in Russian Vol 42 No 1, pp 4-17

[Article by V.F. Babenko and A.A. Ligun, Dnepropetrovsk University]

[Abstract] Development of the best approximation theory since formulation of the diameter problem by A.N. Kolmogorov in 1936 is reviewed, the fundamental concept of best approximation of element x in linear normalized space X being extended to best approximation of an n-diameter in class M in space X and more narrowly its best linear approximation. Research and developments in this area of mathematics are historically divided into two periods. While the best approximations by trigonometric polynomials of $W_{infinity}{}^r$-type classes in $L_{infinity}$ metric and of $W_1{}^r$-type classes in L_1

metric were sought till 1961, since then the best approximations by trigonometric polynomials of class H^{ω} in uniform metric are sought after N.p Korneychuk has found the exact value of such an approximation. The review covers classes of periodic functions and exact values of their diameters, best approximations and best linear approximations of convolution classes by trigonometric polynomials in C and L_1 metrics, approximation of classes of functions definable by moduli of continuity with applicable duality theorems and comparison theorems, best L_1-approximations of classes of functions definable with the aid of commutation-invariant sets, and exact inequalities of D. Jackson type. References 62.

UDC 517.927

Solution of Multipoint Boundary-Value Problem for System of Linear Ordinary Differential Equations With Holomorphic Coefficients

907L0095B Kiev UKRAINSKIY MATEMATICHESKIY ZHURNAL in Russian Vol 42 No 1, Jan 90 pp 125-128

[Article by V.A. Churkov, Kherson Industrial Institute]

[Abstract] Two theorems are proved which establish the necessary and sufficient conditions for existence and uniqueness of a holomorphic solution to a boundary-value problem with general linear boundary conditions for a system of linear first-order ordinary differential equations with holomorphic coefficients x'= T(t)x + f(t) and Σ(i= 0 to m)A_ix(t_i) + Σ(i= 1 to m)Integral(t_i= 1 to t_j)Φ_i (t)x(t)dt= h, where both the nXn-dimensional matrix T(t) and the n-dimensional vector f(t) are holomorphic in the vicinity absolute value of (t- t_0) smaller than r while the Φ_i(t) matrices are bounded and continuous in (t_{i-1},t_i) (i= 1 to m; m are natural numbers from 1 to n1), A_j (j from 0 to m) are nXn-dimensional matrices, and h is an n-dimensional numerical A_j-vector. References

UDC 512.546

Expanding Group Topology of Denumerable Group to Complete One

907L0086A Novosibirsk SIBIRSKIY MATEMATICHESKIY ZHURNAL in Russian Vol 31 No 1, Jan-Feb 90 pp 3-13

[Article by V.I. Arnautov and Ye.I. Kabanova, Kishinev]

[Abstract] The first step is taken toward resolution of the hypothesis that in a denumerable group any nonexpandable topology τ in the class of all nondiscrete ones is complete. Properties of a topological group (G,τ) which satisfies the first axiom of denumerability are established and verified with the aid of lemmas, using a group G in multiplicative notation and its unit e as well as the strength of a set X and the set N of all natural numbers. Two theorems are then proved, the first one confirming that hypothesis about a denumerable group G having a nondiscrete group topology τ^* which is com-plete and thus not smaller than topology τ. The second theorem states that the original topology τ_0 in the denumerable topological group (G,τ_0 is the lower bound of set T of all topologies in group G not smaller than topology τ_0. References 5.

UDC 517.11

Hyperidentities of QZ-Algebras

907L0077A Novosibirsk SIBIRSKIY MATEMATICHESKIY ZHURNAL in Russian Vol 30 No 6, Nov-Dec 89 pp 132-139

[Article by I.A. Maltsev and D. Schweigert, Novosibirsk]

[Abstract] An algebra A= and the set P_A all operations on A (pre-iterative Post algebra over set A) are considered, of concern being the properties of subalgebras of the Post algebra and of the clones among them, i.e., those which contain selectors. Their properties are established by five theorems, the first one proved here on the basis of two lemmas (proofs not given) and the following four proved with the aid of an additional lemma each. References 11.

UDC 519.54

Homomorphism Diagrams over Groups of Surfaces

907L0077B Novosibirsk SIBIRSKIY MATEMATICHESKIY ZHURNAL in Russian Vol 30 No 6, Nov-Dec 89 pp 150-171

[Article by A.Yu. Olshanskiy, Moscow]

[Abstract] Following an outline of the theory of diagrams, including three lemmas which pertain respectively to a disk diagram over group G, existence of a holomorphism diagram, and existence of a solution-to-equation diagram, the theory is further extended to diagrams over a free groups such as O-rings. A theorem with two corollaries is proved for holomorphisms of groups of surfaces in a free group A lemma is proved for simple diagrams with edge and a theorem is proved for quadratic equations in a free group A corollary having already established when and only when an element of a free group is a commutator, two theorems are now stated pertaining to products of commutators and (with a corollary) to products of squares respectively. Three ways of reformulating the Poincare hypothesis about homomorphism of a 3-sphere of any singly-connected compact 3-manifolds being possible by virtue of the Stollings-Jaco theorem, a-rings are considered next. A theorem is proved for them with the aid of a lemma and is demonstrated on an example. There follow diagrams over hyperbolic groups, specifically δ-groups and solutions to quadratic equations, a theorem for them being proved with the aid of five auxiliary lemmas. Figures 8. references 13.

END OF FICHE

DATE FILMED

5 Aug. 1990